D. BOZALİOĞLU METU 2007

EVALUATION OF MINIMUM REQUIREMENTS FOR LAP SPLICE DESIGN

DOĞU BOZALİOĞLU

MARCH 2007

EVALUATION OF MINIMUM REQUIREMENTS FOR LAP SPLICE DESIGN

A THESIS SUBMITTED TO
THE GRADUATE SCHOOL OF NATURAL AND APPLIED SCIENCES
OF
MIDDLE EAST TECHNICAL UNIVERSITY

BY

DOĞU BOZALİOĞLU

IN PARTIAL FULFILLMENT OF THE REQUIREMENTS
FOR
THE DEGREE OF MASTER OF SCIENCE
IN
CIVIL ENGINEERING

MARCH 2007

Approval of the Graduate School of Natural and Applied Sciences

Prof. Dr. Canan ÖZGEN
Director

I certify that this thesis satisfies all the requirements as a thesis for the degree of Master of Science

Prof. Dr. Güney ÖZCEBE
Head of Department

This is to certify that we have read this thesis and that in our opinion it is fully adequate, in scope and quality, as a thesis for the degree of Master of Science

Asst. Prof. Dr. Erdem CANBAY
Supervisor

Examining Committee Members

Prof. Dr. Tuğrul TANKUT (METU, CE) _____

Asst. Prof. Dr. Erdem CANBAY (METU, CE) _____

Prof. Dr. Güney ÖZCEBE (METU, CE) _____

Assoc. Prof. Dr. Barış BİNİCİ (METU, CE) _____

Dr. B. Afşin CANBOLAT (YÜKSEL PROJE) _____

I hereby declare that all information in this document has been obtained and presented in accordance with academic rules and ethical conduct. I also declare that, as required by these rules and conduct, I have fully cited and referenced all material and results that are not original to this work.

Name, Last name: Doğu Bozalioğlu

Signature :

ABSTRACT

EVALUATION OF MINIMUM REQUIREMENTS
FOR LAP SPLICE DESIGN

BOZALİOĞLU, Doğu
M.S., Department of Civil Engineering
Supervisor: Asst. Prof. Dr. Erdem CANBAY

February 2007, 121 Pages

Minimum requirements for lap splices in reinforced concrete members, stated in building codes of TS-500 and ACI-318, have a certain factor of safety. These standards have been prepared according to research results conducted previously and they are being updated according to results of recent studies. However the reliability of lap splices for minimum requirements needs to be investigated. For this purpose, 6 beam specimens were prepared according to minimum provisions of these standards. The test results were investigated by analytical procedures and also a parametric study was done to compare two standards. For smaller diameter bars both standards give safe results. Results showed that the minimum clear cover given in TS500 is insufficient for lap spliced bars greater than or equal to 26 mm diameter.

Keywords: Lap splice, reinforced concrete, beam, bond.

ÖZ

MİNİMUM KOŞULLARIN BİNDİRMELİ EKLER
AÇISINDAN İNCELENMESİ

BOZALİOĞLU, Doğu
Yüksek Lisans, İnşaat Mühendisliği Bölümü
Tez Yöneticisi: Y. Doç. Dr. Erdem CANBAY

February 2007, 121 Sayfa

TS-500 ve ACI-318 standartlarında belirtilen bindirmeli ekler için minimum koşullar belli oranda güvenlik faktörü içermektedir. Bu şartlar önceki araştırmalardan çıkan sonuçlara göre hazırlanmış ve yeni yapılan araştırmalara göre de güncellenmektedir. Ancak bindirmeli eklerin güvenirliliğinin minimum şartlar için incelenmesi gerekmektedir. Bu amaçla 6 kiriş numunesi standartlarda belirtilen minimum şartlara göre hazırlanmıştır. Deney sonuçları analitik yöntemlerle incelenmiş ve ayrıca iki şartnameyi kıyaslamak için bir durum çalışması yapılmıştır. Daha küçük çaptaki donatılar için her iki şartnamede güvenli sonuçlar vermektedir. Sonuçlar, TS500'de verilen minimum paspayı mesafesinin 26 mm çapına eşit veya büyük donatılarla yapılan bindirmeli ekler için yetersiz olduğunu göstermiştir.

Anahtar Kelimeler: Bindirmeli ekler, betonarme, kiriş, aderans.

ACKNOWLEDGEMENTS

This study was conducted under the supervision of Asst. Prof. Dr. Erdem Canbay. I wish to express my deepest appreciation to him for his suggestions in the creation of the scope of this study.

I would like to give my sincere thanks to Assoc. Prof. Dr. Barış Binici for his precious contributions.

I would like to give my thanks to the stuff of structural mechanics laboratory who were helped and supported me throughout the experimental study.

Last, but not least thanks to my family for being with me all the way.

TABLE OF CONTENTS

LIST OF TABLES

TABLES

LIST OF FIGURES

FIGURES

LIST OF SYMBOLS

a	Distance of the point load to the support
A_s	Total cross-sectional area of all longitudinal reinforcement in section
A_{tr}	Total cross-sectional area of all transverse reinforcement which is within the spacing s and which crosses the potential plane of splitting through the reinforcement being developed
b_w	Width of specimen
c_b	$c_{\min} + 0.5\, d_b$ (mm)
c_{bb}	Clear cover of reinforcement being developed or lap spliced, measured to tension face of member
c_c	Side and bottom clear cover
$c_{\max}$	Maximum value of c_s or c_{bb}
$c_{\min}$	Minimum value of c_s or c_{bb}
c_s	Minimum value of c_{si} + 6 mm or c_{so}
c_{si}	One-half of average clear spacing between bars or lap splices in a single layer
c_{so}	Clear cover of reinforcement being developed or lap spliced, measured to side face of member
d	Effective depth of specimen
h	Depth of specimen
d_b	Diameter of reinforcing bars
d_m	Clear distance between lap spliced and transverse reinforcement
d_{tr}	Diameter of transverse reinforcement
f'_c	28 days cylinder compressive strength of concrete
f_c	Cylinder compressive strength of concrete
f_{ct}	Tensile strength of concrete
f_{ct}	Design tensile strength of concrete

f_{cts} Split tensile strength of concrete

f_{su} Longitudinal reinforcement ultimate strength

f_y Longitudinal reinforcement yield strength

f_y Longitudinal reinforcement design yield strength

f_{yt} Yield strength of transverse reinforcement

K_{tr} Transverse reinforcement index

K'_{tr} Transverse reinforcement index

ℓ_b Development length of tension reinforcement by means of straight embedment

ℓ_d Development length

ℓ_o Splice length

ℓ_s Development or splice length

n Number of bars or wires being spliced or developed along the plane of splitting

r Ratio of spliced reinforcement to total reinforcement at that section

s Maximum center-to-center spacing of transverse reinforcement within ld

$t_{A/C}$ Tangential deviations between points A and C

$t_{B/C}$ Tangential deviations between points B and C

t_d The bar diameter factor

u Mean unit bond strength

α_1 Multiplying factor for ℓ_b

Δ_A Deflection at point A

Δ_C Deflection at point C

ϕ Reinforcement bar diameter

ϕ_t Transverse reinforcement diameter

λ Lightweight aggregate concrete factor

ω Factor calculated from $c_{\max}$ and $c_{\min}$

ψ_t Reinforcement location factor

ψ_e Coating factor

ψ_s Reinforcement size factor

CHAPTER 1

INTRODUCTION

1.1. General

Although various types of construction materials are available in today's construction world, reinforced concrete is still the most widely used material.

One of the basic assumptions for calculating the reinforced concrete members' capacities is the perfect bond assumption between concrete and steel. Perfect bond means that the strain on reinforcing steel and surrounding concrete is the same and there is no slip or splitting type of failure prior to the yielding of reinforcing steel bar. If failure occurs before yielding of reinforcing bar, the reason may be the insufficient bond strength. Therefore, performance of the reinforced concrete structures depends on the adequate bond strength. Bond strength may be investigated in two categories: Development strength (i.e. bond strength of bars embedded in concrete) and splice strength (i.e. bond strength of splicing bars). Splicing of reinforcing bar causes a local deficiency in the member at splice region due to stress concentration. However, avoiding of bar splices completely is impossible because of the production limitations in length. Previous earthquakes showed that many of the collapses were caused due to insufficient lap splice, lack of confinement along the spliced region or short anchorage lengths.

Bond strength was related to bearing strength between the ribs of reinforcement and surrounding concrete. Therefore it was assumed that bond strength is related to

material properties only. In modern codes, lap splice or development of reinforcing bars are not only related to the material properties but also related to the geometric properties of members. Such as configuration of reinforcing bar along the member, cover thickness, confinement ratio and relative rib area of reinforcing bars.

1.2. Bond Behavior

Bond strength between reinforcing steel and concrete is provided mainly by adhesion forces and friction forces for plain bars. For deformed bars, bearing forces resulting from lugs of reinforcement against surrounding concrete is the main reason of bond strength. With the initiation of slip of plain bar in concrete, adhesion and other chemical resistances between reinforcing bar and concrete are lost. Bond strength is provided only by frictional forces. Resistance of surface roughness for plain bar is very small. Therefore the type of failure for plain bars is usually slip. Splitting of concrete cover is not a concern for plain bars. For deformed bars failure mechanism is different than plain bars. Lugs (ribs or deformations) of deformed bars increase the surface contact between bar and concrete, resulting in an increase of frictional forces. But, mainly bearing forces resulting from lugs on surrounding concrete provides the most important part for bond strength. The tensile forces on the rebar cause inclined reaction forces on the lugs. These forces are illustrated in Figure 1.1.

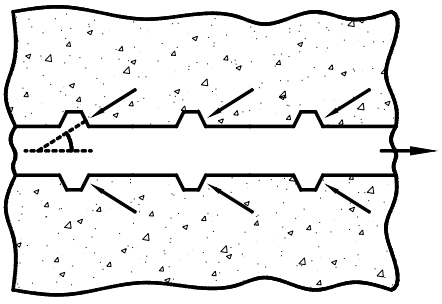

Figure 1.1 Bearing forces on lugs.

These forces can be divided into horizontal and vertical components. The horizontal component causes shear force in the concrete between successive lugs. On the other hand, the vertical component produces radial internal pressure and this force creates tensile forces on the surrounding concrete. These tensile forces may cause splitting of concrete cover or concrete between adjacent bars. Hence, it has been proven that the clear cover, clear spacing and amount of transverse reinforcement are also important factors influencing the bond strength for deformed bars.

1.3. Research Needs

Bond strength of bars has been studied by many researchers for more than 100 years. Code provisions and design expression have been continuously modified for bond. Starting from 1977 ACI 318 Building Code [23] concrete cover, spacing between rebars and amount of transverse reinforcement have been included in the code provisions. A database is provided by ACI Committee 408 [25] and it has a very important role for development of design expressions on bond. This study aims to fulfill some of the gaps in the database.

Another important research need is that there is no specific research that investigates the bond characteristics of design provisions of the Turkish Code TS500 [22].

The main philosophy of the design codes is to provide simple and safe equations while maintaining the economy. However, the tendency of the current codes, like ACI 318-05 [24] move towards more sophisticated, confusing and complex equations. The Turkish Standard for Reinforced Concrete Structures [22] (TS 500) is much simpler when compared to those codes. However, accuracy and/or safety concerns arise for TS 500 which has to be studied carefully.

1.4. Objective and Scope

The objective of this study is to verify the validity of the lap splice provisions for minimum requirements. In this study TS500 and ACI318-05 codes were considered. Totally six specimens were designed according to minimum requirements of cover, spacing between bars and transverse reinforcement.

In this scope 6 real size beam specimens were prepared. Three of them were constructed according to TS 500 and the other three according to ACI 318-05 provisions. Lap splices of the longitudinal bars were made at the midspan where the moment was constant and shear was zero. All bars were spliced at the same location. Beams were tested as inverted simply supported beam. Tip and mid deflections and strains on longitudinal and transverse reinforcement were acquired during the tests.
The scope of this study includes:

- Understanding the bond behavior especially for lap splicing by reviewing previous publications and researches.
- Preparation and testing of six beam specimens fulfilling the requirements of testing protocol of ACI Committee 408.
- Evaluation of data gathered during tests.
- Comparison of test results with the analytical predictions.

CHAPTER 2

LITERATURE SURVEY

Since 1913 starting with Abrams [1] bond behavior of reinforced concrete members have been studied. Today, thanks to these researchers, bond behavior of conventional reinforced concrete members is well known. Based on the comprehensive literature survey, important observations and conclusions of the previous researchers are summarized below. The survey is presented in chronological order to preserve the historical prospective.

Chinn, Ferguson, and Thompson [8] conducted experiments on 40 beams with a constant moment region. They observed from their experiments that splice strength increases by 15 to 40 percent by doubling beam width. Also, the splice strength of shorter splices increases 7 to 15 percent by doubling cover. They stated that bottom split failures were not sensitive to small changes in concrete strength, but for side splitting, doubling the concrete strength, splice strength was increased 37 percent. They noticed that as splice length increases, the bond stress decreases accordingly, but not as rapidly as the surface area increased. Also they concluded that using stirrups or ties around a splice increased the strength 45 percent. They also stated that bar size had an effect on bond strength even when cover, splice length, and beam width were constant in terms of bar diameter.

Chamberlin [4] conducted experiments on beams containing one single bar or two bars spliced in the constant moment region. According to the test results it was concluded that the ACI Building Code requirement of "minimum overlap for a lapped splice shall be 24 bar diameters, but not less than 12 in." causes yielding of

bar even the final failure was side splitting. Thus, load carrying capacity of concrete beams increased with wider spacing of unspliced bars.

Ferguson and Breen [10] observed that specimens with shorter splices showed splitting over a large part of their length, whereas longer splice lengths generally showed less splitting over their length. They concluded that longer splice lengths appeared to stabilize with a substantial center length remaining unsplit until a final violent failure occurred. They assumed that the developed bond stress varied as the square root of concrete compressive strength. They observed that crack width is not related with bar diameter, since for same stress levels different bar diameters resulted in almost the same crack widths. But with beams heavy stirrup along the lap splice resulted with greater crack widths. They observed that beams with stirrups showed greater splice strengths than those without stirrups and stirrups eliminated the sudden and violent failure which characterized splices without stirrups.

Ferguson and Briceno [11] developed a splitting theory for splices. They assumed in their calculations that the radial and longitudinal stress components in concrete are equal, and at ultimate the variation in steel stress along the splice is essentially linear from zero at one end to a maximum at the other. Their splitting theory for splices fit into their test results with errors generally less than 15 percent.

Ferguson and Krishnaswamy [12] noticed that splice strength does not vary linearly with either length or lateral spacing of adjacent splices. They concluded that the most important variables defining splice strength was the clear lateral spacing between adjacent splices and the clear cover over the splices. They also noticed that lateral, the average tensile stress in concrete appeared to be more nonuniform as the spacing between adjacent splices was increased. In their study, the splitting stress over the entire splice length and the entire net concrete width per splice was calculated to resist an assumed splitting force related to the bond stress.

Goto [13] conducted a series of tests on axially loaded specimens. A single deformed bar encased concentrically in a long concrete prism. Specimens loaded with axial tension through the exposed ends of the bar. By injection of ink into specimens, he observed crack patterns. He concluded that both lateral and transverse cracks appearing on concrete surface were both primary and secondary cracks and formed in completely different ways. He also concluded that great numbers of internal cracks were formed in concrete around deformed bars making an about 60 degree angels relative to the bar axis.

Thompson, Jirsa, Breen, and Meinheit [19] conducted a series of beam tests to examine the strength and behavior of wide sections containing multiple lap splices. Beam specimens were constructed to simulate splice conditions in a typical cantilever retaining wall section with the main reinforcement in the wall stem lap spliced to anchor bars that extend up from the base. They observed that splice strength increases with increasing splice length, clear cover, and increasing concrete tensile strength. They stated that the edge splices in a section normally proved to be the weakest splices. They also stated that the inclusion of transverse reinforcement in the splice section improves the performance of the splice and providing transverse reinforcement increased strength of splice and cracking was reduced.

Orangun, Jirsa, and Breen [15] developed an expression for calculating the development and splice lengths for deformed bars. The expression is based on a nonlinear regression analysis of test results of beams with lap splices and reflects the effect of length, cover, spacing, bar diameter, concrete strength, and transverse reinforcement on the strength of anchored bars. The expression proposed in their study forms the basis of splice strength provisions of ACI 318-05.

Zekany, Neumann, Jirsa, Breen [20] investigated the effects of level of shear, amount of transverse reinforcement and casting position on the strength of lap splices. They concluded some following important results according to their experimental studies:

- The level of shear had a negligible influence on the strength of lapped splices. With substantial increases in the level of shear, only negligible changes in the bond strength were observed.

- Transverse reinforcement was found to be effective in resisting splitting produced by anchorage distress. The entire area of transverse reinforcement can be considered in calculating shear capacity and splice length.

- Top splices had average strengths of 90 percent (with a standard deviation of about 8 percent) of the bottom splice strength.

- Shifting the splice away from the section of maximum moment did not improve the capacity of the splice. The load sustained was about the same as if the splice had been located at the critical section (maximum moment).

Sozen and Moehle [18] developed a simple design procedure to determine development/splice lengths for deformed reinforcing bars. A total of 233 test results were included in this study. They noticed a decreasing trend between the normalized bond strength, $u/\sqrt{f_c'}$, and development length ratio, ℓ_s/d_b. They also observed a plausible trend for strength, $u/\sqrt{f_c'}$, to increase with cover, $c_{\min}/d_b$. For as-rolled deformed bars (without epoxy coating) with less than 12-in. of concrete cast beneath them, the proposed method required a development length of 40 bar diameters using a specified yield stress is 60,000 psi (413 MPa) and a concrete compressive strength of 4,000 psi (27 MPa).

Rezansoff, Konkankar and Fu [16] conducted tests on 40 simply supported beams with a constant moment region. They studied the confinement limits for tension lap splices under static loading. They observed that the reinforced concrete beams containing lap splices with heavy reinforcement performed as well as beams in which the splices were lightly confined. They also observed that specimens with larger concrete covers showed marginally lower splice strengths than specimens with

smaller covers. Confinement provided by concrete was a little less efficient than the equivalent confinement provided by stirrups. They observed a large scatter at low confinement levels, whereas the prediction was reasonable with large confinement.

Sakurada, Morohashi, Tanaka [17] conducted series of beam tests in order to investigate the effect of inner transverse reinforcement on dynamic behavior of lap splices. They observed that inner supplementary ties decreased the crack width. They also observed that the main reinforcement in the intermediate section combined with inner supplementary ties showed greater bond stress than the main reinforcement without inner supplementary ties.

Azizinamini, Stark, Roller and Ghosh [3] studied the bond performance of reinforcing bars embedded in high-strength concrete. They concluded that the assumption of a uniform bond stress distribution at the ultimate stage may not hold true for high-strength concrete and the nonuniform bond stress distribution could be more pronounced as the splice length increases or concrete cover decreases. For high-strength concrete, in the case of small covers, increasing the splice length is not an efficient approach for increasing bond capacity. A better approach would be to require a minimum amount of transverse reinforcement over the spliced length. Also they observed that for small cover, top cast bars appear to perform better with respect to bond and this was in contrast to the performance of such bars in normal strength concrete.

Azizinamini, Chisala and Ghosh [2] investigated the minimum stirrup requirement over the splice region. According to their previous research they concluded that inclusion of a minimum amount stirrup over lap splice is a better approach rather than increasing lap splice length. They observed that the strain distribution over the splice region is not uniform near the maximum midspan displacement; however, as the splice length decreases, strain distribution shows a more uniform value. In general, only the outer-most stirrup over the splice region reaches the yield strain at maximum midspan displacement, with the remaining stirrups over the splice region reaching strains values below yielding.

Darwin, Zuo, Tholen and Idun [8] developed statistically an expression for the force bond strength of confined and unconfined splices. The expression includes concrete strength, cover, bar spacing, development/splice length, transverse reinforcement, and the geometric properties of the developed/spliced bars. They suggested the use of the power ¼ instead of ½ for the concrete compressive strength to accurately represent the effect of concrete strength on bond strength.

Zuo and Darwin [21] evaluated effects of concrete strength, coarse aggregate quantity and type, and reinforcing bar geometry on splice strength. They proposed a new expression that represents the development/splice strength of bottom-cast uncoated bars as a function of member geometry, concrete strength, relative rib area, bar size, and confinement provided by both concrete and transverse reinforcement.

Hamad, Najjar, Jumma [14] conducted two series of beam tests with high strength concrete. In one series steel fibers of different volume fractions were used. In second series transverse reinforcement was placed in various amounts. In both series 12 full-scale beams were tested with three different bar (20, 25 and 32 mm) sizes. Some of the conclusions are listed below.

- Increasing the amount of steel fibers or the number of stirrups increased in the splice region improved the ductility of mode of failure of the high strength concrete beam specimens.

- Presence of hoop stirrups in the splice region produced a relatively more ductile and gradual mode of failure than beams with fiber reinforcement.
- For all tested specimens increasing the fiber content in the spliced region increased the average bond strength of tension lap splices.

Canbay, Frosch [5] evaluated the bond strength of lap – spliced bars and developed an expression to calculate bond strength. They verified the expression with 203

unconfined and 278 confined beam tests which were in consistency with the ACI 408 Database 10-2001 (ACI Committee 408 2003). They concluded the following results.

- The relation between splice strength and splice length can be expressed approximately by the square root of the ratio of splice length to bar diameter, $\sqrt{\ell_s / d_b}$.

- In agreement with the latest viewpoint of ACI Committee 408 (2003), the fourth root of the concrete strength provides an improved estimate regarding the behavior of lapped splices as compared with the square root.

- Since the effect of the thickness of the concrete cover surrounding the bar is not linear, the decreasing impact of larger covers can be incorporated by the square root of the cover to the bar diameter ratio, $\sqrt{c/d_b}$.

- Large bar spacing has a positive effect for face – splitting failure, especially for slab – type members. This trend can be represented by a linear increase in bond strength.

Canbay, Frosch [6] investigated the development of a simple and reliable design expression. Equations on development and splices of reinforcement in ACI 318-05 along with other design proposals were critically assessed in light of 203 unconfined and 278 confined beam tests where the splice region was subjected to constant moment. A simple design provision was developed that was based on a physical model of tension cracking of concrete in the lap spliced region.

$$\frac{\ell_d}{d_b} = 3.12 \times 10^{-4} \frac{f_y^2 \sqrt{d_b}}{\sqrt{f_c'}}$$

(2.1)

They found that the proposed design expression, given in equation 2.1, provides excellent overall results and was applicable for the design of beams as well as slabs. Furthermore, the proposed expression was applicable beyond the concrete strength limitation of ACI 318-05 and can be used for concrete strengths up to 16,000 psi (110 MPa).

Darwin, Lutz and Zuo [9] recommend a new design proposal for ACI318-05 Code. Recommended provision has two basic development length calculations. First approach is the simple one and considers only the steel strength and concrete strength. However, there are two different equations which are used according to clear cover and spacing limitations. Following equations 6.1 and 6.2 are used as basic approach.

$$\frac{\ell_d}{d_b} = \left(\frac{f_y}{2.2 f_c'^{1/4}} - 21 \right) \psi_t \psi_e \lambda \tag{6.1}$$

$$\frac{\ell_d}{d_b} = \left(\frac{f_y}{1.5 f_c'^{1/4}} - 31 \right) \psi_t \psi_e \lambda \tag{6.2}$$

In order to use Equation 6.1, clear spacing of the bars being spliced shall not be less than d_b, and stirrups or ties throughout ℓ_d provide a value $K'_{tr}/d_b \geq 0.5$ or clear spacing of the bars being spliced shall not be less than $2d_b$ and clear cover is not less than d_b. If these requirements are not satisfied than Equation 6.2 have to be used.

The advanced approach in the proposal is as follows:

$$\frac{\ell_d}{d_b} = \frac{\left(\frac{f_y}{f_c'^{1/4}} - 48\omega \right) \psi_t \psi_e \lambda}{1.5 \left(\frac{c_b \omega + K'_{tr}}{d_b} \right)} \tag{6.3}$$

$\left(\frac{c_b \omega + K'_{tr}}{d_b} \right)$ shall not be greater than 4.0.

The factor ω shall be taken as 1.0 or calculated as

$$\omega = 0.1\frac{c_{\max}}{c_{\min}} + 0.9 \le 1.25 \tag{6.4}$$

The transverse reinforcement index K'_{tr} shall be calculated as

$$K'_{tr} = \frac{6t_d A_{tr}\sqrt{f'_c}}{sn} \tag{6.5}$$

The bar diameter factor t_d shall be calculated as

$$t_d = 0.03d_b + 0.22 \tag{6.6}$$

$c_b = c_{\min} + 0.5\,d_b$ (mm)

c_{bb} = clear cover of reinforcement being developed or lap spliced, measured to tension face of member. (mm)

$c_{\max}$ = maximum value of c_s or c_{bb}. (mm)
$c_{\min}$ = minimum value of c_s or c_{bb}. (mm)
c_s = minimum value of c_{si} + 6 mm or c_{so}. (mm).
c_{si} = one-half of average clear spacing between bars or lap splices in a single layer. (mm)
c_{so} = clear cover of reinforcement being developed or lap spliced, measured to side face of member. (mm)

ACI408 proposal has the main difference in concrete strength. In ACI 318-05, the strength of concrete is incorporated into the equation with its square root. In ACI408 proposal, however, the fourth root of concrete strength is considered. ACI 318-05 expression considers only yield strength of transverse reinforcement in the K_{tr} calculations. On the other hand, ACI408 proposal considers square root of strength of concrete rather than yield strength o transverse reinforcement.

CHAPTER 3

EXPERIMENTAL PROGRAM

3.1. General

Six reinforced concrete beams were tested in this study. Specimens were prepared according to the minimum requirements given in TS 500-2000 and ACI 318-05 for clear cover, bar spacing, lap splice length and quantity of stirrups for confinement. The diameters of longitudinal bars were 16, 22 and 26 mm. TS and ACI in the naming of specimens stand for designs according to provisions of Turkish Standards-500 and American Concrete Institute-318-05, respectively. The numbers in the naming show the diameter of rebars. Formworks were prepared in the structural mechanics laboratory and concrete was supplied by a ready mixed concrete firm. All reinforcement work, including set-up of strain gauges, were made in the structural laboratory.

3.2. Materials

3.2.1. Concrete

As previously mentioned, concrete was supplied from a ready mix concrete company. The target strength for concrete was 30 MPa and as expected it gained its full strength at the end of 28 days. Due to some unexpected problems occurred during the experimental program; specimens had to be tested after 5 months. At the

end of the final experiment, after 172 days, f_c was reached to 38 MPa. At the first two weeks curing was applied properly by covering the specimens with wet burlap. However, curing process was stopped after realizing that concrete gained its strength very fast.

Concrete of all specimens was molded at the same time from a mixer and test cylinders were taken randomly during the placement of concrete. Concrete strength was determined by testing these standard cylinders. Cylinders were 150 mm in diameter and 300 mm in height. The curing of cylinders was the same as specimens.

At the end of each test, three of concrete cylinders were tested to determine compressive strength and three of them to determine split tensile strength of concrete. Table 3.1 shows the date of experiment, strength values and relevant experiments for the data.

Table 3.1 Concrete strength of specimens

Age of concrete (days)	Date	f_c (MPa)	f_{cts} (MPa)	Experiments Done
30	08.03.2006	30.96	N.A.	N.A.
65	12.04.2006	36.60	2.30	TS26
85	02.05.2006	37.00	2.38	ACI22
154	10.07.2006	37.70	2.46	ACI26
171	27.07.2006	37.70	3.11	TS16, ACI16, TS22

3.2.2. Steel

In each specimen, three longitudinal reinforcing bars were used with the diameters of 16, 22 and 26 mm. For shear reinforcement, 8 mm bars were used as stirrups. At the top of the beams, two 12 mm bars were used as assembly bars. All reinforcing bars

were taken from the same batch and all of them were deformed bars. Turkish classification for bars is S420.

Two test coupons were taken from each full length reinforcements. Coupons had a length of 600 mm for bars with the diameters of 22 and 26 mm, length of 400 mm for bars with the diameters of 16 and 12 mm, and 300 mm for 8 mm bar. These coupons were tested at the Materials Laboratory of Civil Engineering Department. Generally all reinforcing bars had greater elongation percent than 12% which is minimum requirement for S420 reinforcing steel in Turkish Codes. Table 3.2, 3.3 shows the properties of the reinforcing bars used in the specimens.

Table 3.2 Geometrical properties of reinforcing bars.

Test Coupon	Weight (gr)	Length (cm)	Diameter (mm)	Area (mm^2)
ϕ8_1	129.00	30.50	8.29	54
ϕ8_2	130.60	30.40	8.35	55
ϕ12_1	347.90	40.00	11.88	111
ϕ12_2	348.60	40.10	11.88	111
ϕ16_1	635.20	40.00	16.05	202
ϕ16_2	636.00	39.90	16.08	203
ϕ22_1	1798.90	60.40	21.99	380
ϕ22_2	1786.10	60.00	21.98	379
ϕ26_1	2411.30	60.00	25.54	512
ϕ26_2	2388.90	60.00	25.42	508

Table 3.3 Properties of reinforcing bars.

Test Coupon	Yield Strength (f_y) (N/mm^2)	Ultimate Strength (f_{su}) (N/mm^2)	Elongation Percent
ϕ8_1	482	705	20.0
ϕ8_2	482	719	21.0
ϕ12_1	433	681	18.0
ϕ12_2	447	686	16.5
ϕ16_1	435	672	17.5
ϕ16_2	423	669	18.0
ϕ22_1	453	722	16.7
ϕ22_2	459	727	16.7
ϕ26_1	468	742	15.3
ϕ26_2	469	753	16.1

3.3. Specimens

3.3.1. Specimen Geometry

All specimen geometries had different dimensions except their depths, which was 400 mm for all. Widths of the specimens were determined according to the minimum spacing and clear cover limitations of code provisions. Dimensions for six specimens and their *a*/*d* ratios are shown in Table 3.4. *a* is the distance of the point load to the support. For all specimens it is equal to 1.4 m and *d* is the effective depth of the specimen. The *a*/*d* ratio for all specimens was approximately equal to 4. Since adequate lateral reinforcement supplied to the specimens, the expected behavior was flexural.

Table 3.4 Dimensions of Specimens.

Specimen	Dimension ($h \times b_w \times \underline{\ell}$)	a/d
ACI26	$400 \times 306 \times 5500$ mm	4.11
ACI22	$400 \times 285 \times 5500$ mm	4.08
ACI16	$400 \times 255 \times 5000$ mm	4.05
TS26	$400 \times 324 \times 5500$ mm	3.97
TS22	$400 \times 284 \times 5000$ mm	3.90
TS16	$400 \times 234 \times 5000$ mm	3.85

3.3.2. Formwork

Formworks were prepared in the Structural Mechanics laboratory. In order to produce six beams at the same time, 6 adjacent formworks were made by using steel plates and steel profiles. 5 mm thick steel plates were used to get smooth surface. Steel plates were cut to get 4m×400 mm surface. 400 mm was the depth of beam specimens. Two steel square sections (box section), which had 20×20×2 mm dimensions and 4 m in length were welded to the edges of the steel plates. Then 360 mm long steel sections were welded as stiffeners on the side steel plates vertically with a 250 mm of spacing. Between these vertical stiffeners 430 mm diagonal cross stiffeners were also welded. Another steel plate was welded on the stiffeners and a two sided smooth thick plate was produced. Figure 3.1 shows the details of the formwork.

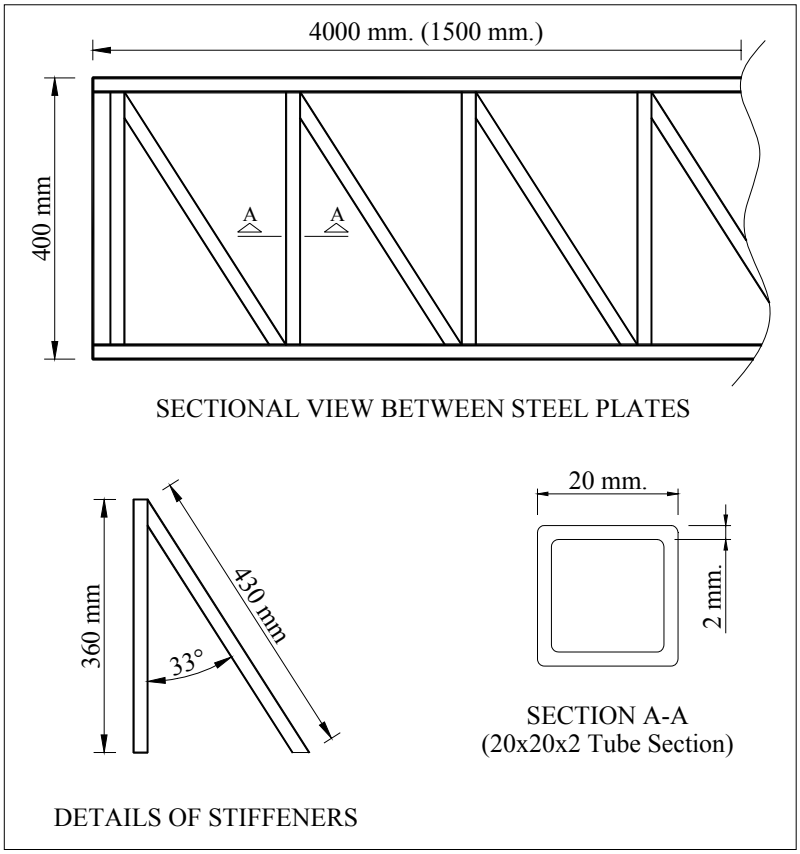

Figure 3.1 Details of formwork.

1.5 m long steel forms were also prepared to get a total of 5.50 m long formwork. The square steel sections provided the required stiffness to the formworks against out of plane bending.

After side parts of formwork were completed they were set on a smooth steel table according to their predefined beam widths. The surface of table was also produced with 5 mm thick steel plate. The ends of formwork were closed with similar steel plates. The steel plates were precisely assembled using water level and 90^{o} angles to form perfectly straight and orthogonal formworks. Finished view of formwork is shown in Figure 3.2.

Figure 3.2 Finished view of formwork.

3.3.3. Reinforcement

The diameter of the longitudinal bars used in specimens were 16 mm, 22 mm, and 26 mm. Lap splice lengths, spacing between bars and bottom and side clear cover depths were determined according to minimum requirements of TS 500 and ACI 318-05 standard specifications for splice length. All these data were calculated for cylindrical compressive concrete strength of 30 MPa and 420 MPa yield strength for both transverse and longitudinal reinforcing bars.

3.3.4. Lap Splice Calculations and Spacing Requirements for ACI 318 Code.

Spacing limit for longitudinal reinforcements, clear cover limitations and bend diameters for transverse reinforcement was taken from Chapter 7 – Details of Reinforcement.

Lap splice length was calculated from the provisions stated in Chapter 12 – Development and Splices of Reinforcement.

3.3.4.1. Spacing and Clear Cover Requirements

In Chapter 7, Clause 7.6 following limitations are required for spacing.

- The minimum clear spacing between parallel bars in a layer shall be equal to the bar diameter and not less than 1 in (25.4 mm) (7.6.1). Code also limits the spacing according to the maximum aggregate size. This is stated in Clause 3.3.2. Coarse aggregate size shall not be larger than ¾, of the minimum clear spacing between individual reinforcing bars.

- Clause 7.7 limits the minimum clear cover requirements. Minimum cover shall be greater than 1.5 in (38 mm) for cast-in-place concrete beams or columns. (7.7.1)

3.3.4.2.Lap Splice Requirements

In Chapter 12, Clause 12.2 there are two equations. First one is the simple approach and in these equations clear cover and spacing dimensions, and the amount of transverse reinforcement are not considered. The equations in the basic approach are given in tabulated form. Depending on some conditions 4 different equations can be selected. The other one is a more advanced approach and it considers cover and

spacing dimensions and the amount of transverse reinforcement. Equation 3.1 given below shows the advanced approach for the calculations of the development length (ℓ_d).

$$\frac{\ell_d}{d_b} = \frac{9}{10}\frac{f_y}{\sqrt{f'_c}}\frac{\psi_t\psi_e\psi_s\lambda}{\left(\frac{c_b + K_{tr}}{d_b}\right)} \qquad (3.1)$$

$\left(\frac{c_b + K_{tr}}{d_b}\right)$ shall not be greater than 2.5.

ψ_t : Reinforcement location factor. For horizontal reinforcement placed such that more than 300 mm (12 in.) of fresh concrete is cast below the splice, ψ_t is 1.3. For other situations it is 1.0.

c_b: Use the smaller of either the distance from the center of the bar or wire to the nearest concrete surface or one-half the center-to-center spacing of the bars or wires being developed.

ψ_e : Coating factor. For epoxy-coated bars or wires with cover less than $3d_b$, or clear spacing less than $6d_b$, ψ_e is 1.5. For all other epoxy-coated bars or wires it is 1.2. For uncoated reinforcement it is 1.0.

The product of $\psi_t\psi_e$ need not be grater than 1.7.

ψ_s : Reinforcement size factor. For 19 mm (No.6) diameter and smaller bars and deformed wires ψ_s is 0.8. For 22 mm (No.7) and larger bars it is 1.0.

λ : Lightweight aggregate concrete factor. When lightweight aggregate concrete is used λ is 1.3. However, when f_{ct} is specified, λ shall be permitted to be taken as $\sqrt{f'_c}/1.8f_{ct}$ but not less than 1.0. When normal weight concrete is used it is 1.0.

K_{tr} : Transverse reinforcement index.

$$= \left(\frac{A_{tr} f_{yt}}{1500sn} \right)$$

A_{tr} : Total cross-sectional area of all transverse reinforcement within spacing s that crosses the potential plane of splitting through the reinforcement being developed.

f_{yt} : Yield strength of transverse reinforcement.

n : Number of bars being spliced.

s : Spacing of transverse reinforcement.

In Chapter 12, Clause 12.15 Lap splice length is defined in two different ways. For Class A, splice lap splice length is $1.0\ell_d$ and for Class B splice it is $1.3\ell_d$. Lap splice length shall not be less than 300 mm (12 in.). Class A and Class B type lap splices summarized in Table 3.6.

Table 3.5 Definition for Class A and Class B type of lap splice. [24]

$\frac{A_s \text{ provided}^*}{A_s \text{ required}}$	Maximum Percent of spliced within required lap length	
	50	100
Equal to or greater than 2	Class A	Class B
Less than 2	Class B	Class B

*Ratio of area of reinforcement provided to area of reinforcement required by analysis at splice region.

The main reason for 1.3 multiplier in lap splice length is primarily to encourage designers to splice bars at points of minimum stress and to stagger splices to improve behavior of critical details. Therefore, this multiplier is not considered in this study.

Basically, the splice lengths given below are the development lengths according to the code.

Detailed calculations for lap splice lengths, spacing and clear covers are showed in Appendix A. Table 3.7 lists these values for ACI16, ACI22, ACI26. Figures 3.4, 3.5 and 3.6 show the details of specimens ACI26, ACI22 and ACI16, respectively.

Table 3.6 Lap Splice, spacing and cover dimensions for ACI specimens.

Specimen Name	c_{so} **(mm)**	$2c_{si}$ **(mm)**	c_b **(mm)**	**Lap Splice Length (mm)**	**Lap Splice Length (In terms of d_b)**
ACI16	38.0	25.4	38.0	500	31 d_b
ACI22	38.0	25.4	38.0	1060	48 d_b
ACI26	38.0	26.0	38.0	1380	53 d_b

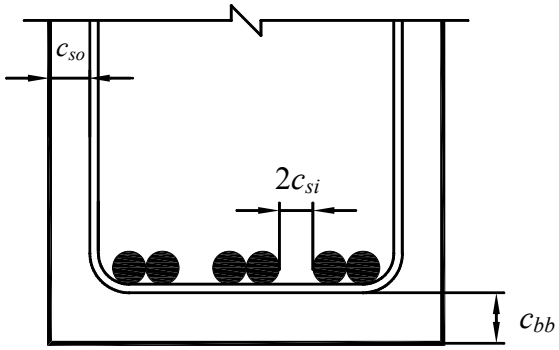

Figure 3.3 Definitions for c_{so}, c_{si}, c_{bb}.

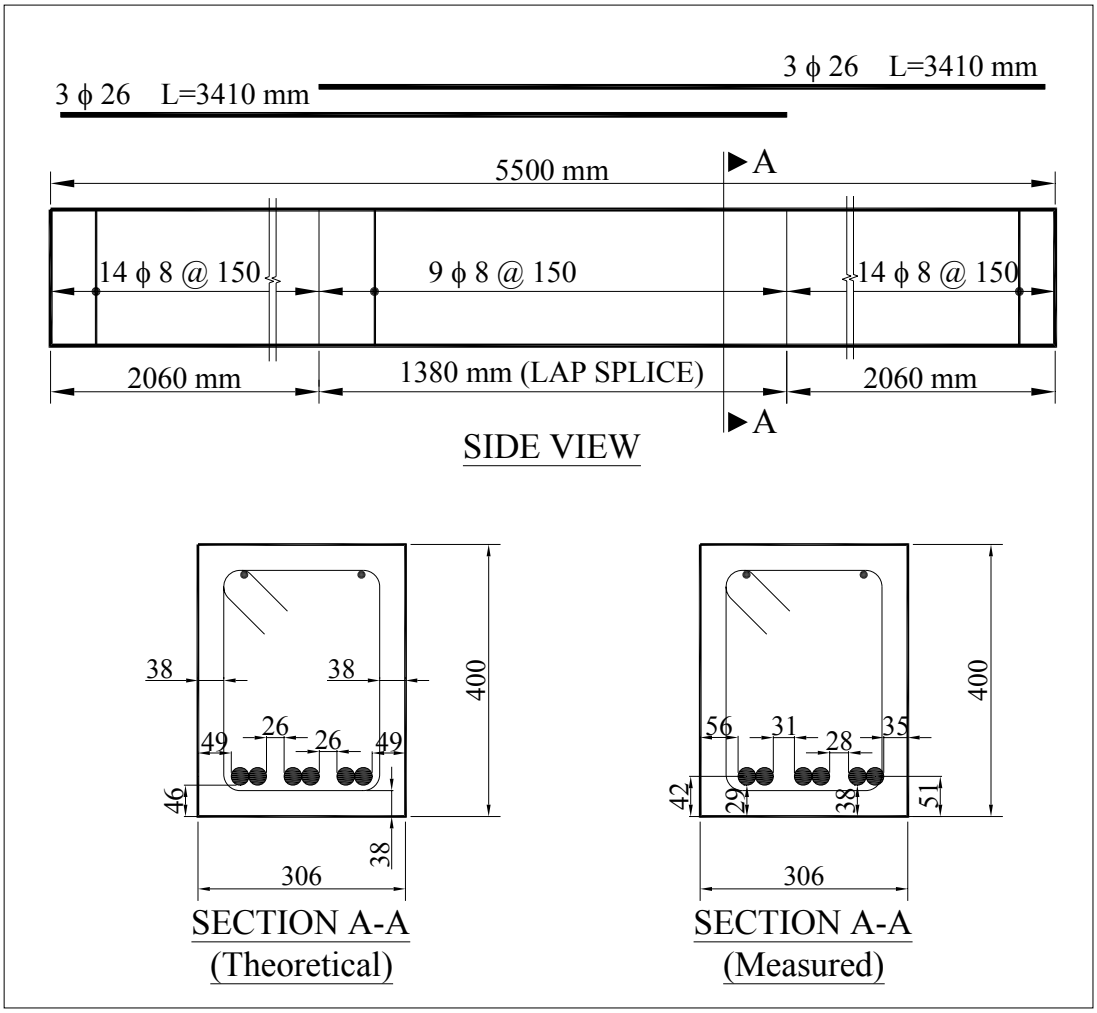

Figure 3.4 Details of Specimen ACI26.

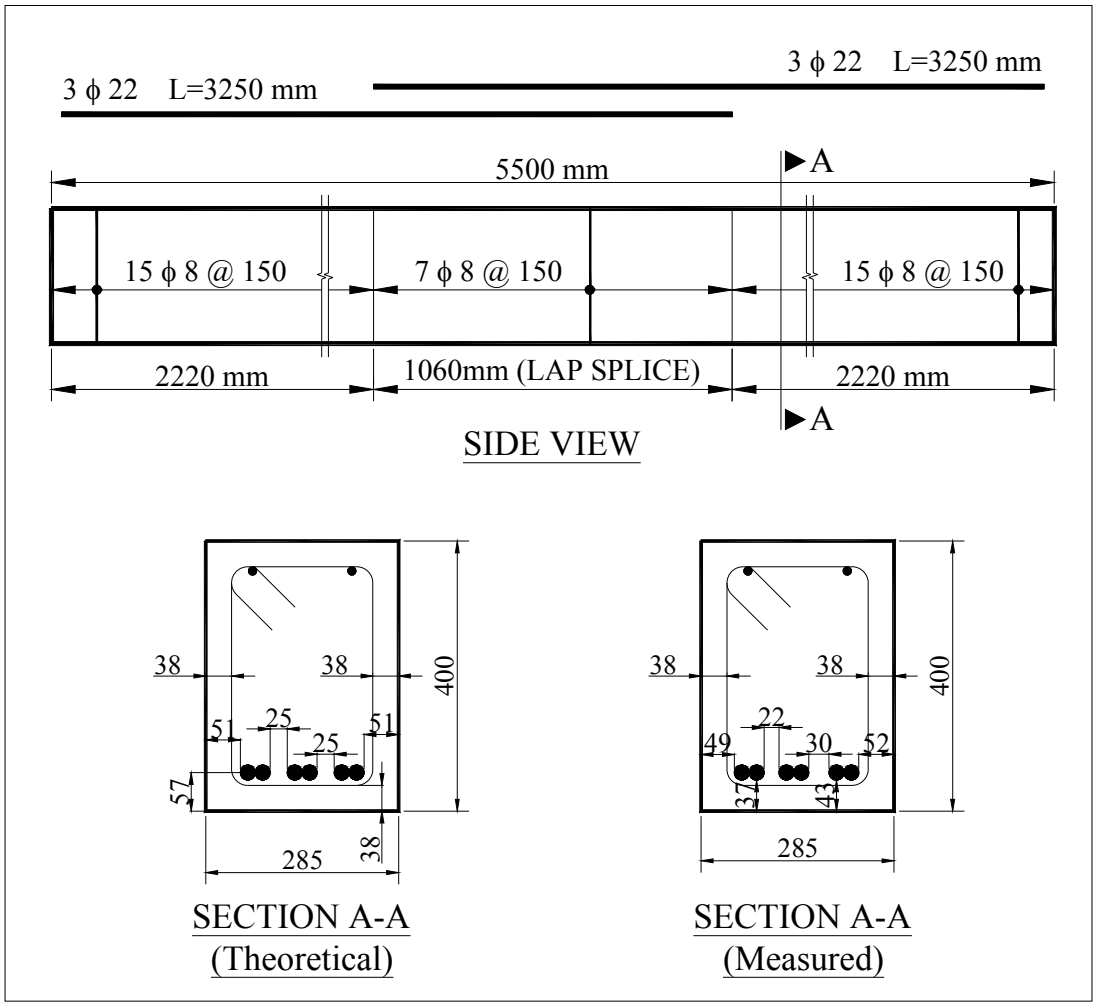

Figure 3.5 Details of Specimen ACI22.

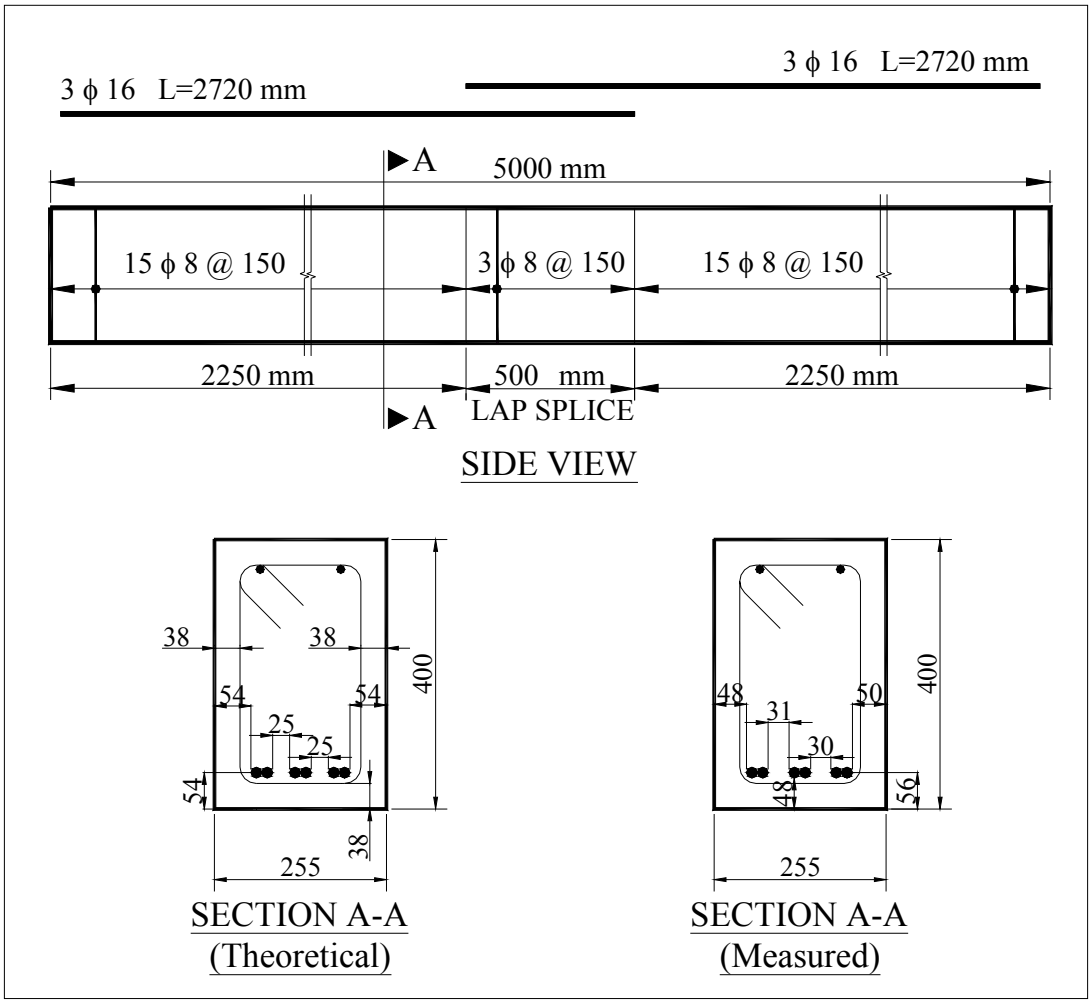

Figure 3.6 Details of Specimen ACI16.

3.3.5. Lap Splice Calculations and Spacing Requirements for TS – 500 Code.

The rules and specifications for anchorage and placement of reinforcement are defined in Chapter 9. This section covers both lap splice length, spacing and clear cover requirements.

3.3.5.1. Spacing and Clear Cover Requirements

In Chapter 9, Clause 9.5 defines the limitations for placement of reinforcing bars. According to the code, clear cover should be larger than or equal to 20 mm for interior columns and beams not exposed to earth.

The clear spacing of reinforcing bars at the same layer shall not be less than either the diameter of the reinforcing bar times 4/3 the nominal coarse aggregate size or 25mm. These limits are also applicable in locations where lap splices exist.

3.3.5.2. Lap Splice Requirements

In Chapter 9, clause 9.1.3 equation 3.2 defines the development length of tension reinforcement by means of straight embedment.

$$\ell_b = \left(0.12 \frac{f_{yd}}{f_{ctd}} \phi \right) \geq 20\phi \tag{3.2}$$

This development length should be increased by $100/(132-\phi)$ when the diameter of reinforcement is $32\,\text{mm} < \phi \leq 40\,\text{mm}$. When the concrete cover is less than the diameter of the reinforcing bars or the clear spacing between reinforcing bars in a layer is smaller than one and a half times the diameter of the reinforcing bars, the development lengths calculated by using Equation 3.2 should be multiplied by 1.2.

The reason of this multiplier also is to encourage designer to use greater clear cover lengths with the increasing of bar diameter. Therefore, all specimens prepared according to this requirement in order to use basic development length.

TS 500 also increase the development length according to placement of reinforcement during concrete casting. TS 500 defines two placement conditions. If the reinforcement is in the Case I condition, development length shall be increased by 1.4. These two casting conditions are as stated below.

- Case I: General Situation (All bars not in Case II).

- Case II: Reinforcing bars making an angle of 45^o-90^o with the horizontal during casting as well as reinforcing bars in the lower half of the section or at least 300 mm away from the upper face of the section which are horizontal or which make an angle less than 45^o with the horizontal.

In Clause 9.2.5, requirements for splices of reinforcing bars in tension are defined. According to Eq. 3.3 splice length is determined by multiplying development length calculated from Eq. 3.2 with α_1 factor.

$$\ell_o = \alpha_1 \ell_b$$
$$\alpha_1 = 1 + 0.5r \qquad (3.3)$$

Here "*r*" is the ratio of spliced reinforcement to total reinforcement at that section. For members where the whole section is in tension, α_1 is taken as 1.8.

Similar to ACI 318, the reason of α_1 multiplier is to encourage the designers to use staggered lap splice. Therefore, in the design of specimens α_1 is not considered.

In TS 500, there is a minimum transverse reinforcement requirement for lap splices. According to Clause 9.2.5, confining reinforcement along lap splice should have a

minimum diameter of 1/3 of diameter of lap spliced bar and should not be less than 8 mm. At least six hoops should be present along the splice length. The spacing of the confinement reinforcement cannot be more than either ¼ of the member depth or 200 mm.

Detailed calculations for lap splice lengths, spacing and clear covers are shown in Appendix A. Table 3.8 lists the required lap splice length for TS16, TS22 and TS26. Figures 3.7, 3.8 and 3.9 show the details of specimens TS26, TSI22 and TS16, respectively.

Table 3.7 Lap Splice, spacing and cover dimensions for TS specimens.

Specimen Name	c_{so} **(mm)**	$2c_{si}$ **(mm)**	c_{bb} **(mm)**	**Lap Splice Length (mm)**	**Lap Splice Length (In terms of d_b)**
TS16	20.0	25.0	20.0	550	34 d_b
TS22	22.0	33.0	22.0	750	34 d_b
TS26	26.0	39.0	26.0	890	34 d_b

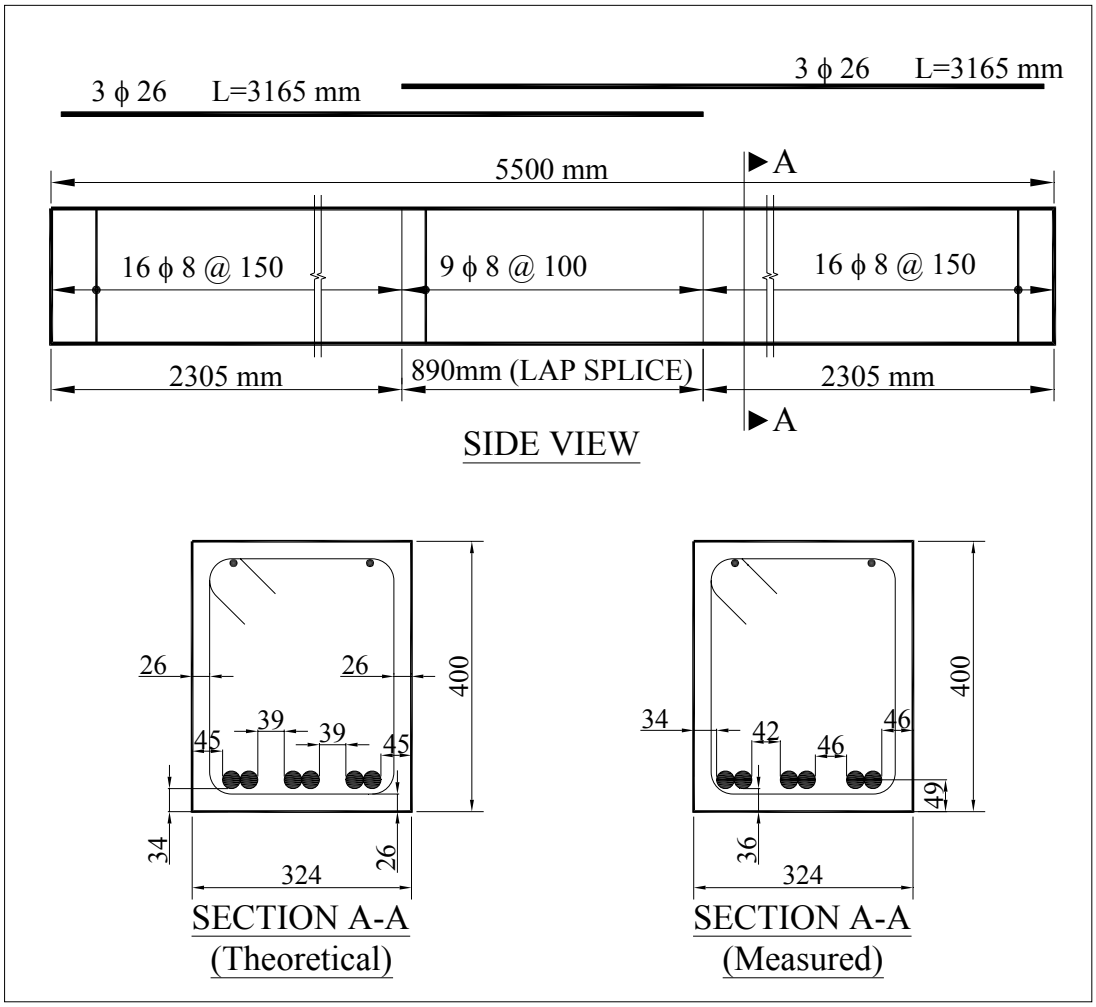

Figure 3.7 Details of Specimen TS26.

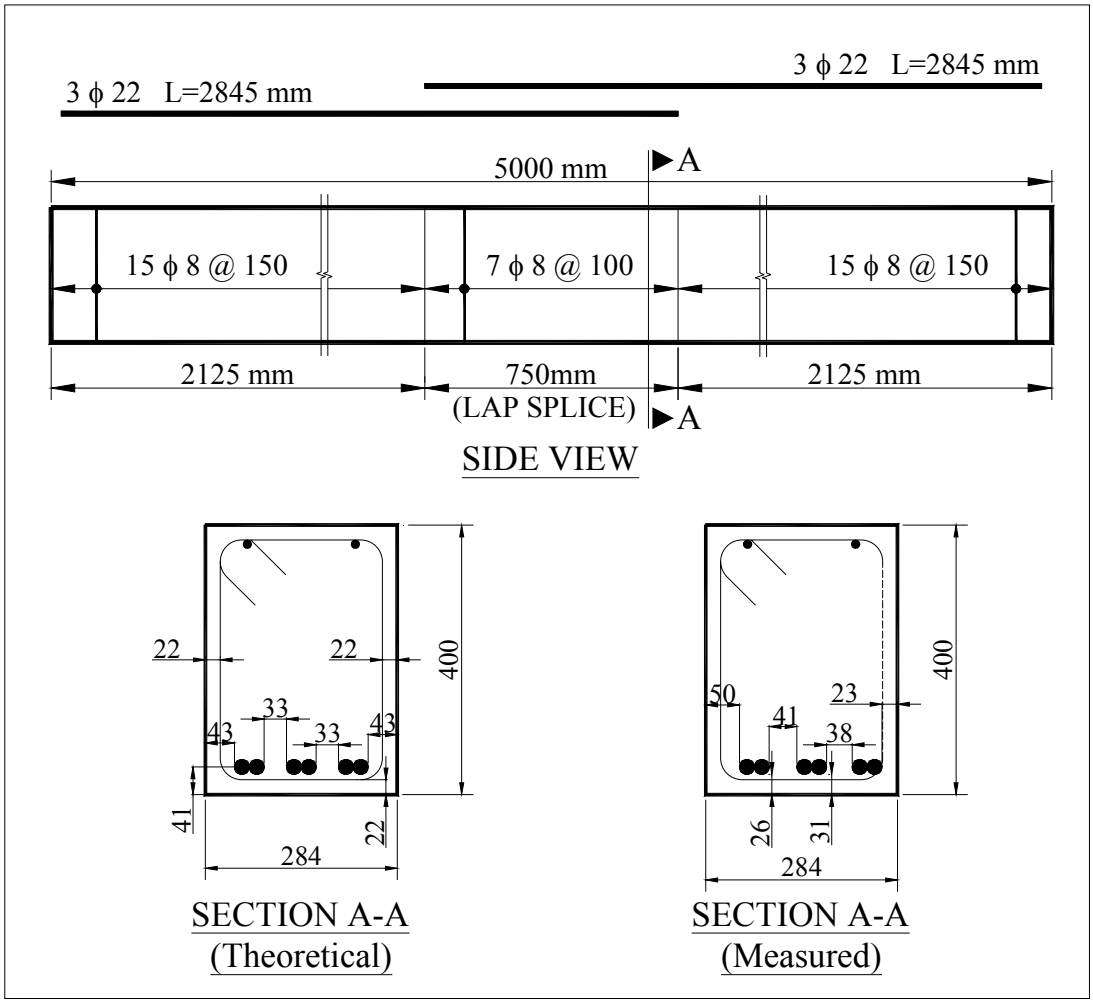

Figure 3.8 Details of Specimen TS22.

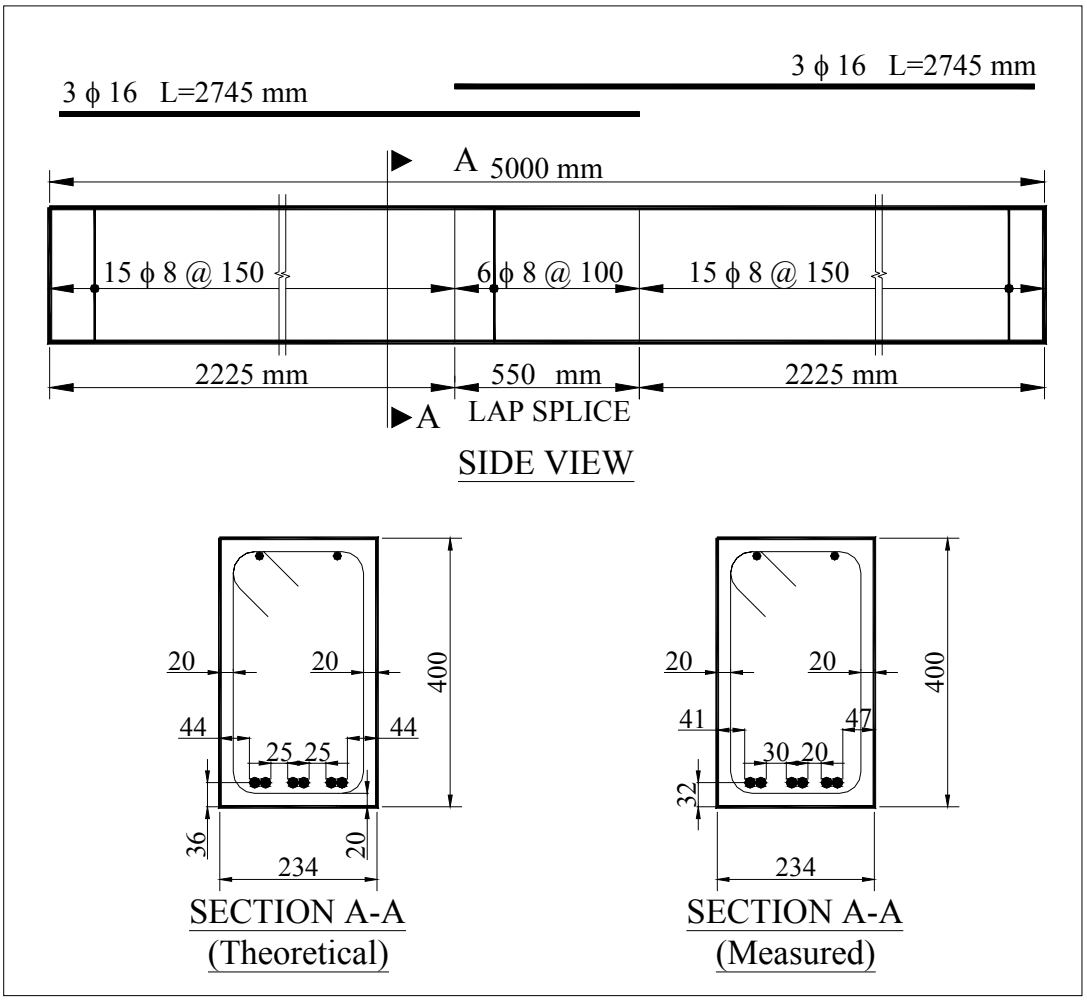

Figure 3.9 Details of Specimen TS16.

3.4. Test Setup and Loading

Specimens were tested in a loading frame which was already located in the Structural mechanics Laboratory of METU.

Two concrete blocks were put on the strong floor 1.20 m. apart from the mid point of beam's left and right sides. On these blocks two steel supports were placed. One of these supports was roller and the other one was rectangular. These supports were chosen to simulate simple and roller type of support. Loading of specimens was done by using two hydraulic rams. Hydraulic rams had 200 mm stroke capacity which was adequate to load the specimens until they were reached their ultimate capacity and failure limits. Hydraulic rams were fixed to test frame by using anchoring bolts. Two steel plates were used to fix the bolts through the screws. Between steel plates a hinge was located to let the hydraulic ram and its stroke rotate freely. Between the beam's upper surface and stroke of the hydraulic ram, load cell and rollers were placed. A rotationally free system was constructed by locating both hinge and roller.

The test setup was reconstructed separately twice because there were two different specimen lengths. Figure 3.10 shows the setup for 5.50 m long specimens which were TS26, ACI26, ACI22 and Fig 3.11 shows the setup for 5.00 m long specimens which were TS22, TS16, ACI16. The only difference between these two setups was the distance between the concrete blocks.

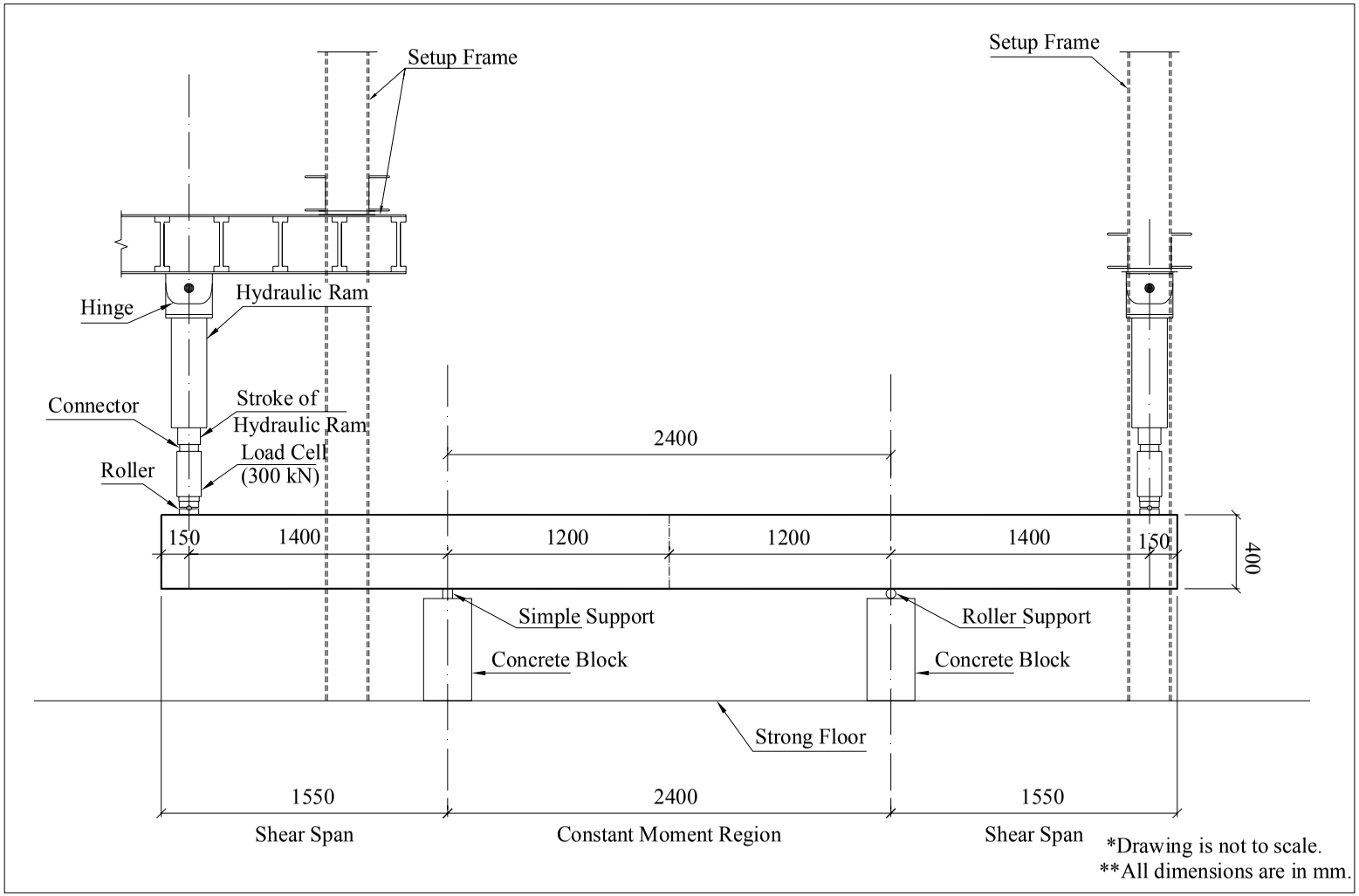

Figure 3.10 Test setup for Specimens TS-26, ACI-26 and ACI22

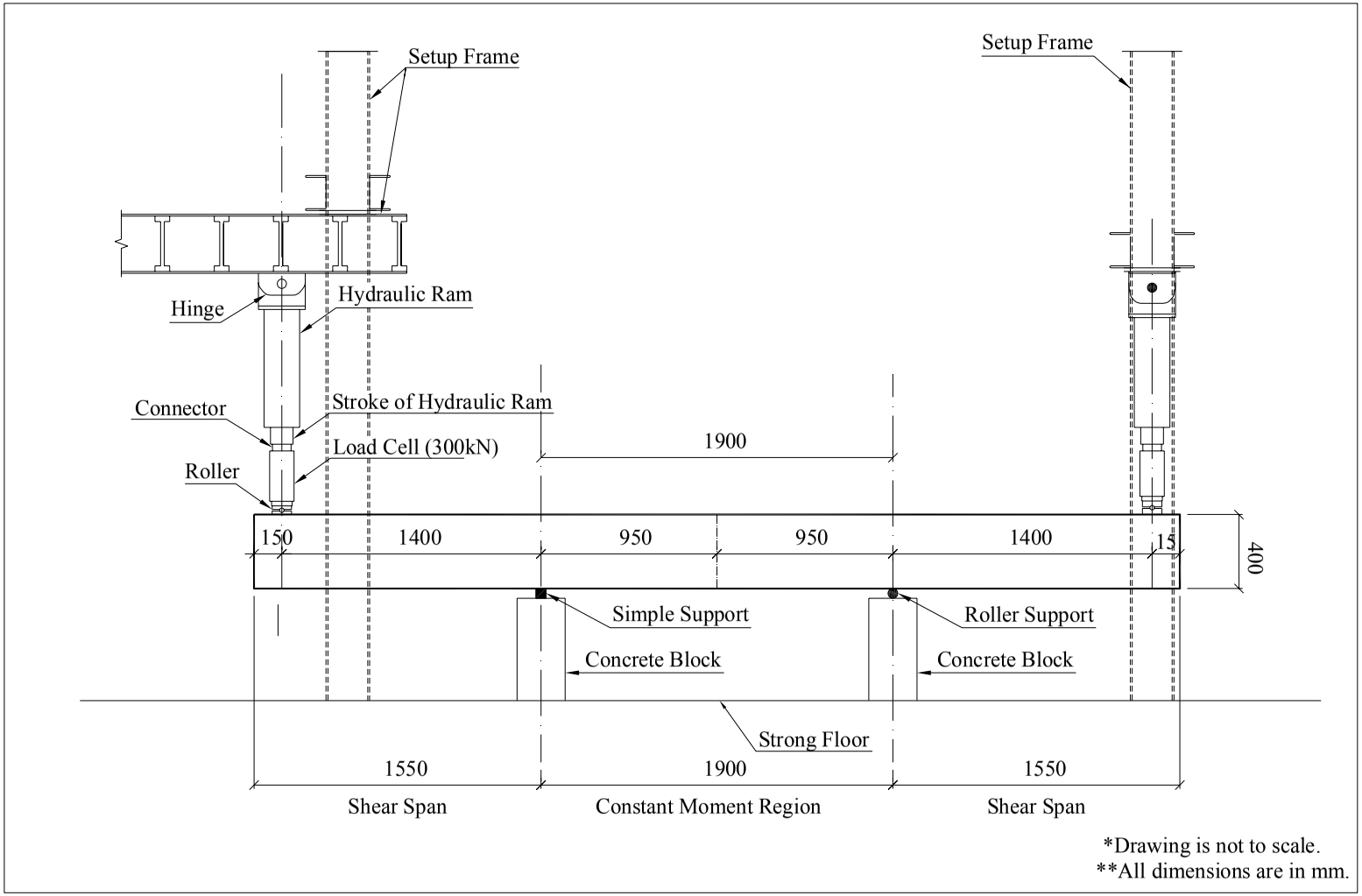

Figure 3.11 Test setup for Specimens TS16, ACI16 and TSI22

3.5. Instrumentation

3.5.1. General

Linear Variable Differential Transformers (LVDTs) and dial gauges were used for displacement measurements of specimen and dial gauges were also used to determine slip displacement of the longitudinal reinforcement. Two load cells were used for load measurements. For the strain measurement of longitudinal bars and transverse reinforcement totally 12 strain gauges were used.

Voltage outputs from the LVDTs, dial gauges and strain gauges were gathered by data acquisition system using a software, which was written by the supplier of the data acquisition system and installed on a personal computer. These voltage outputs were stored as engineering units like strains, displacements and loads by means of this software and data acquisition system. Also load – displacement curve of the specimens were followed by means of graphic display property of the software.

3.5.2. Displacement Measurement

Displacement measurements were taken from the following points of the specimens.

- Vertical tip displacements were monitored at the both ends of specimen where load was exerted. At these points two LVDTs were located. Heavy concrete blocks with steel rods were used to fix the LVDTs to the strong floor. The brand of LVDTs was Kyowa and they had stroke capacity of 100 mm. This capacity was adequate for yield and ultimate capacities of the specimens.

- The mid-span deflection is the most important measurement of the test. Therefore, the measurement was taken with a backup system. Vertical mid span

displacement of the specimens were monitored by one LVDT and one dial gauge with a stroke capacities of 100 mm and 50 mm respectively.

- Support displacement was also monitored in order to examine the vertical settlement of the specimen at the location of the supports. Theoretically it had to be zero but during experiments there was a little vertical displacement due to the support settlement. Two dial gauges which had a 20 mm of stroke capacity were located at the supports. They were fixed to strong floor by means of heavy steel sections and they were come to same level with specimen by means of stiff timber section attached to these heavy sections.

- Slip displacement of longitudinal bars were monitored also by using dial gauges with stroke capacities of 10 mm. This type of dial gauges were selected because slip displacement was less than the other displacements and also setup of this dial gauges on the top of the beam surface with limited area was somewhat harder than the other gages. In order to monitor slip displacement M5 bolts were welded at the free end of the lap splice of two longitudinal reinforcing bars. One of these bars was the edge bar and the other one was the middle bar. Before casting of concrete, M5 bolts were wrapped with tapes in order to prevent the concrete to fill into the bolt. A piece of styrofoam was also attached to bar ends where M5 bolts were welded. The styrofoam was extended up to the surface of the beam. Prior to test, the stryfoam was removed and a small free space was achieved nearby the end of the lap spliced bar. A steel bar was screwed to the bolt which was welded at the end of the bar. Dial gauges were fixed to the concrete surface and their ends are connected with thin wires to this steel bar.

The locations of displacement transducers are shown in Figure 3.12. Also detailed view for slip measurement is shown in Figure 3.13.

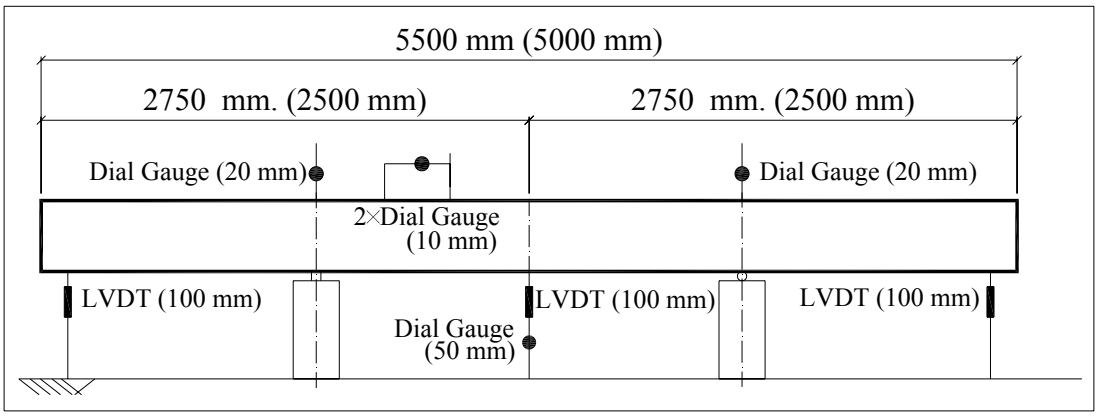

Figure 3.12 Schematic view of instrumentation.

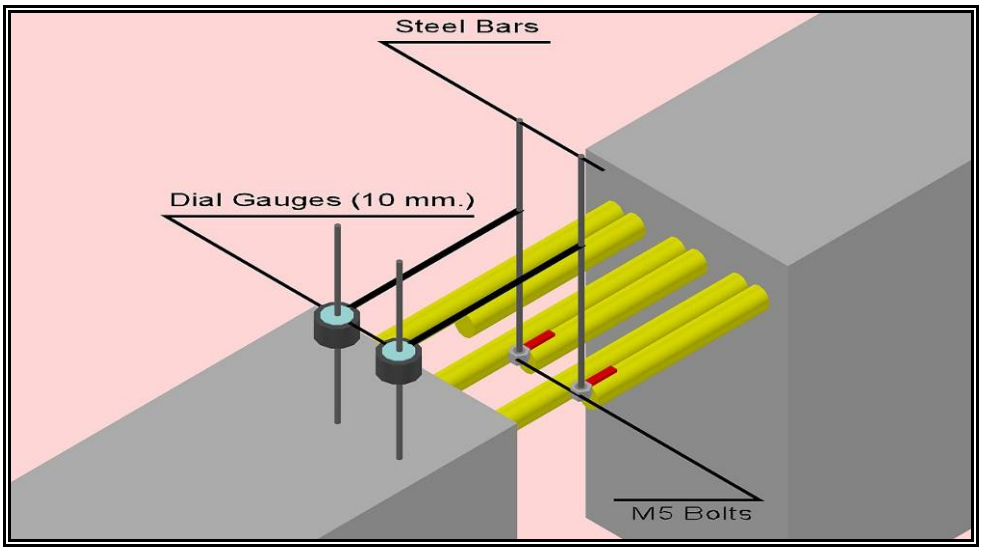

Figure 3.13 Detailed view for slip measurement.

3.5.3. Load Measurement

Specimens were loaded at the ends of the specimen by means of hydraulic rams. Two concrete blocks were used as supports to create a constant moment region and lap splice for all specimens was located in this constant moment region. Between the hydraulic rams and specimen surface as defined previously two load cells were located. These load cells had compressive and tensile capacities of 300 kN. During

the tests, reversed cyclic loads were not considered because the main objective was to investigate the behavior of lap splice under static loading only. Since the maximum load for all specimens was around 150 kN, load cell capacity was enough and load cells were safe enough against yielding. The load cells were calibrated both in structural mechanics laboratory and materials of construction laboratory. Figure 3.14 shows the installed load cell.

Figure 3.14 Load cell used in tests.

3.5.4. Strain Measurement

Strain measurements were done by using Kyowa strain gauges with the resistance of 350Ω and 120Ω. 350Ω strain gauges were used in longitudinal bars and the 120Ω strain gauges were used to monitor strains in stirrups.

350Ω strain gauges were located along the lap splice. There were six strain gauges on two longitudinal bars. These were located at the middle of and at the two ends of the lap splice. Figure 3.15 shows detailed view of 350Ω strain gauges.

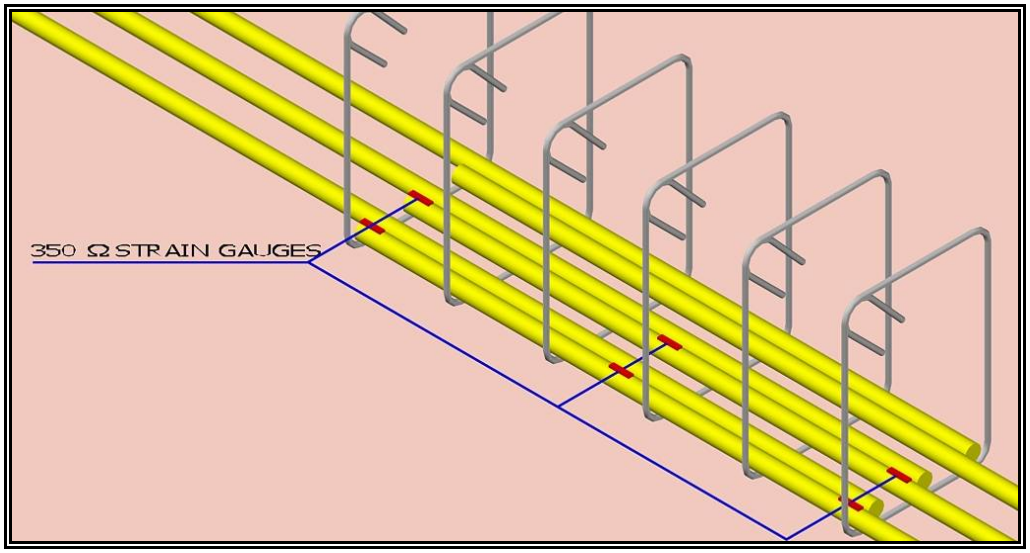

Figure 3.15 Detailed view for location of 350Ω strain gauges.

At both ends of the lap splice it is known that bond stress is maximum and it decreases towards the middle parts of the lap splice. Therefore, it should be expected that at the free end of the rebar steel strains must be zero and at the continuous end of the lap splice rebar strains must be maximum. Since the entire length of lap splice is under the action of same moment, if splitting failure does not occur for the specimen, reinforcement must yield at the continuous end of the lap splice.

120 Ω strain gauges were located on three stirrups along the lap splice. One of these stirrups was the nearest one to the middle of lap splice, second one was the nearest one to end of lap splice and the third one was the center of the first two. Each stirrup had two strain gauges and one of them was located near to the corner of the stirrup at the bottom leg. The other one was located at the middle of the bottom leg. Fig 3.16 shows detailed view for 120Ω strain gauges.

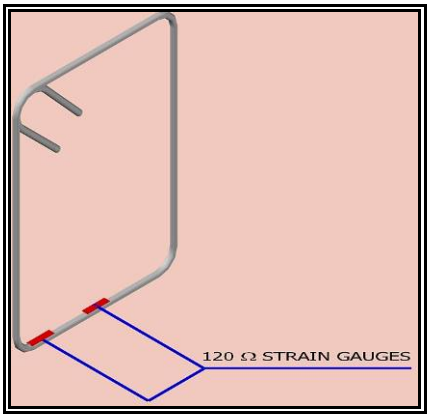

Figure 3.16 Detailed view for location of 120Ω strain gauges.

CHAPTER 4

OBSERVED BEHAVIOUR OF TEST SPECIMENS

4.1. General

In this chapter observed behavior of the beam specimens will be presented. For all specimens displacement and strain measurements were taken simultaneously while applying the load. They are presented in a graphical manner as Load vs. Displacement and Load vs. Strain curves.

4.2. Information of Graphs

For all specimens 9 graphs were drawn according the acquired data during tests except for ACI22. Because of an unexpected failure of the data acquisition system, strain values could not be recorded in this test. All graphs are described below one by one with illustrative figures.

4.2.1. Deflection, Support Settlement and Slip Graphs

Deflection charts were plotted for middle deflection and tip deflection. The instrumentation is shown schematically in Figure. 4.1.

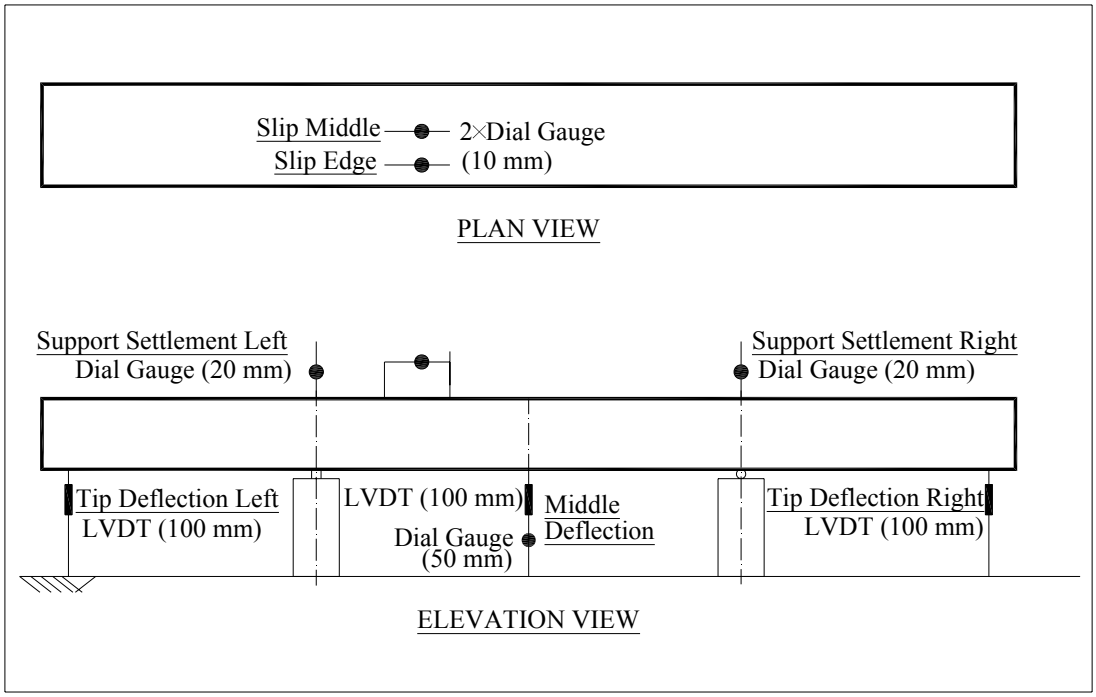

Figure 4.1 Pairs for instrumentation and Graphs.

Since the left and right load cell readings are close to each other as expected, the average of these two readings are used in the load axis of all graphs.

- Tip deflection chart was drawn according to data gathered from LVDTs located at both left and right end of the beam and average load cell readings.

- Middle deflection chart was drawn according to data acquired from Dial Gauge and LVDT located at the middle of the beam.

- The dial gage for the slip measurement was located as close as possible to the end of the spliced bar. However, the distance between the dial gage and the bar end was approximately 100 mm. The displacement recorded from this gage involves not only the slip of the bar but also all cracks formed between the gage and end of bar. Therefore, it is decided not to give slip measurements.

- Support settlement chart was drawn according to data gathered from 20 mm Dial Gauges located at the left and right supports of the beam both left and right side.

4.2.2. Strain Graphs

Strain graphs were plotted for both longitudinal reinforcing bars and stirrups. All strain gauges are numbered from 1 to 12. Locations for these strain gauges can be followed from the Figure 4.2. The resistances of the strain gages from 1 to 6 on the longitudinal bars are 350Ω, and from 7 to 12 on the transverse reinforcement are 120Ω.

Strain gauges 1 and 4 are located at free end of the lap splice. No.1 is located at edge and No.4 is located at the middle longitudinal bar. Expected strain values are in vicinity of zero for these strain gages. Strain gauges 2 and 5 are located at the middle of lap splice No.2 is located at edge and No.5 is located at middle. Expected strain values are larger than zero. Strain gauges 3 and 6 are located at the continuous end of lap splice. No.3 is located at edge and No.5 is located at middle. Maximum strain values are expected at these locations.

Strain gauges 7 and 8 are located on stirrup which is the nearest one to the free end of the lap splice. No.7 is located at the middle and No.8 is located at the corner. Maximum strain values are expected for them. Strain gauges 12 and 11 are located on stirrup close to the middle of lap splice. No.12 is located at middle and No.11 is located at corner of the stirrup. Minimum strain values are expected there. Strain gauges 9 and 10 are located on the halfway of end and center line of lap splice. No.9 is located at middle and No.10 is located at corner. Expected strain values are smaller than the values for No.7 and No.8 and larger than the values for No.12 and No.11.

For each test, the locations of all strain gages are given in a separate figure.

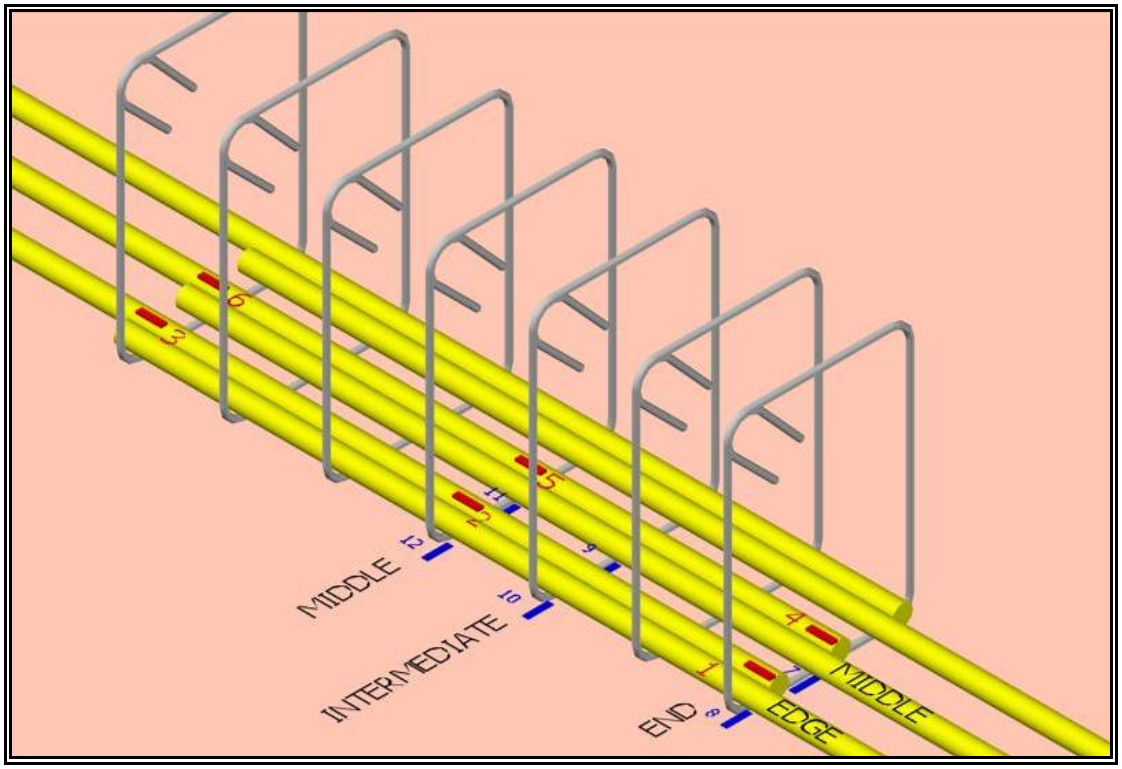

Figure 4.2 Strain gauges numbers and their locations.

4.3. Observed Behavior of Specimens

In this section previously mentioned graphs are drawn according to the raw data for each specimen and the observed behavior of specimens during test is discussed. Also crack pattern of each beam specimen is shown. In the crack pattern figures, the middle strip shows the top face. The top and bottom strips show the side faces crack patterns.

In all specimens, the first cracks are initiated at the end of the lap splices. The bar ends cause discontinuity at those locations and result in cracks. A void was left on concrete at the end of the lap spliced bar in order to measure the slip displacement. This space, however, weakens the cross-section and may cause the first crack to initiate at this location. Moreover, the largest crack width at the end of each test was reached again at these locations.

4.3.1. Specimen: TS26

TS26 beam failed prior to its flexural capacity. The expected yield load was 169 kN. However, beam specimen reached its ultimate load at 140 kN. Failure was brittle and sudden. Failure type was both side and face splitting. Figure 4.3 and 4.4 shows as built strain gauge configuration and crack pattern at the end of the test, respectively.

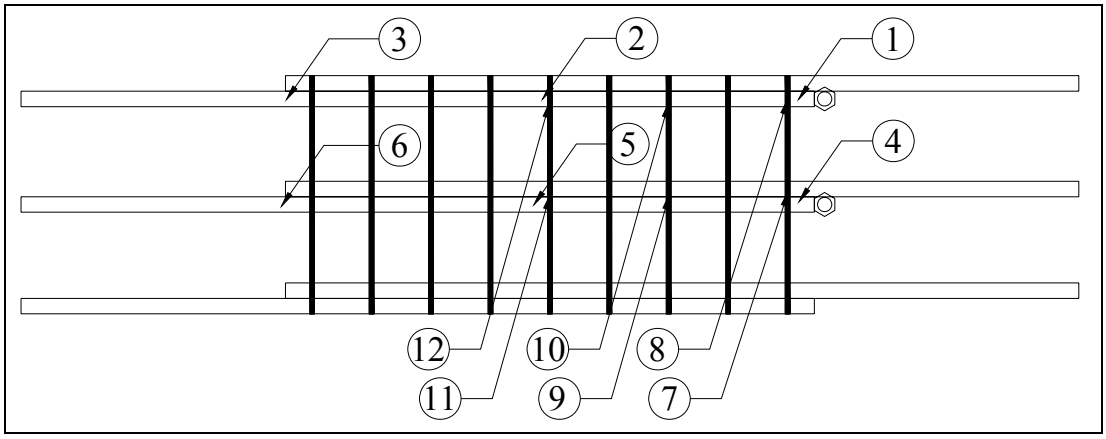

Figure 4.3 Strain gauges numbers and their locations for specimen TS26.

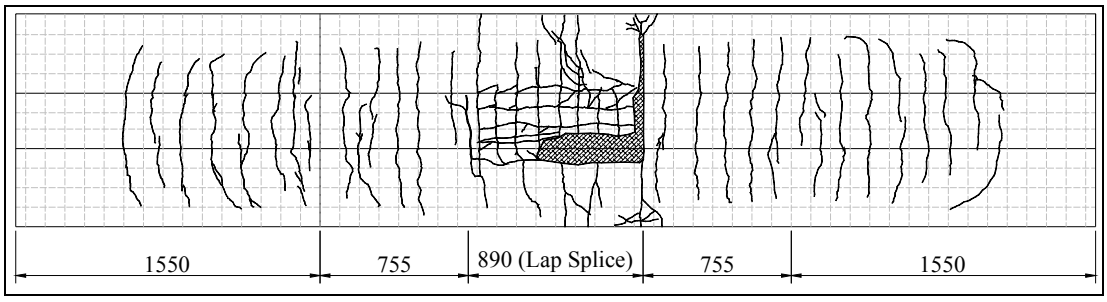

Figure 4.4 Crack pattern for specimen TS26.

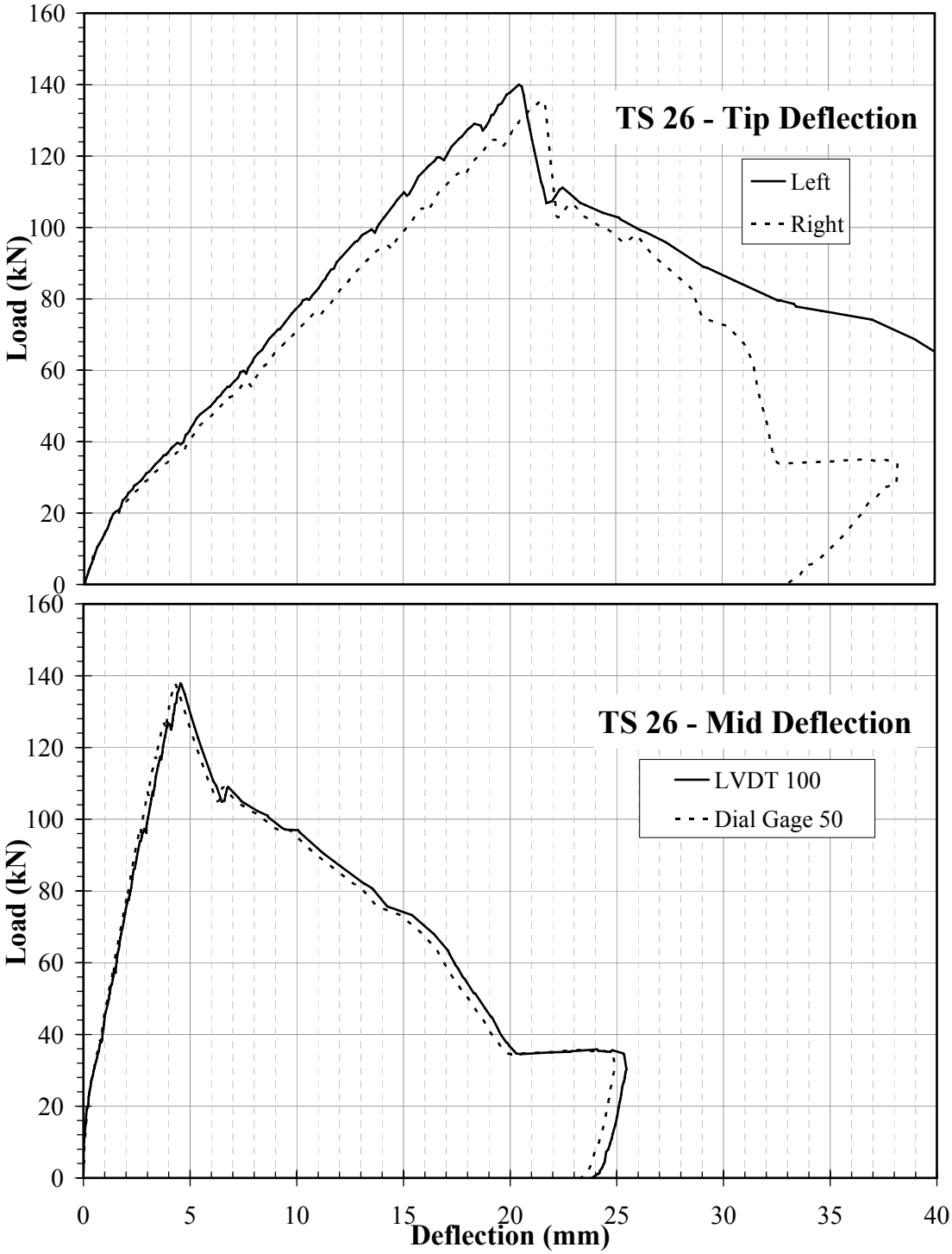

Figure 4.5 TS26 Load vs. Deflection Charts.

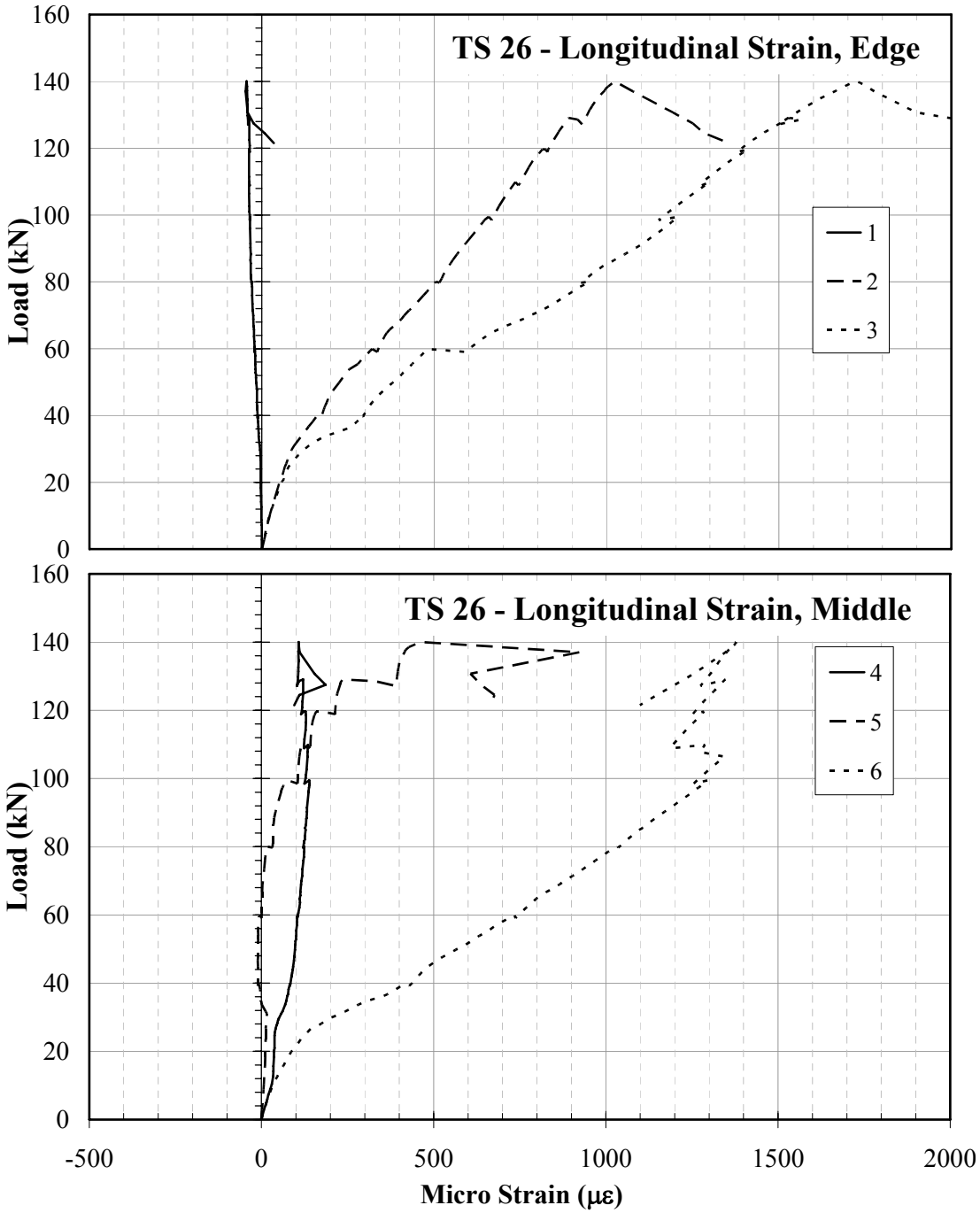

Figure 4.6 TS26 Load vs. Longitudinal Strain Charts.

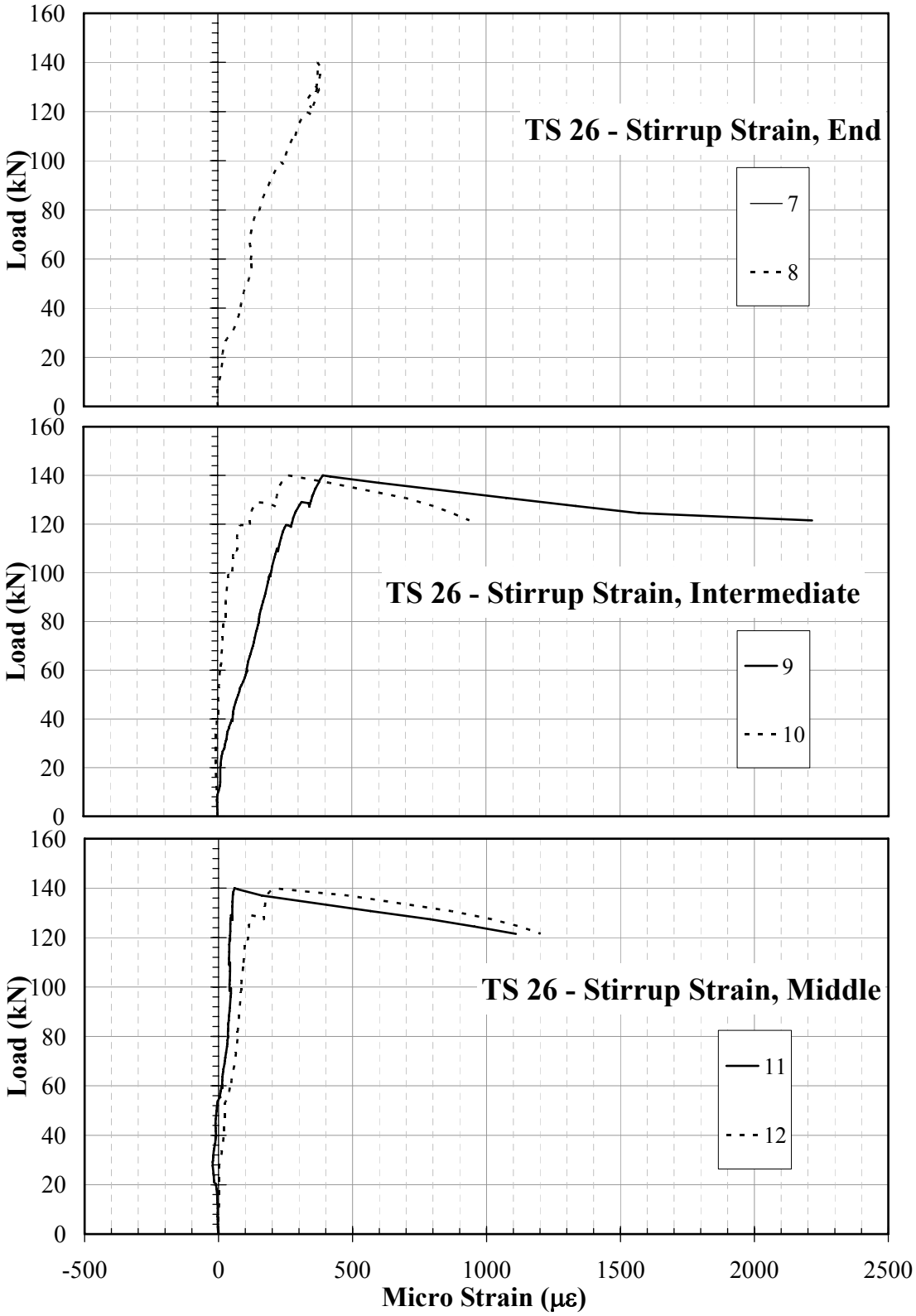

Figure 4.7 TS26 Load vs. Stirrup Strain Charts.

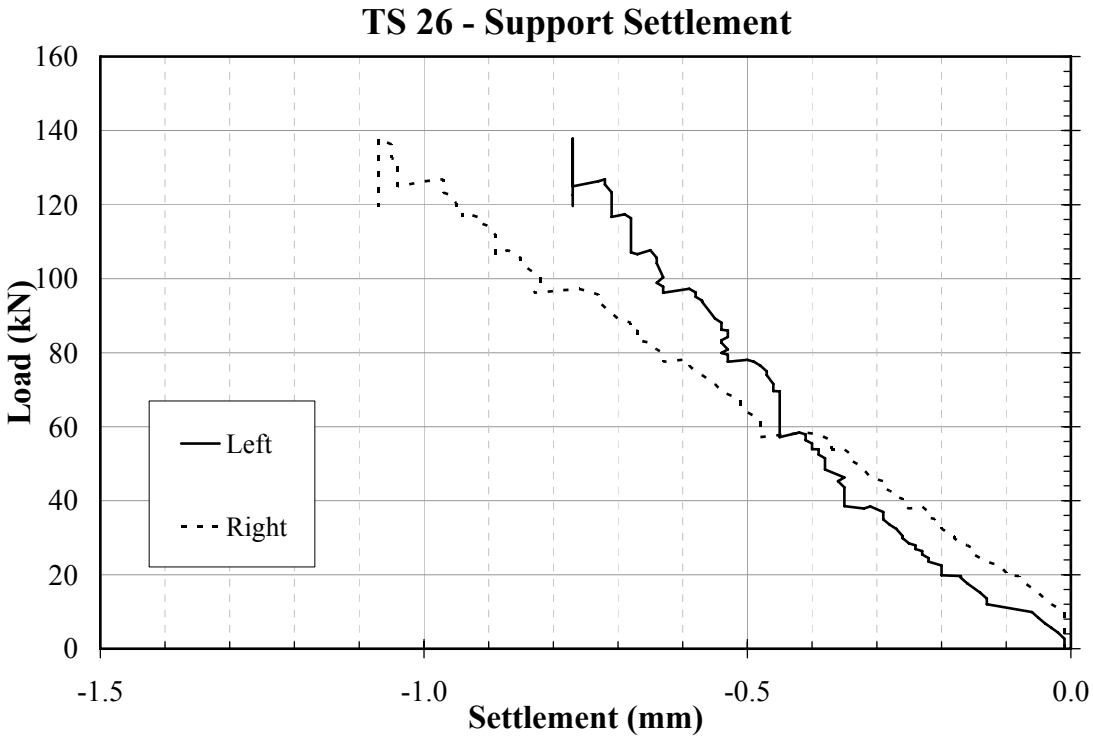

Figure 4.8 TS26 Load vs. Support Settlement.

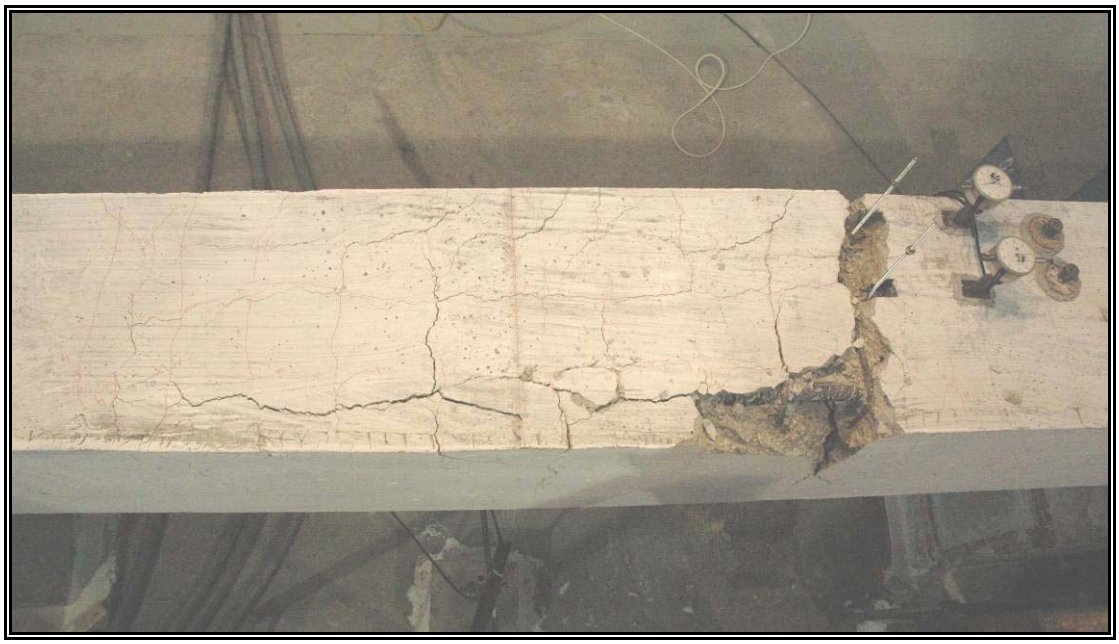

Figure 4.9 TS26 splice region after test.

4.3.2. Specimen: TS22

TS22 beam was failed by reaching its flexural capacity. The theoretical yield value was calculated as 124 kN. The specimen was yielded at 120 kN while observing some longitudinal cracks on the both upper and side faces of specimen at the zone of lap splice. Figure 4.10 and 4.11 shows as built strain gauge configuration and crack pattern at the end of the test, respectively.

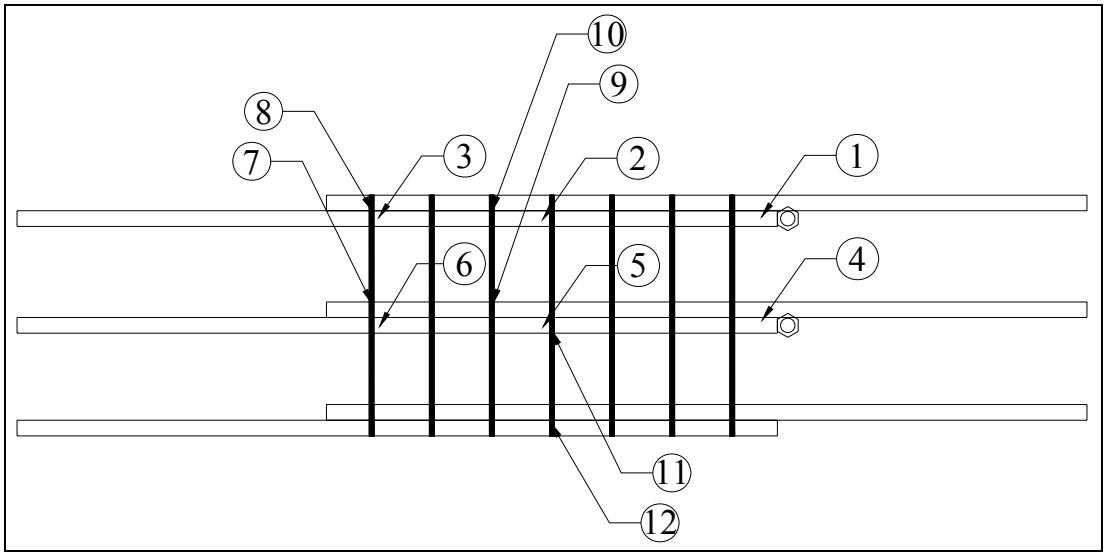

Figure 4.10 Strain gauges numbers and their locations for specimen TS22.

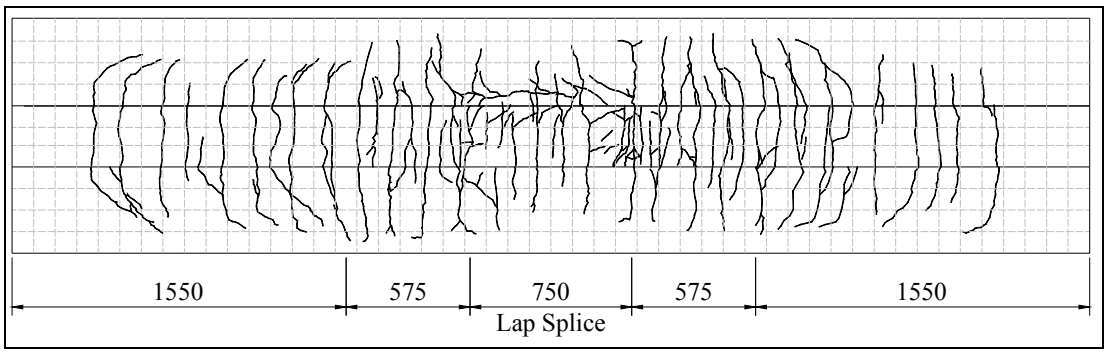

Figure 4.11 Crack pattern for specimen TS22.

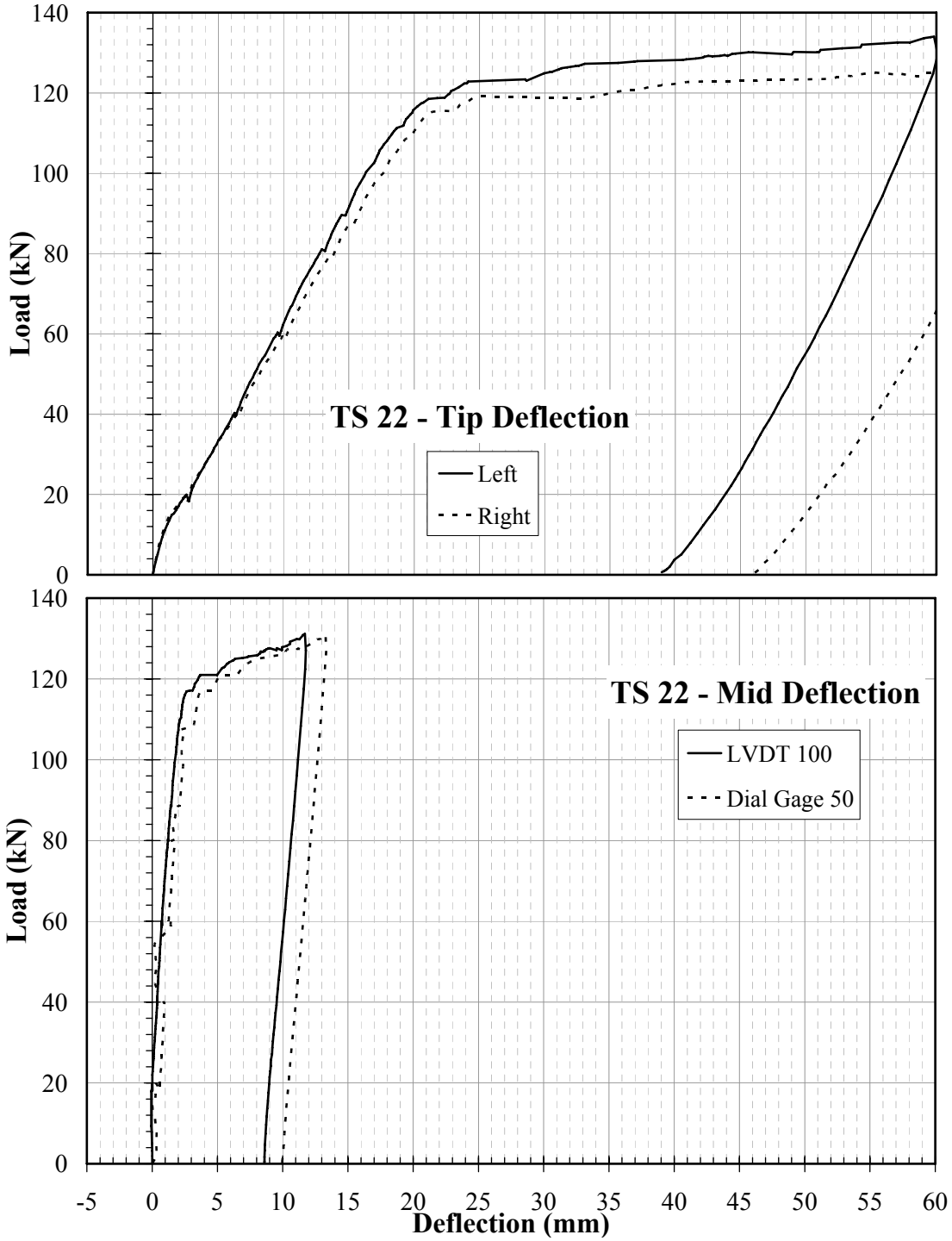

Figure 4.12 TS22 Load vs. Deflection Charts.

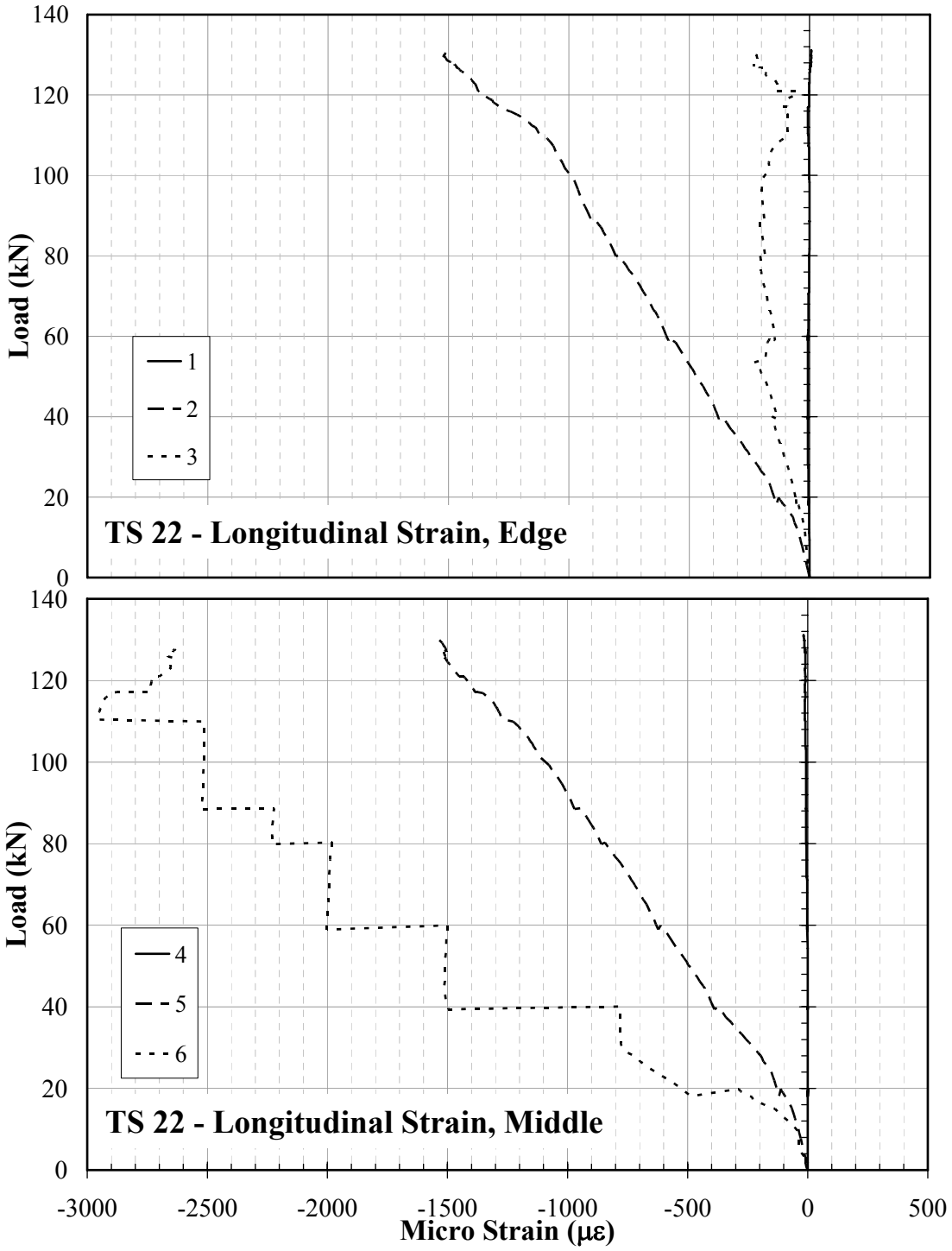

Figure 4.13 TS22 Load vs. Longitudinal Strain Charts.

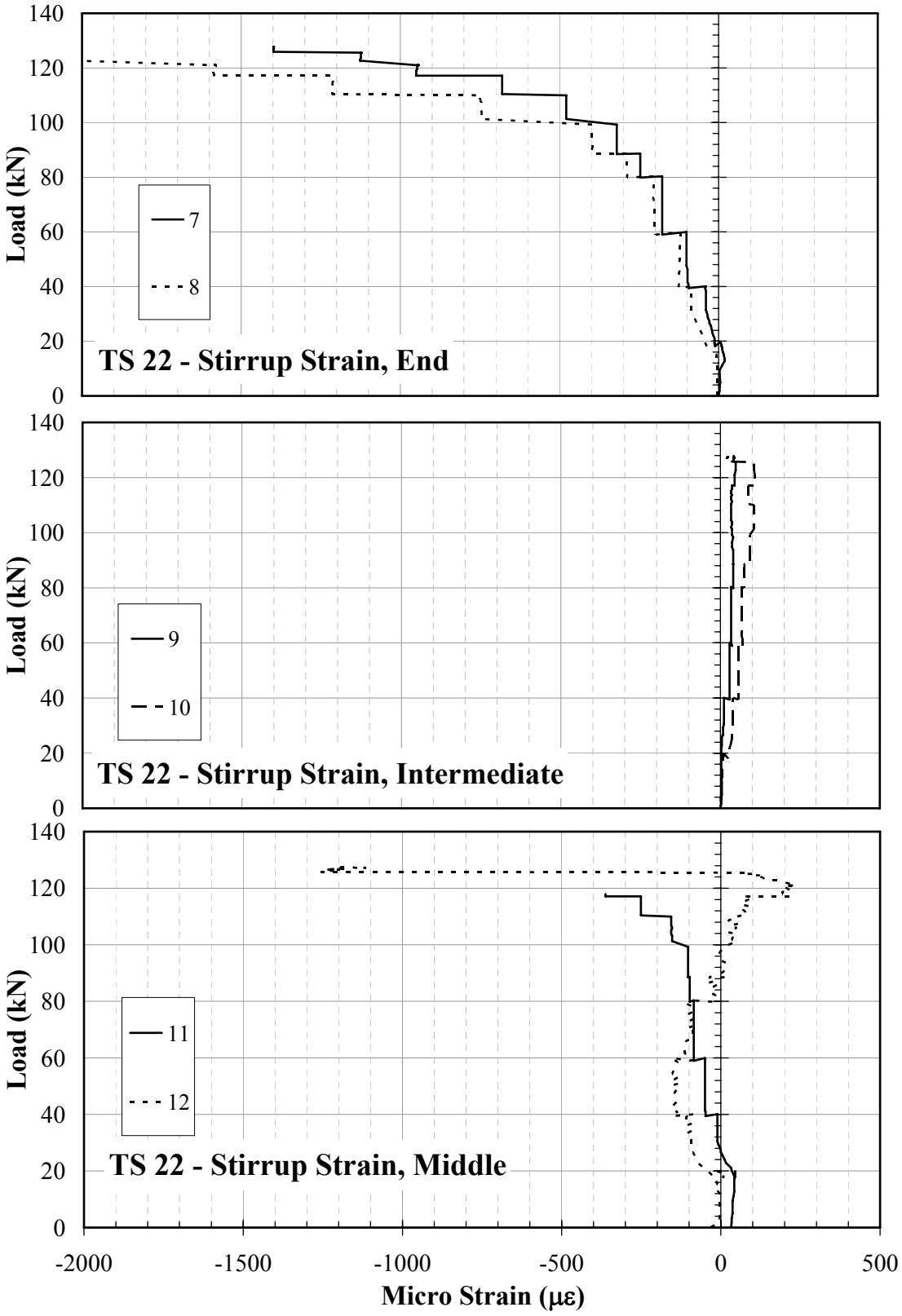

Figure 4.14 TS22 Load vs. Stirrup Strain Charts.

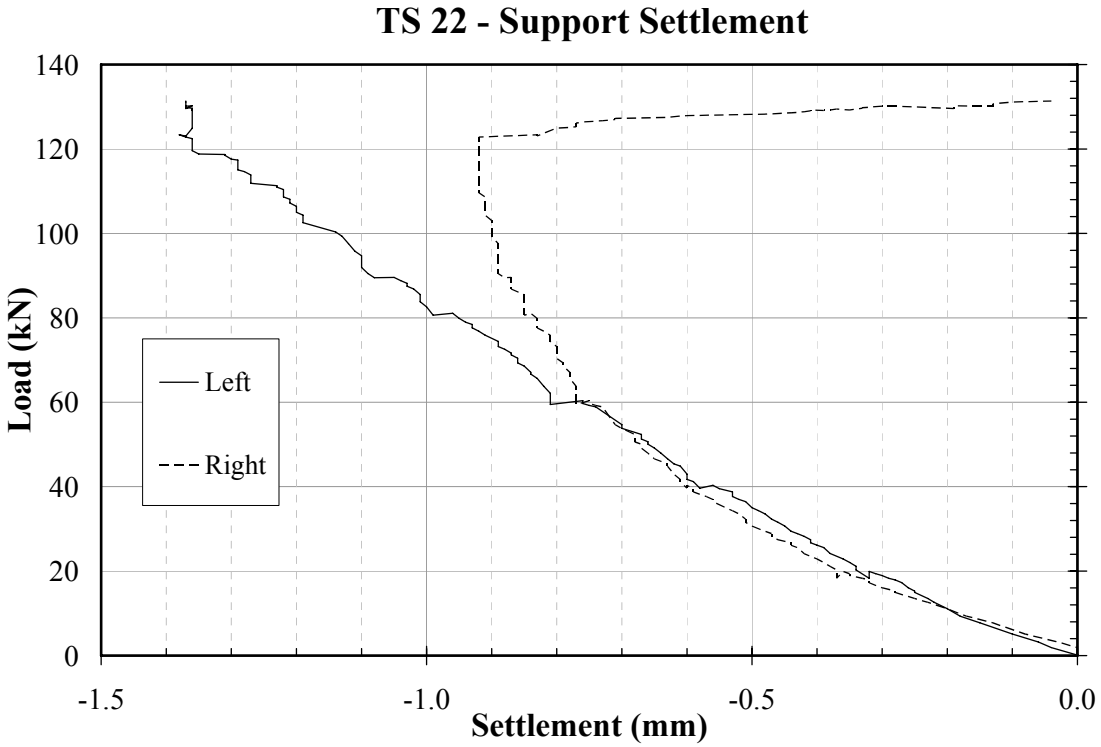

Figure 4.15 TS22 Load vs. Support Settlement.

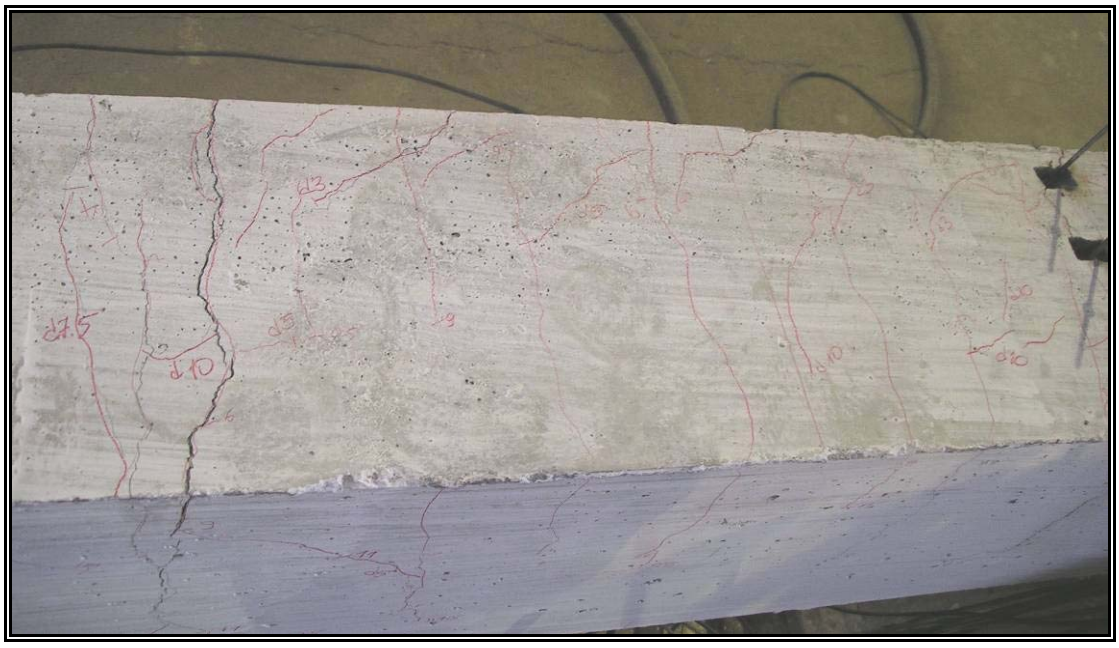

Figure 4.16 TS22 splice region after test.

4.3.3. Specimen: TS16

TS16 beam was failed by reaching its flexural capacity. The theoretical yield value was calculated as 64 kN. Beam was yielded at 60 kN. There were some longitudinal cracks only on the upper face of specimen at the zone of lap splice. Figure 4.17 and 4.18 shows as built strain gauge configuration and crack pattern at the end of the test respectively.

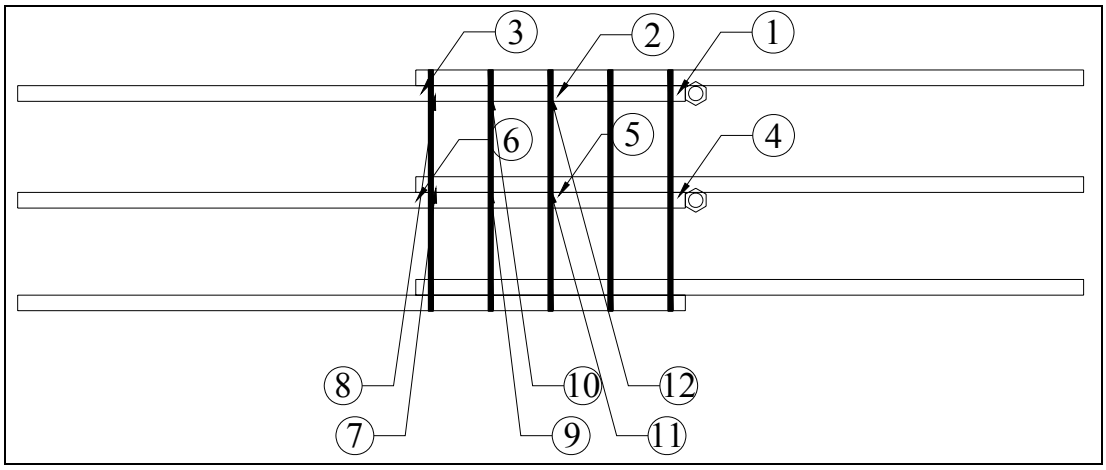

Figure 4.17 Strain gauges numbers and their locations for specimen TS16.

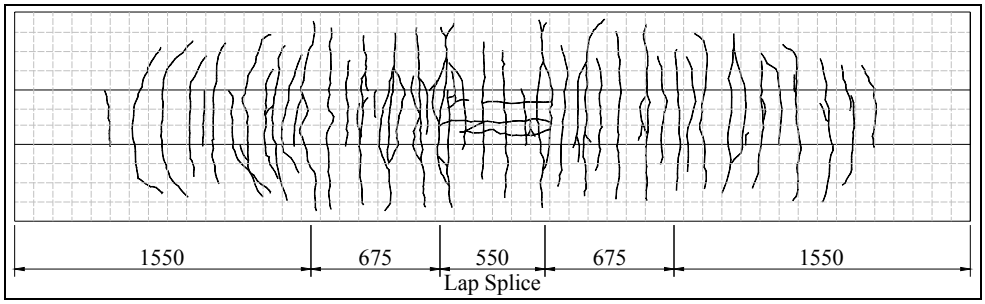

Figure 4.18 Crack pattern for specimen TS16.

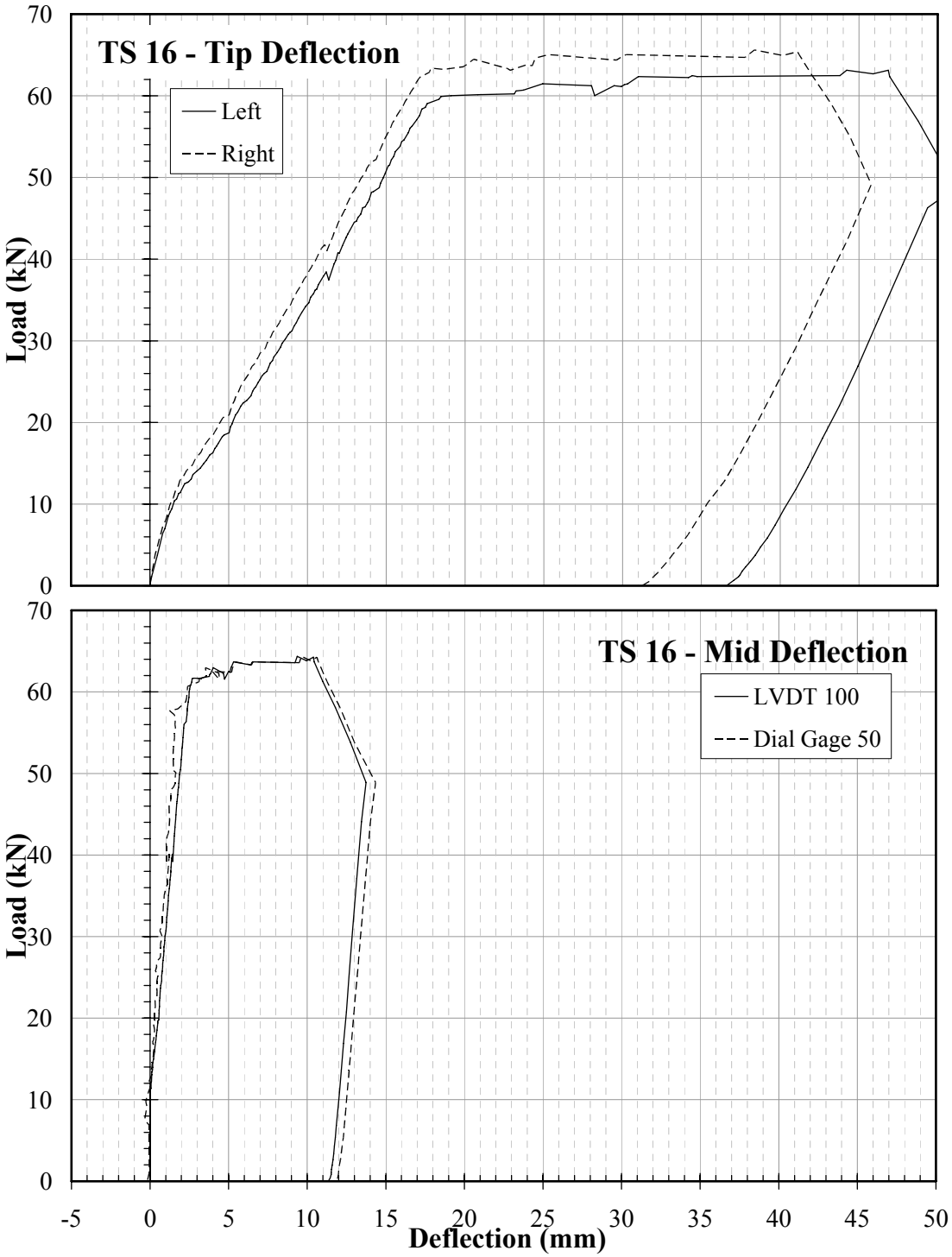

Figure 4.19 TS16 Load vs. Deflection Charts.

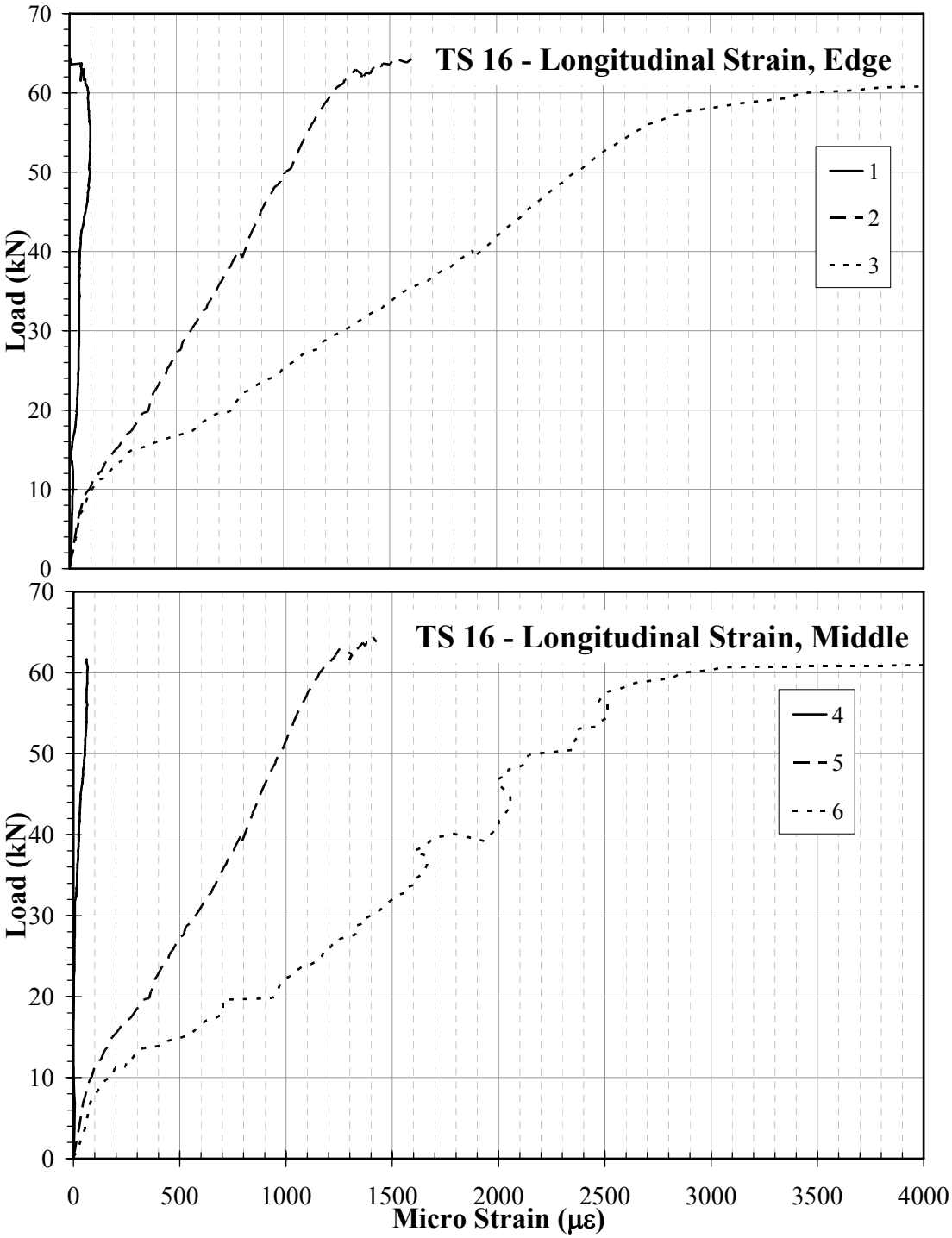

Figure 4.20 TS16 Load vs. Longitudinal Strain Charts.

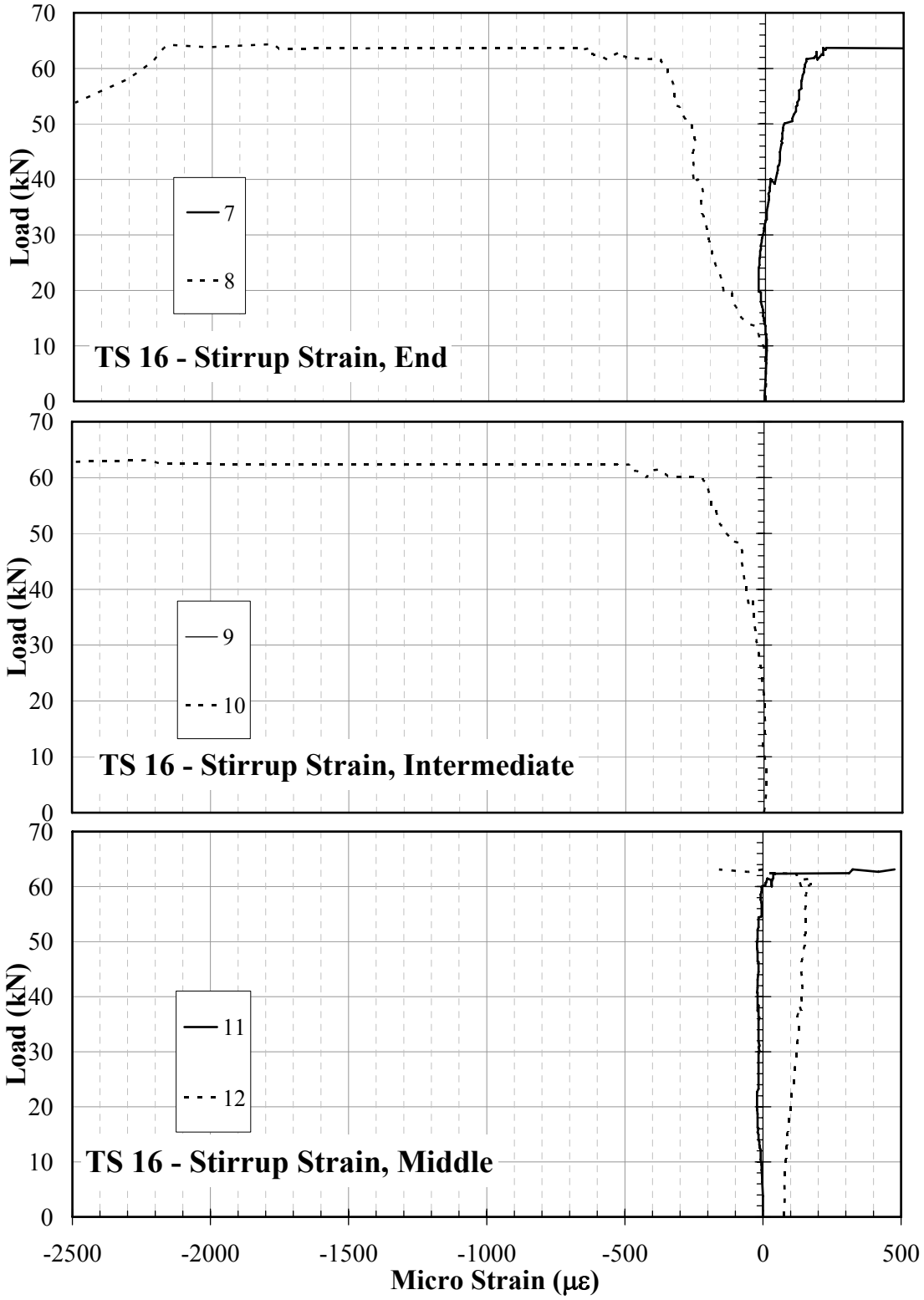

Figure 4.21 TS16 Load vs. Stirrup Strain Charts.

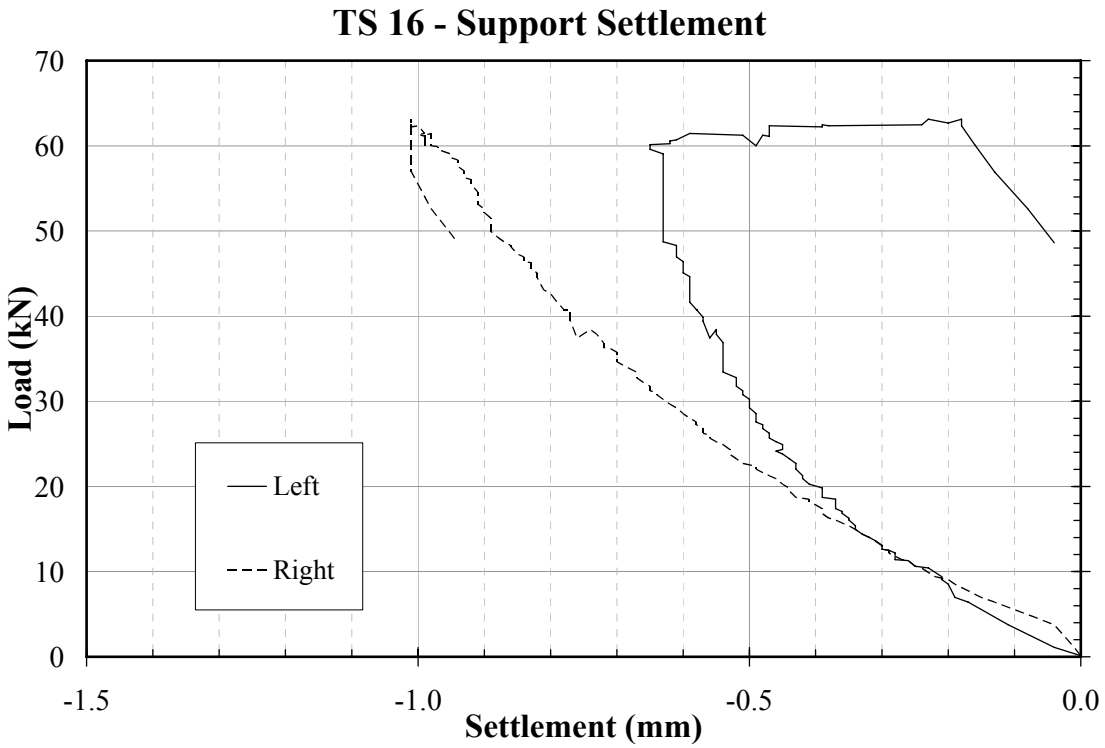

Figure 4.22 TS16 Load vs. Support Settlement.

Figure 4.23 TS16 splice region after test.

4.3.4. Specimen: ACI26

ACI26 specimen was loaded two times, because the rotation capacity of rollers in the first test set-up was not adequate. It was observed that continuing the test would cause safety problems. After increasing rotational capacities of the rollers, specimen was loaded again. L1 code refers to first loading and L2 code refers for second loading. The specimen was failed by reaching its flexural capacity. The calculated yield load value was 169 kN. Beam specimen was yielded at 160 kN. There were some longitudinal cracks only on the upper face of specimen at the zone of lap splice. Figure 4.24 and 4.25 shows as built strain gauge configuration and crack pattern at the end of the test respectively.

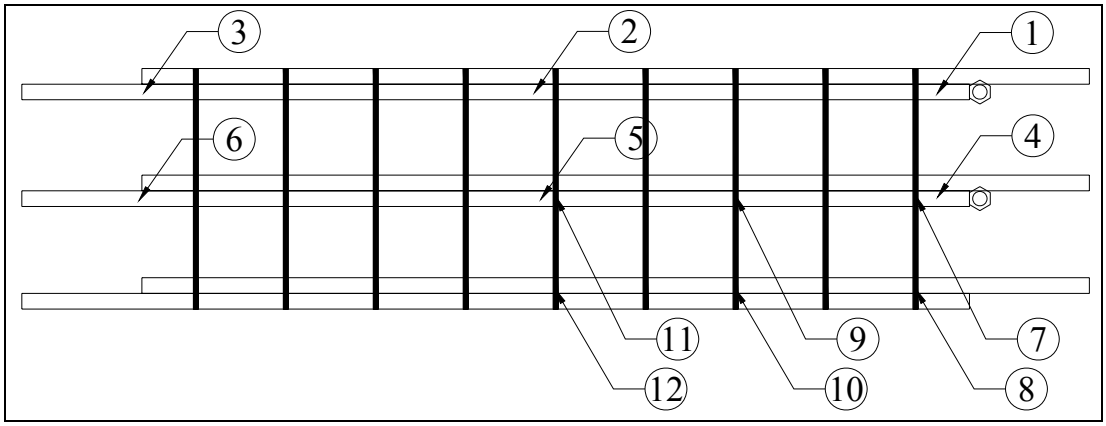

Figure 4.24 Strain gauges numbers and their locations for specimen ACI26.

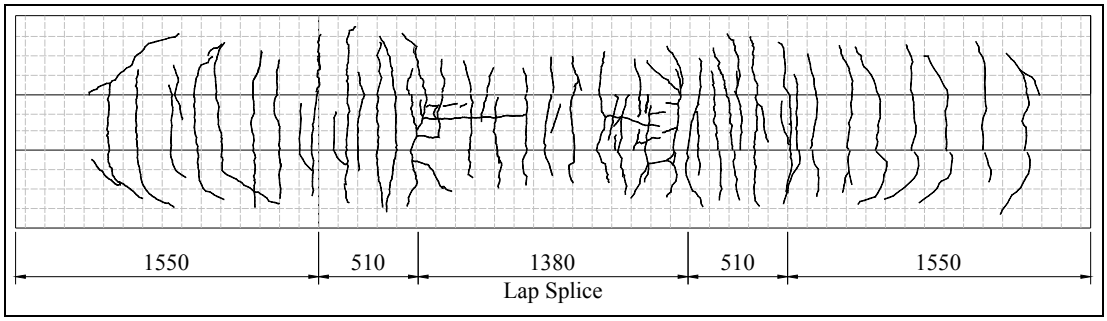

Figure 4.25 Crack pattern for specimen ACI26.

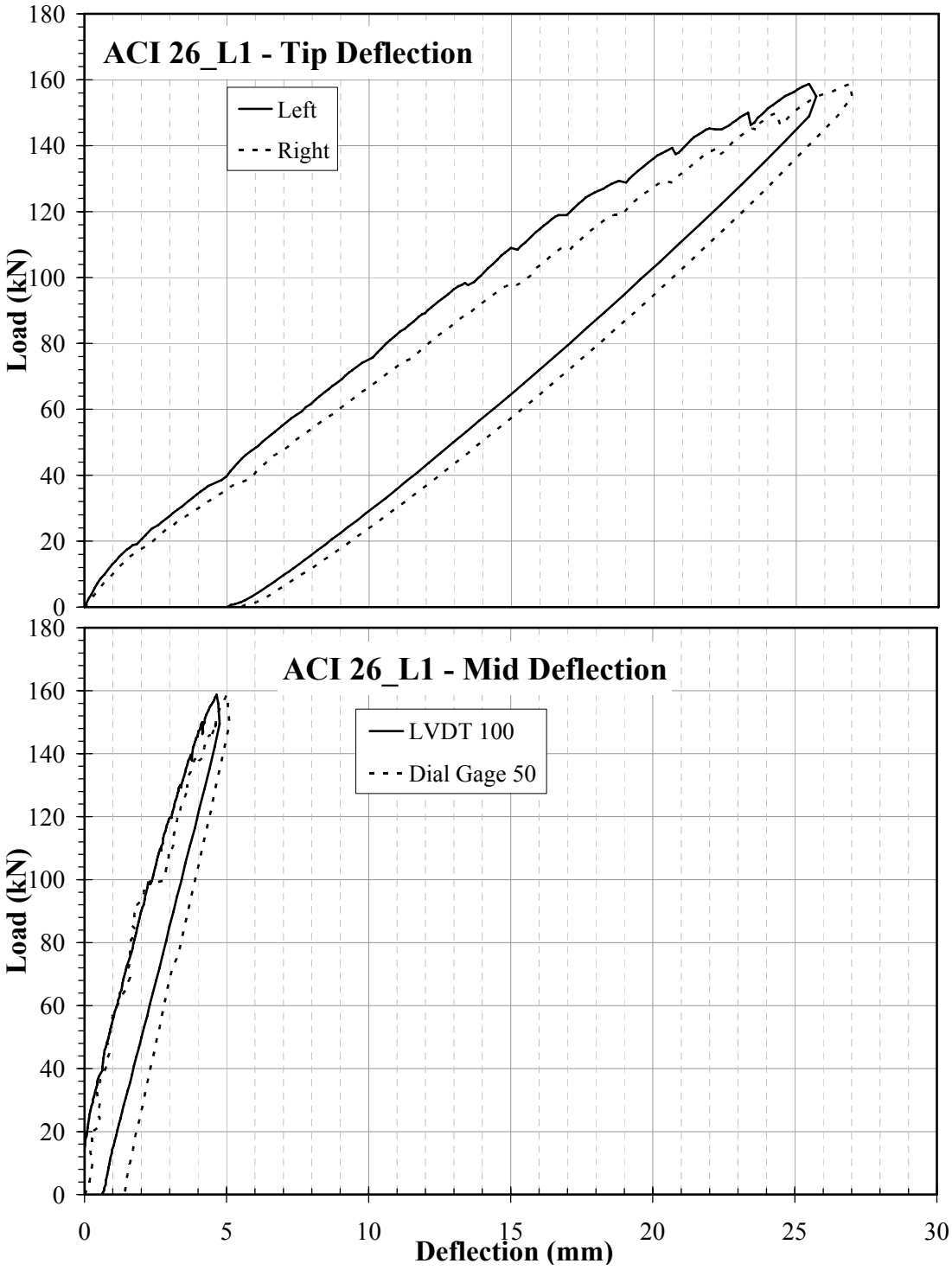

Figure 4.26 ACI26_L1 Load vs. Deflection Charts.

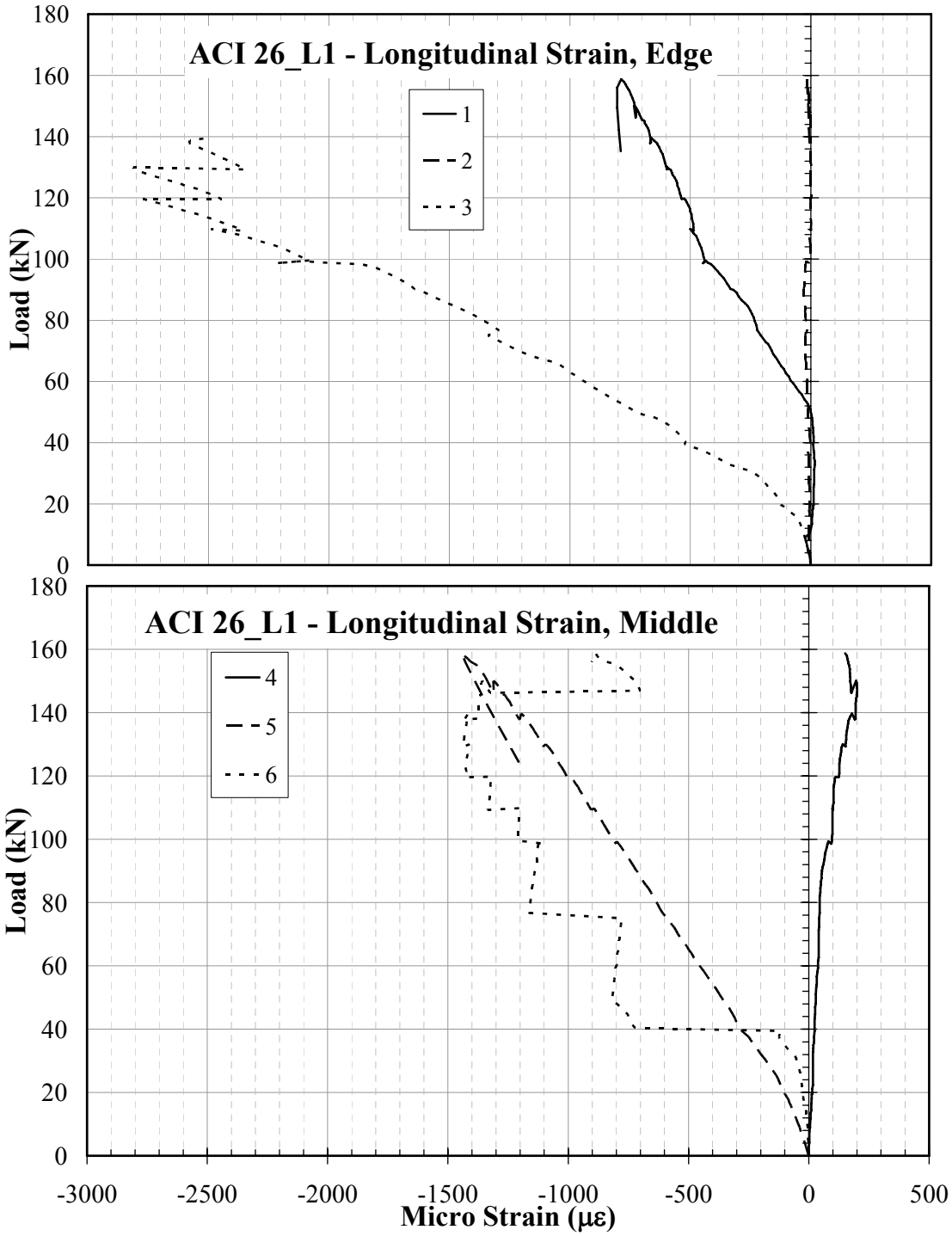

Figure 4.27 ACI26_L1 Load vs. Longitudinal Strain Charts.

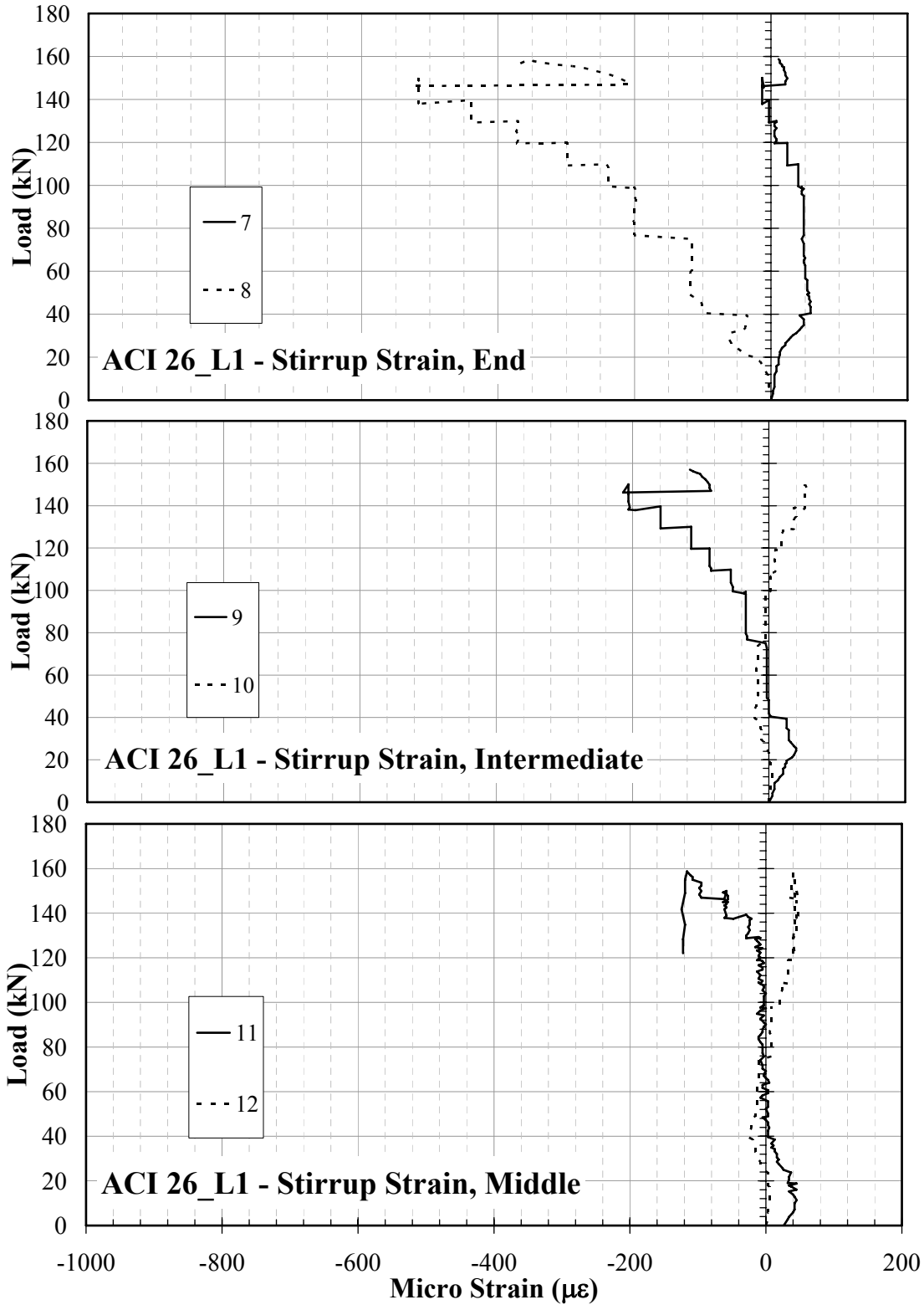

Figure 4.28 ACI26_L1 Load vs. Stirrup Strain Charts.

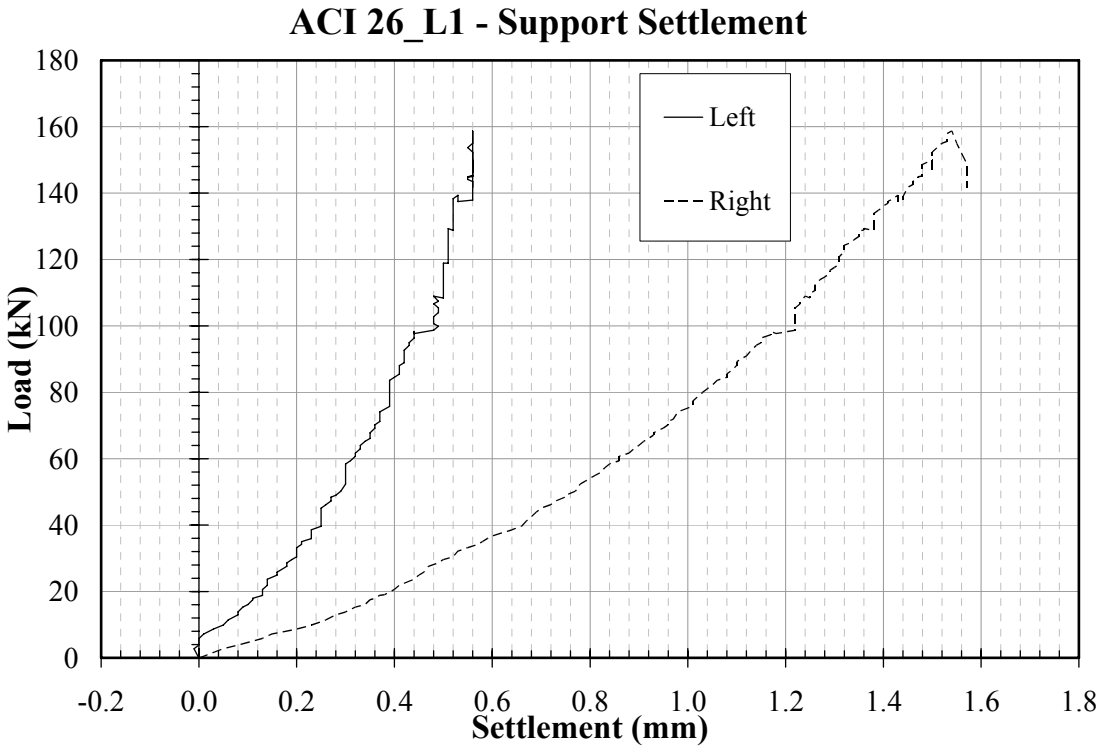

Figure 4.29 ACI26_L1 Load vs. Support Settlement.

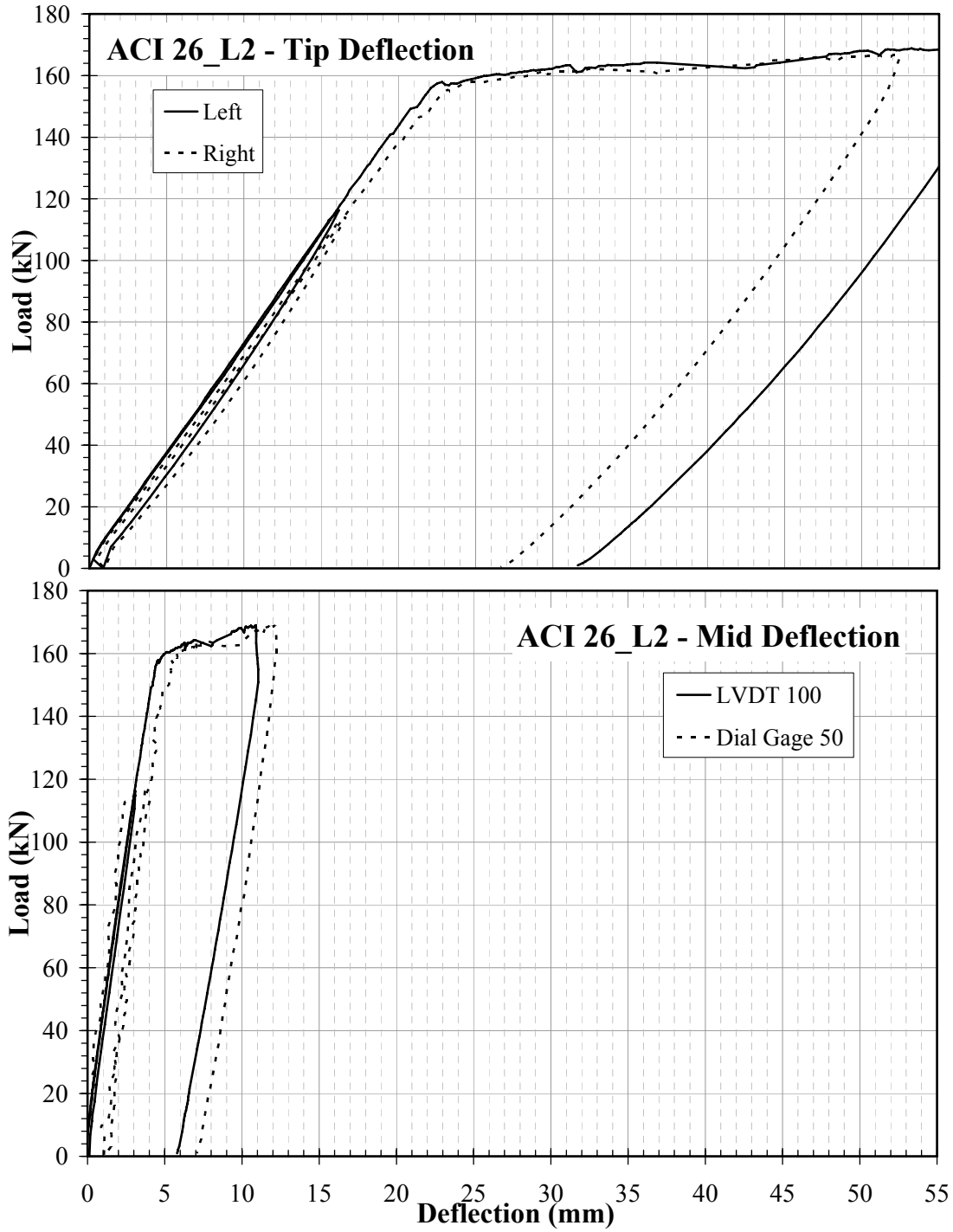

Figure 4.30 ACI26_L2 Load vs. Deflection Charts.

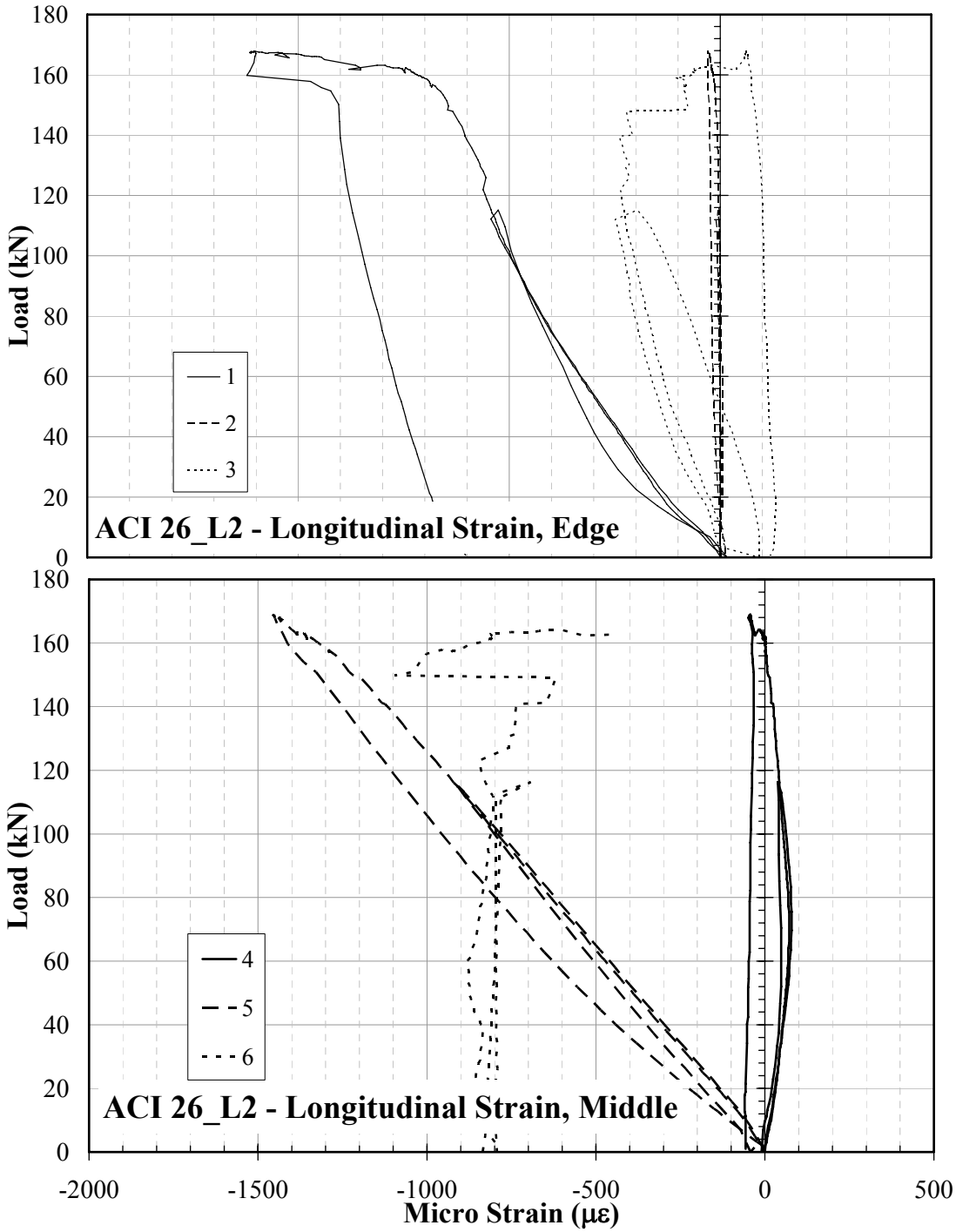

Figure 4.31 ACI26_L2 Load vs. Longitudinal Strain Charts.

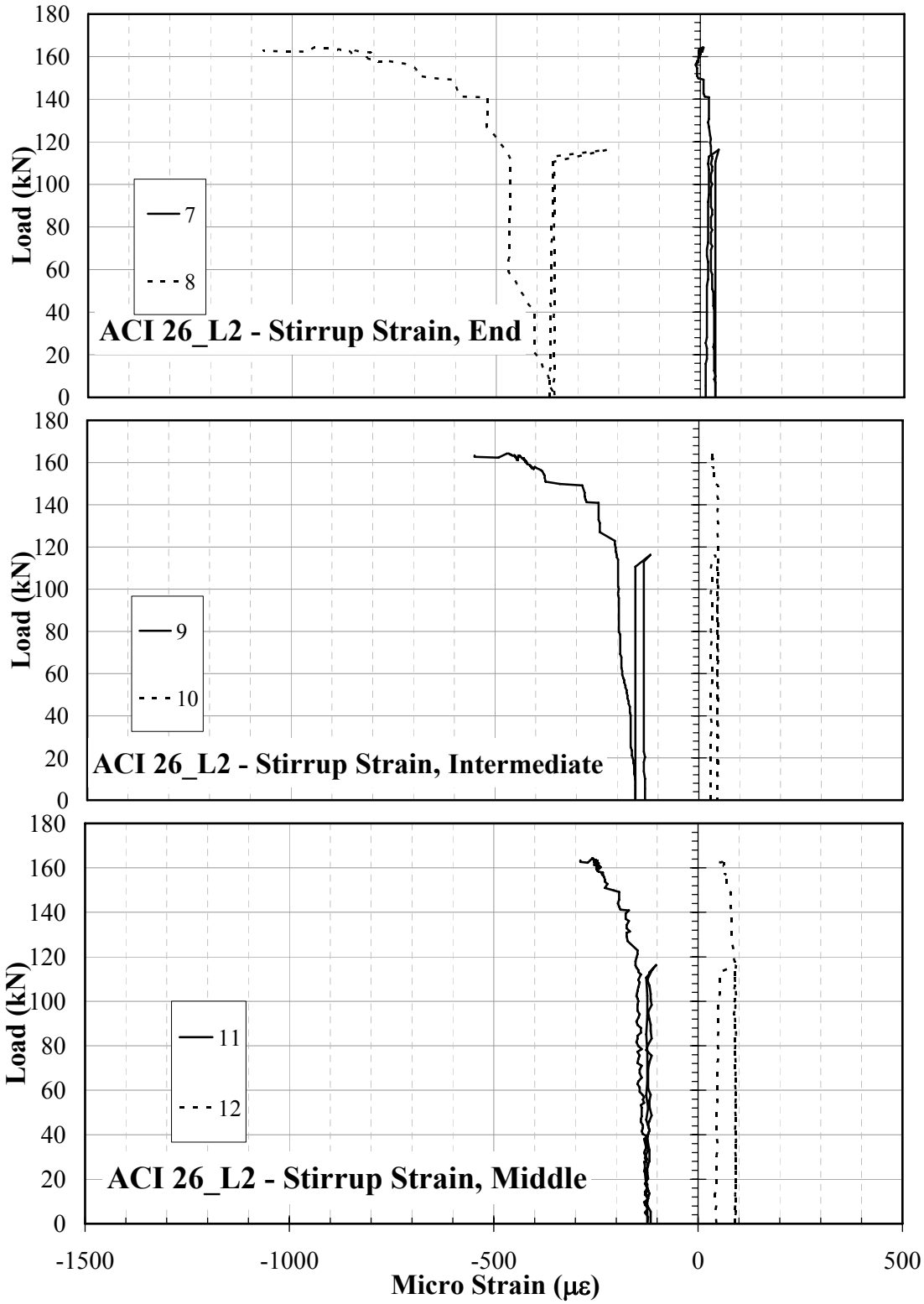

Figure 4.32 ACI26_L2 Load vs. Stirrup Strain Charts.

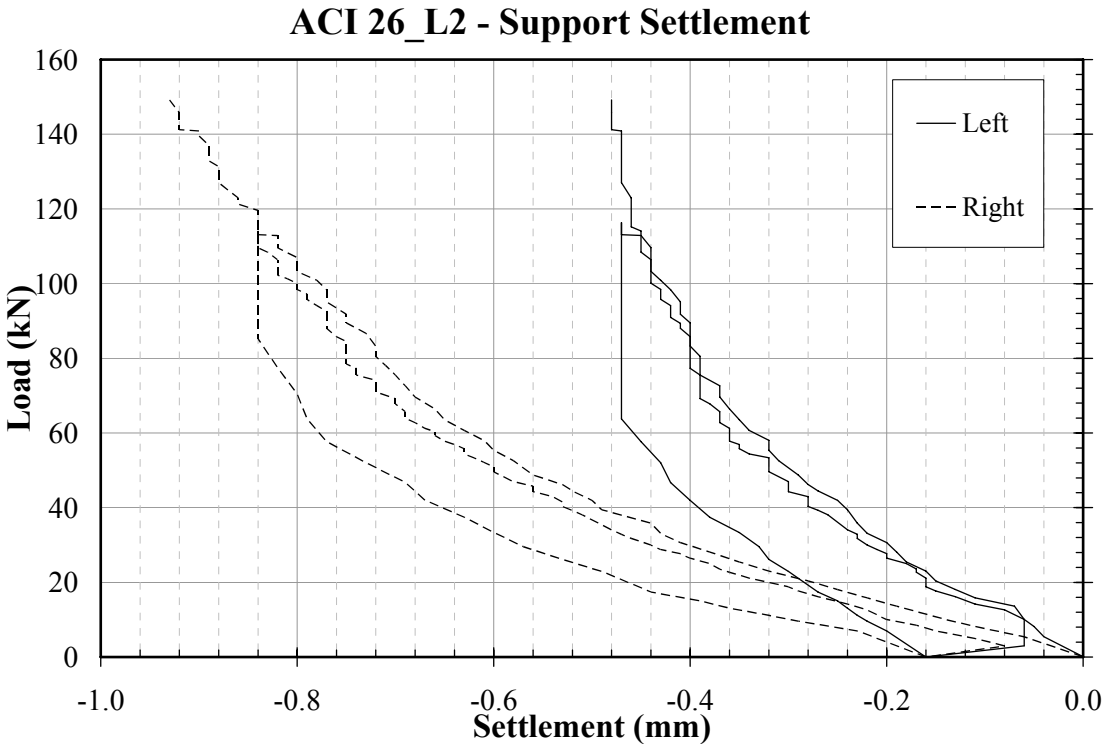

Figure 4.33 ACI26_L2 Support Settlement.

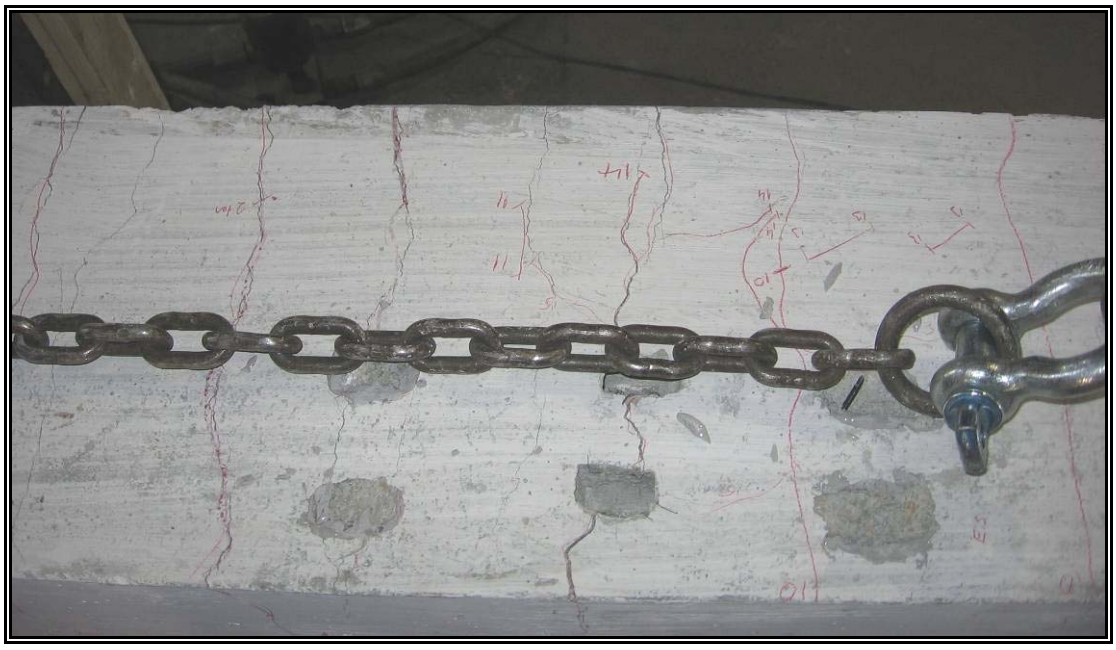

Figure 4.34 ACI26 splice region after test.

4.3.5. Specimen: ACI22

In ACI22 test, strain gauge readings could not be recorded because of the failure of data acquisition system during the test. In order to observe post yielding behavior of the specimen it was loaded once more. L1 code refers to first loading and L2 code is for second loading. Beam specimen yielded by reaching its flexural capacity. The calculated yield load value was 119 kN. Beam specimen was yielded at 125 kN. There were only some longitudinal cracks only on the upper face of specimen at the zone of lap splice. Figure 4.35 and 4.36 show as built strain gauge configuration and crack pattern at the end of the test respectively.

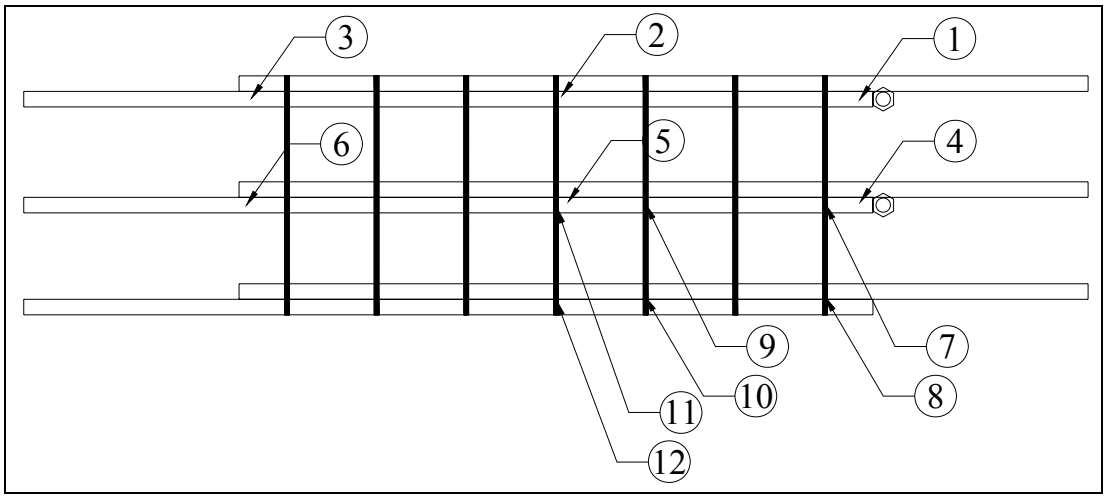

Figure 4.35 Strain gauges numbers and their locations for specimen ACI22.

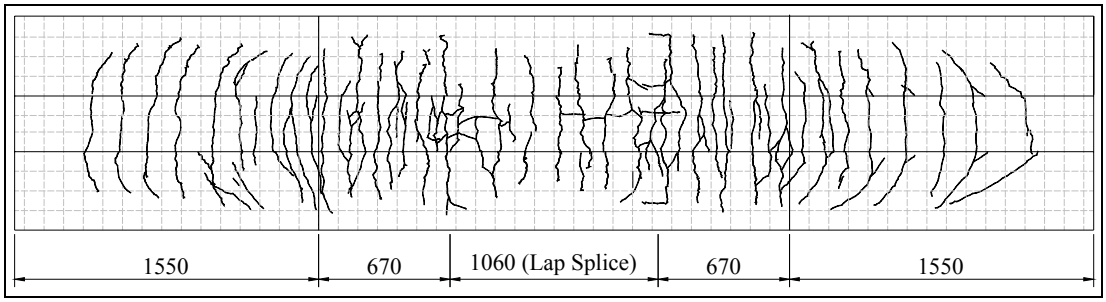

Figure 4.36 Crack pattern for specimen ACI22.

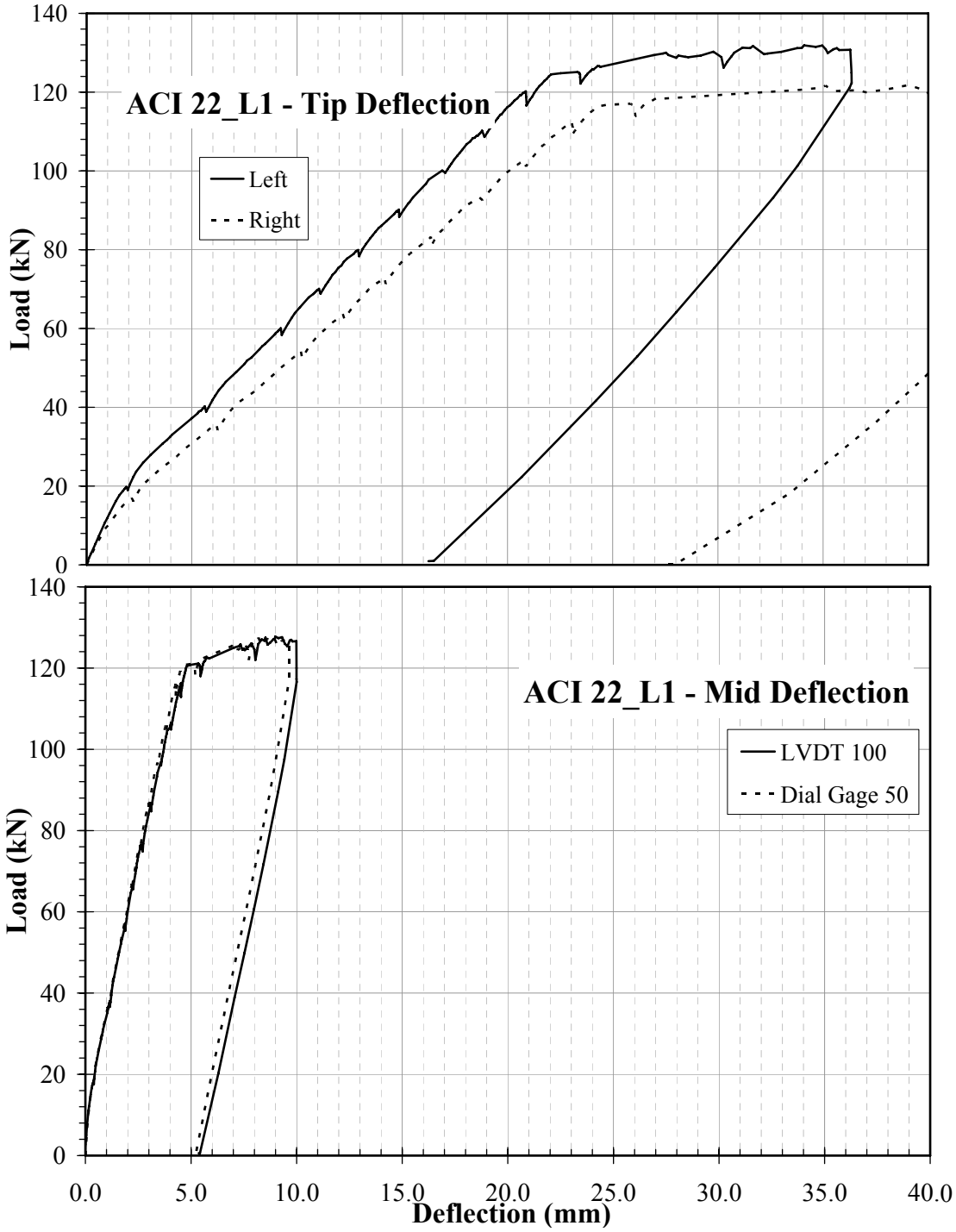

Figure 4.37 ACI22_L1 Load vs. Deflection Charts.

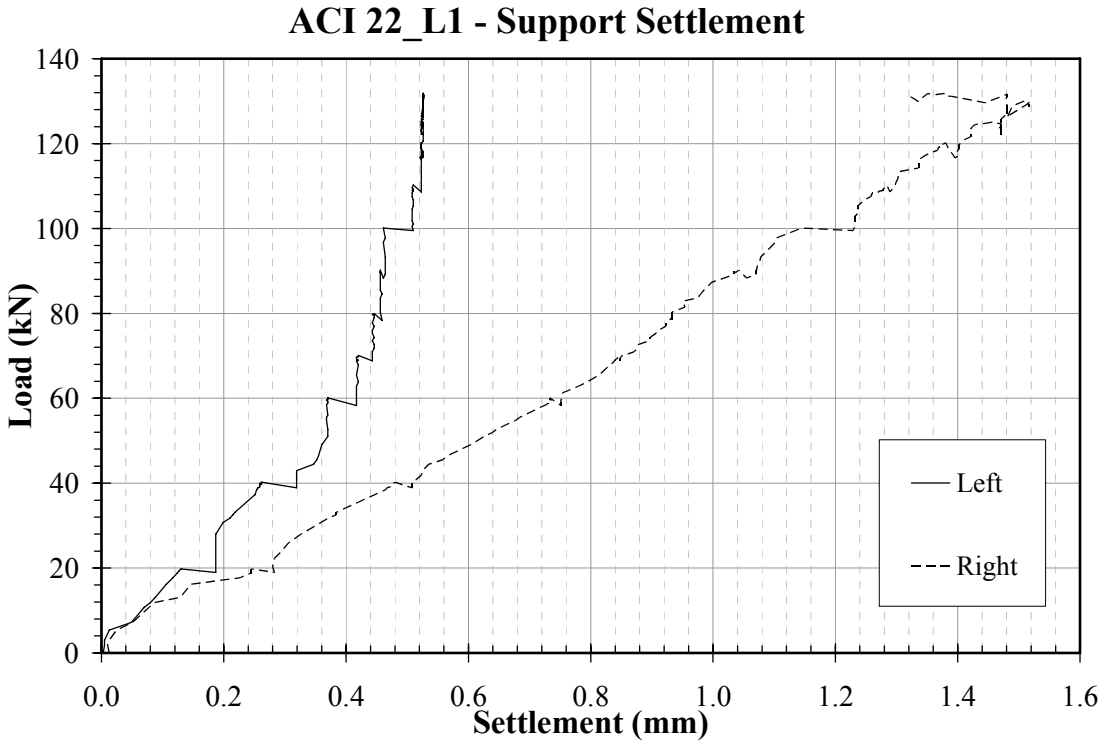

Figure 4.38 ACI22_L1 Load vs. Support Settlement.

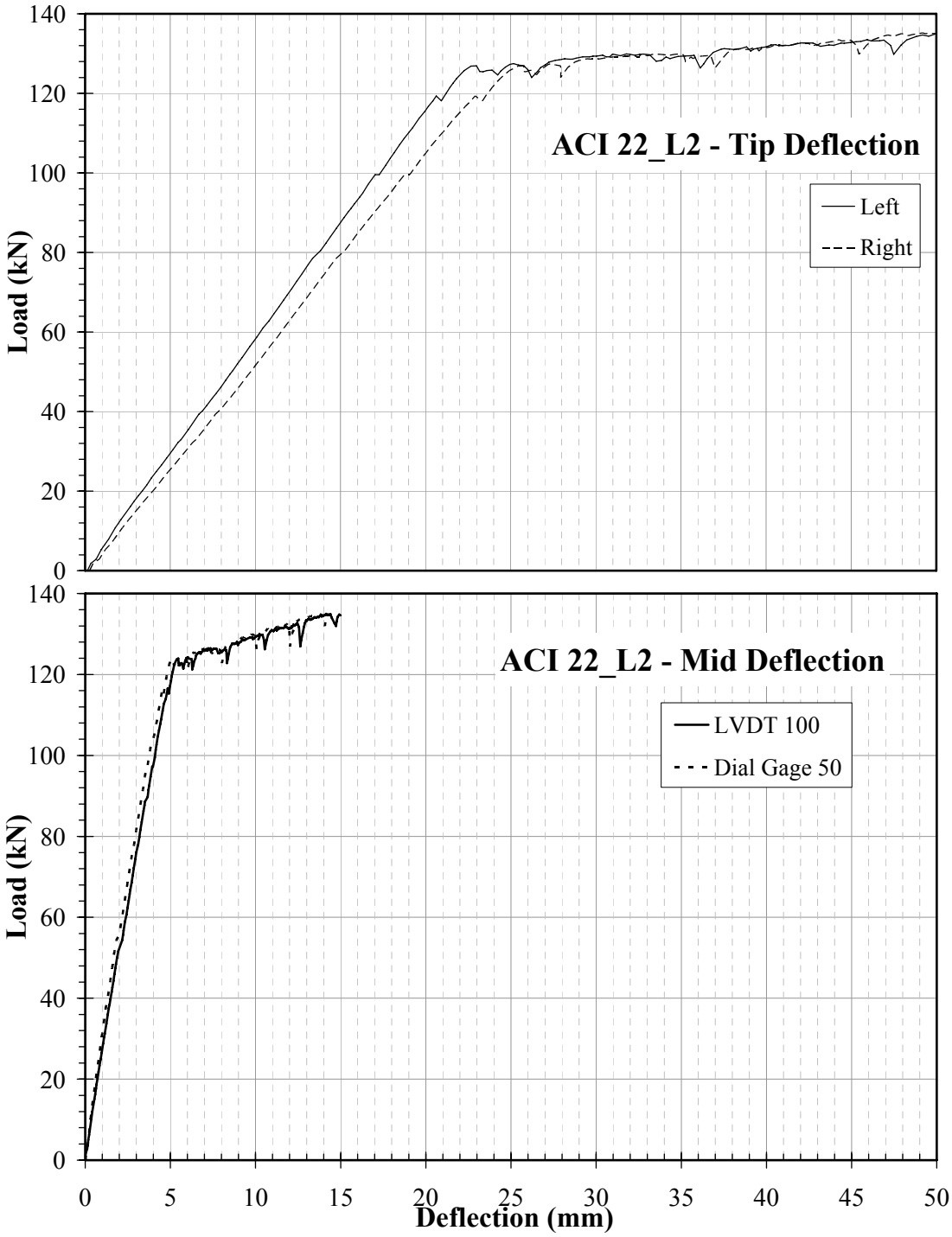

Figure 4.39 ACI22_L2 Load vs. Deflection Charts.

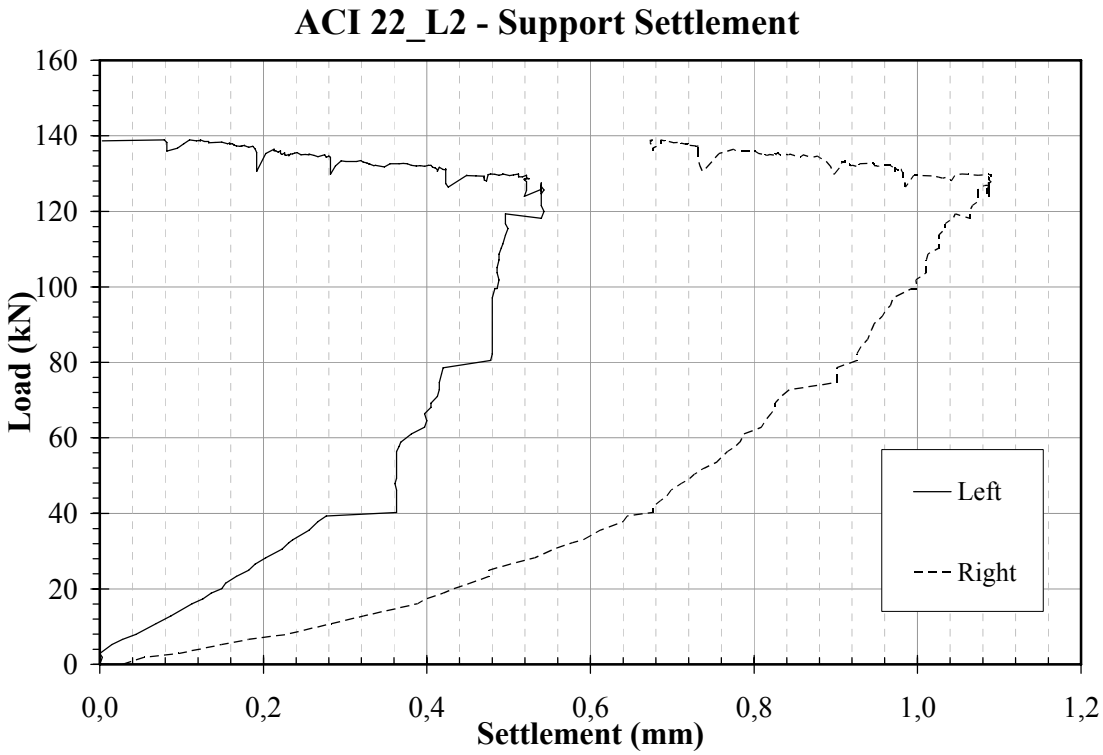

Figure 4.40 ACI22_L2 Load vs. Support Settlement.

Figure 4.41 Splice region after test.

4.3.6. Specimen: ACI16

ACI16 specimen was failed by reaching its flexural capacity. The calculated and measured yielding loads were 60 kN and 55 kN respectively. There were only some longitudinal cracks both on the upper and side faces of specimen at the zone of lap splice. Figure 4.42 and 4.43 show as built strain gauge configuration and crack pattern at the end of the test respectively.

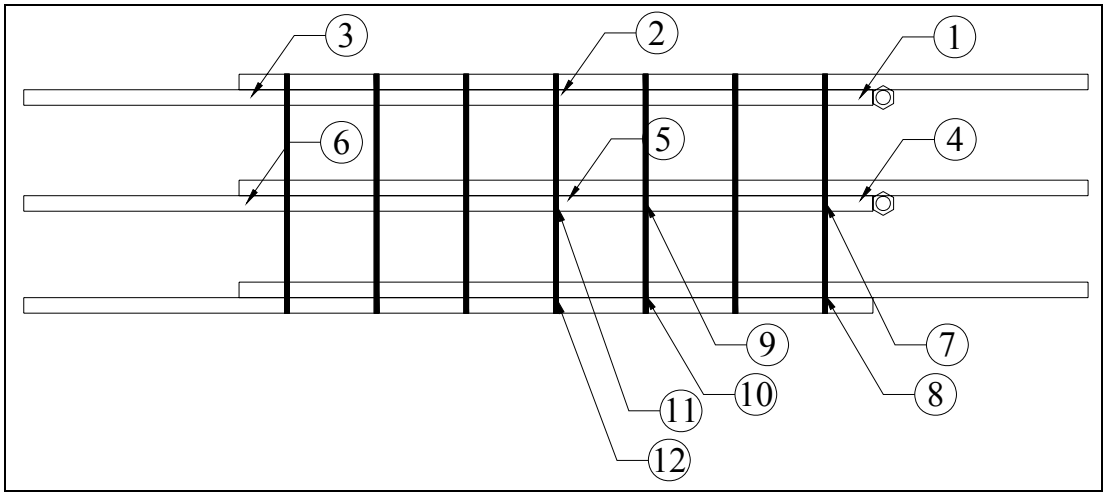

Figure 4.42 Strain gauges numbers and their locations for specimen ACI16.

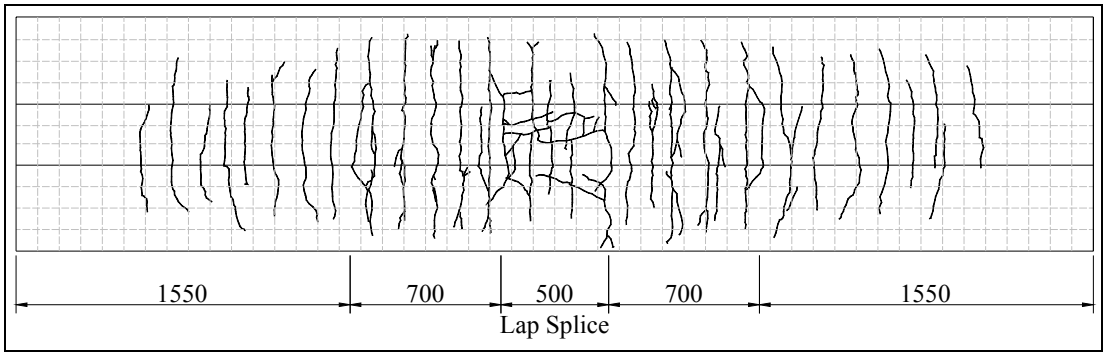

Figure 4.43 Crack pattern for specimen ACI16.

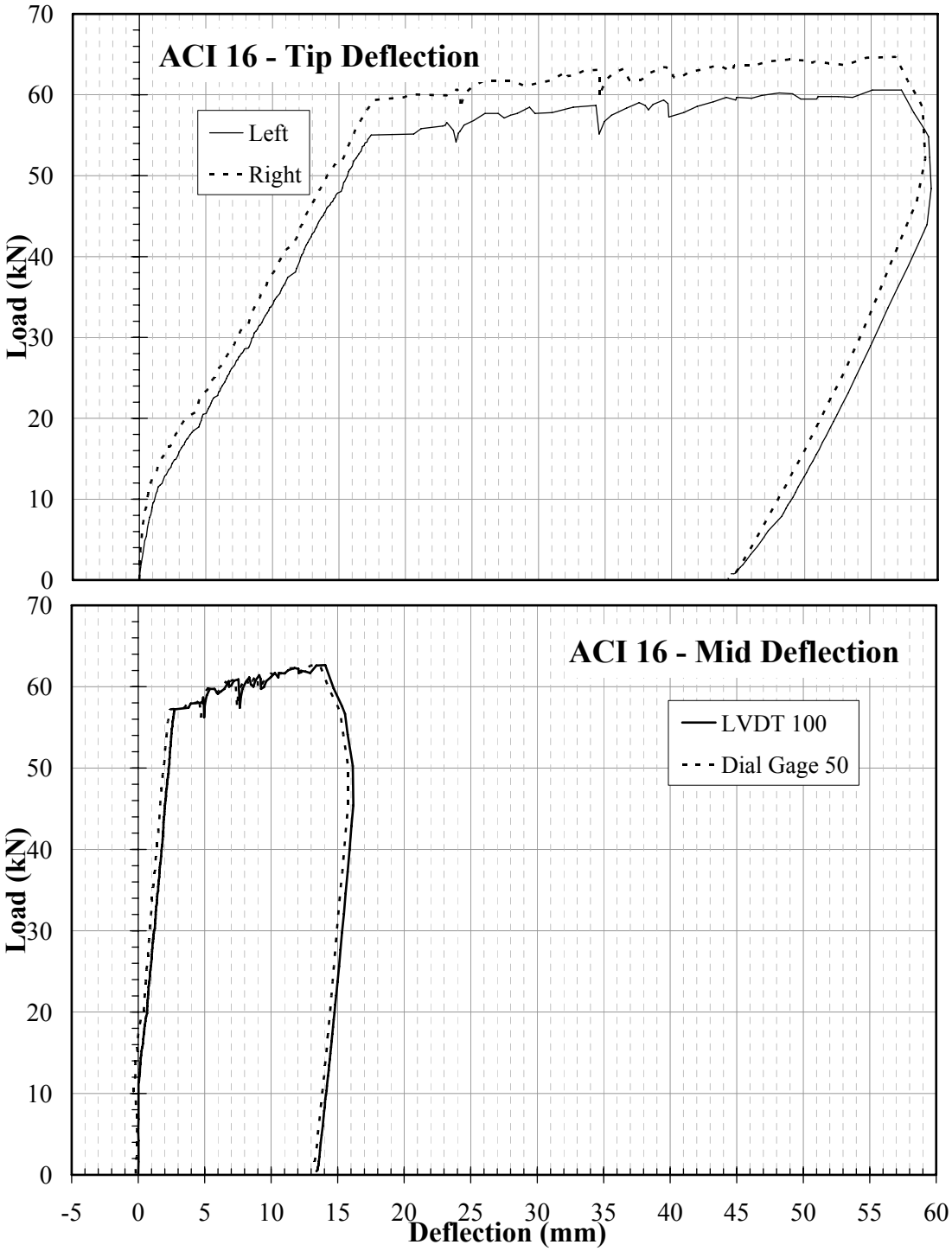

Figure 4.44 ACI16 Load vs. Deflection Charts.

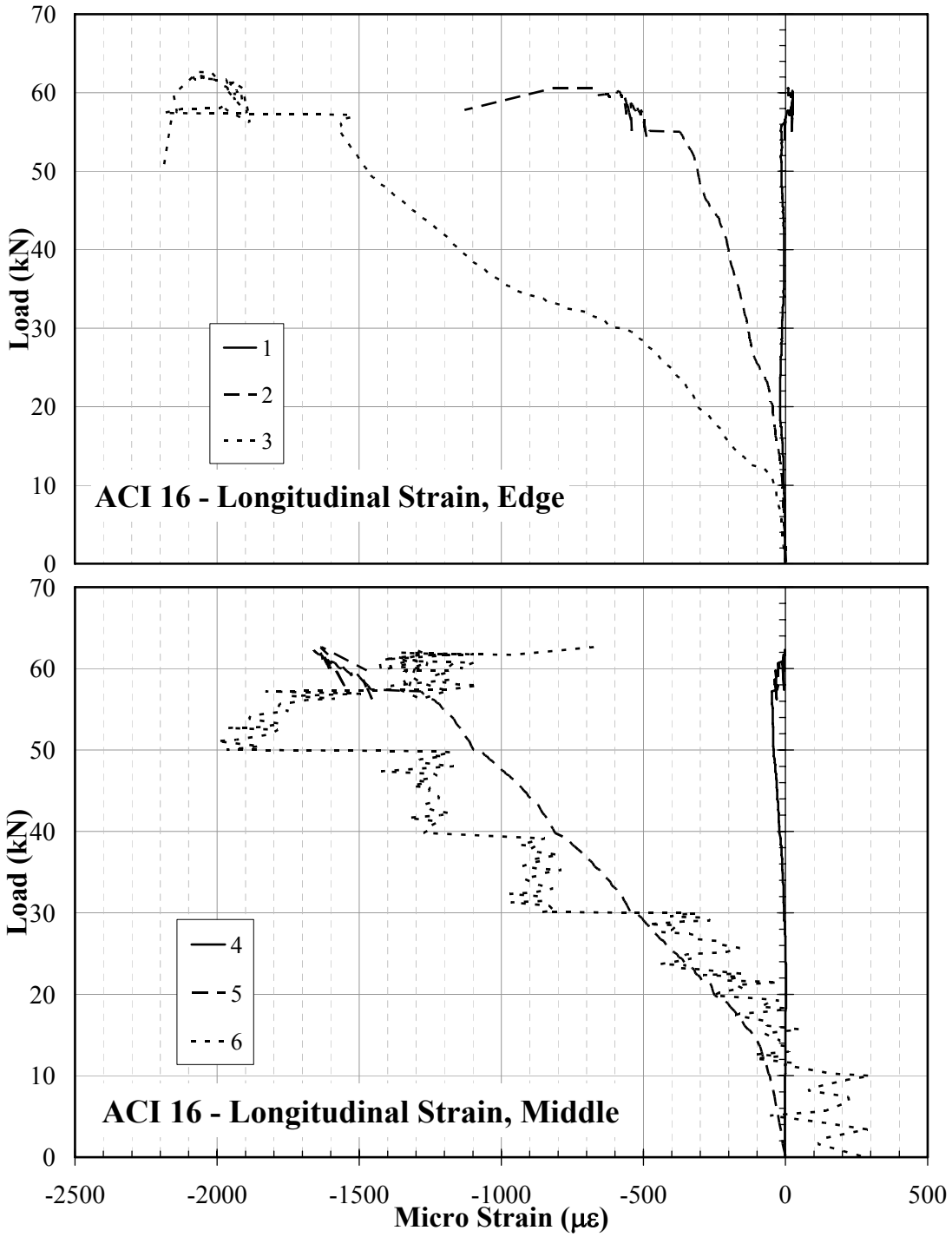

Figure 4.45 ACI16 Load vs. Longitudinal Strain Charts.

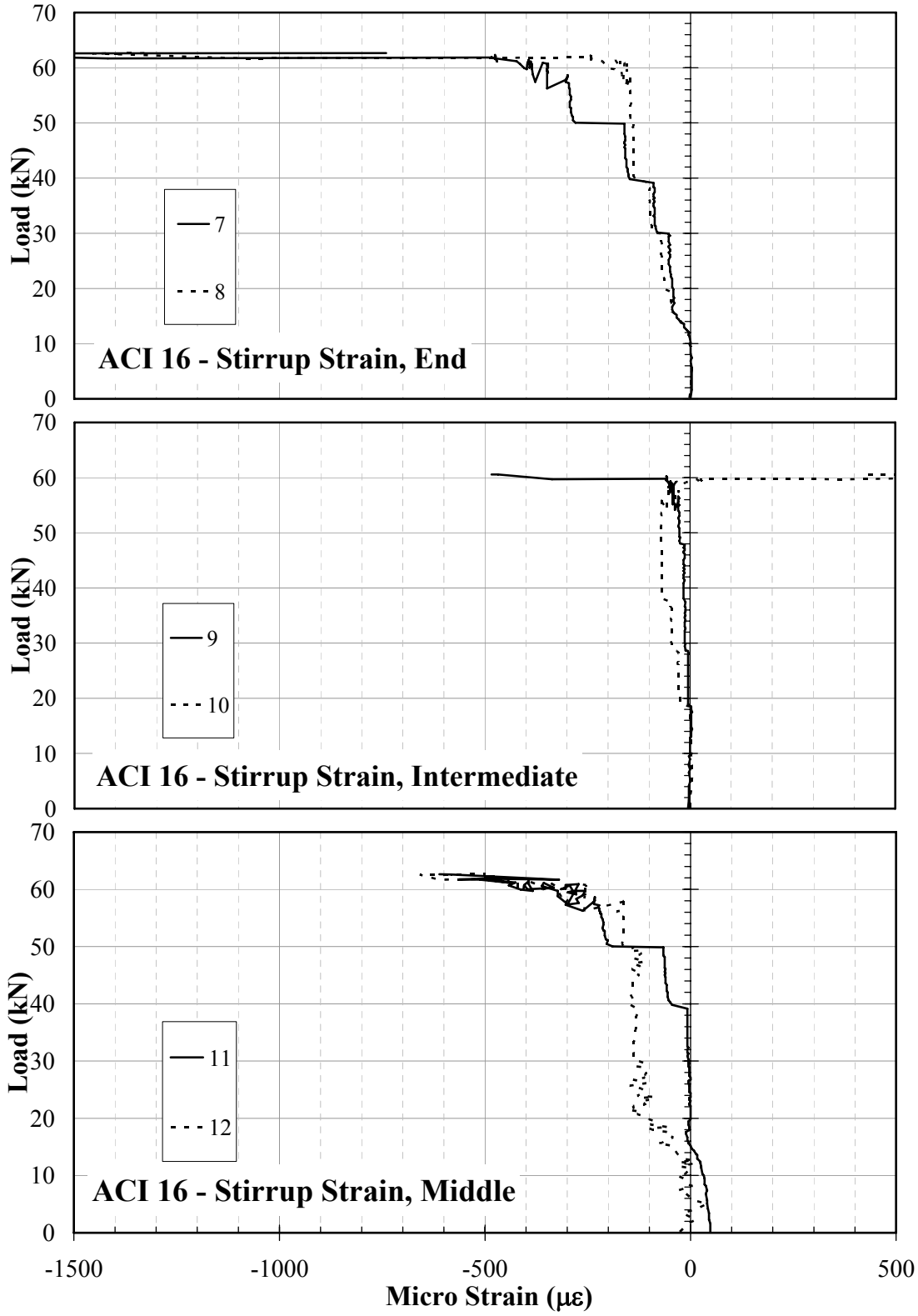

Figure 4.46 ACI16 Load vs. Stirrup Strain Charts.

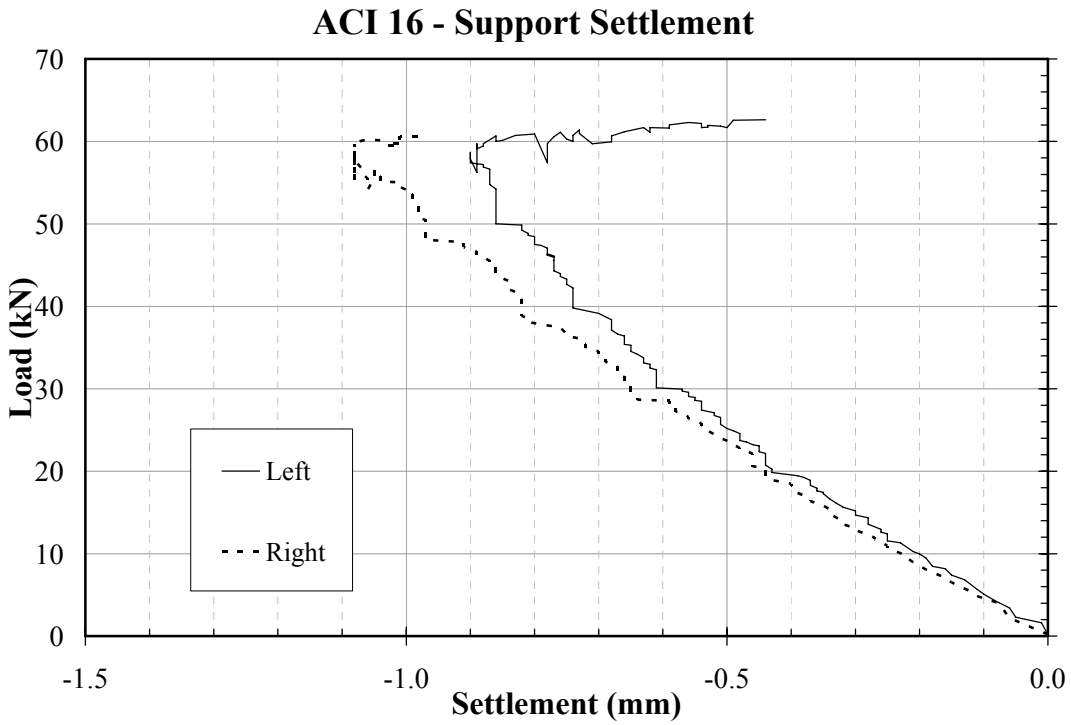

Figure 4.47 ACI16 Load vs. Support Settlement.

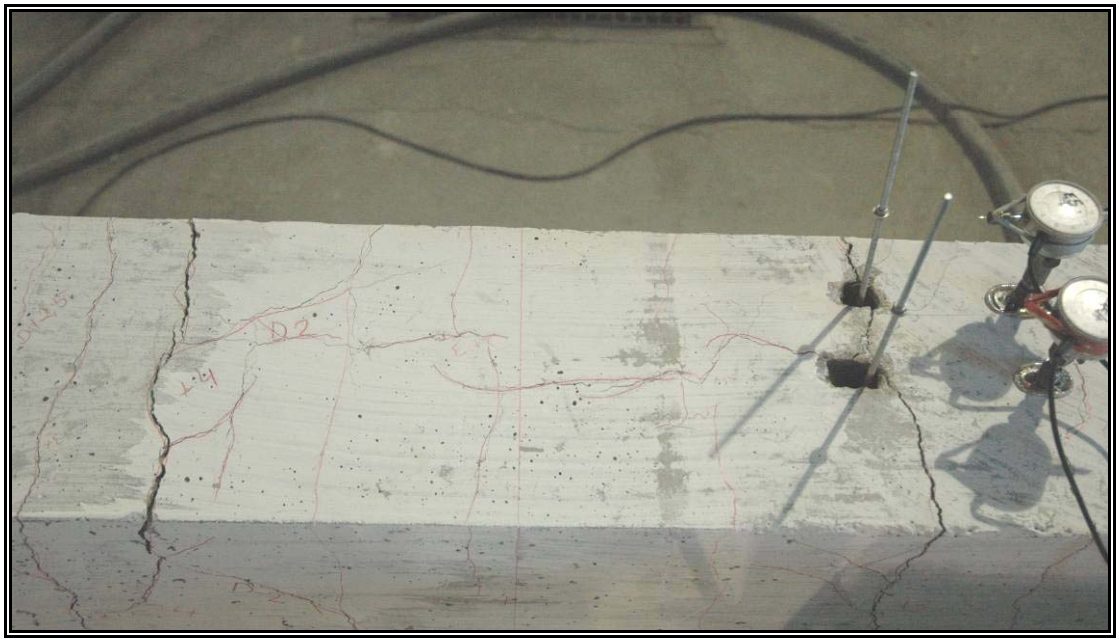

Figure 4.48 Splice region after test.

CHAPTER V

ANALYSIS AND DISCUSSION OF RESULTS

5.1. General

In this chapter, test results were compared with results obtained from analytical studies. Experimentally obtained load-deflection curves were compared with the ones that calculated by analytical methods. Analysis procedure is described in detail in the following parts of this chapter.

5.2. Comparison of the Load-Deflection Curves

Mid deflection and end deflection vs. load curves of the test specimens were compared with the analytically calculated ones. In order to determine the Load-Deflection curves analytically, moment-curvature diagrams of the specimens were calculated first. A non-commercial computer program called RESPONSE 2000 [26] was used to obtain the moment-curvature diagrams. After obtaining moment-curvature diagrams of each specimen, following procedure was fallowed step by step in order to calculate the load-deflection curves.

- After determining moment curvature diagram for each specimen from RESPONSE 2000, as seen from Figure 5.1, test load moment diagram was drawn. Moment is linearly increasing along the shear span. At the end of shear span there is a constant moment region between the supports. The maximum moment occurs throughout this constant moment region and can be calculated simply by multiplying the moment arm with the applied load

(1.4×P). In order to get finer result especially for tip deflection values, moment diagram along shear span was divided to 10 equal strips and moment values for each strip was determined.

- Curvature value was obtained from moment curvature diagram for the corresponding moments. Load increment value which was used in load deflection calculations was equal to 1 kN. During the determination of curvature values for the corresponding moments, interpolation was done between two curvature values. Moment curvature diagrams for each specimen are presented at Appendix B.

- After construction of the curvature diagram, second-moment area theorem was applied to determine tip deflection and mid deflection for each specimen. Equations 5.1, 5.2 and 5.3 were used to calculate tip deflection (deflection at point A). At point C rotation is zero as shown in Figure 5.1. The tangential deviations between points A and C and between points B and C are $t_{A/C}$, $t_{B/C}$ respectively. Difference between $t_{A/C}$ and $t_{B/C}$ gives the deflection at point A (Δ_A). Deflection at point C (Δ_C), the mid point, is directly equal to $t_{B/C}$. Tip and mid deflections were calculated for 1 kN increments until reaching a representative nonlinear behavior of the beam.

$$t_{A/C} = \sum_{1}^{10} A_i \times \delta_{A_i} + A_{11} \times \delta_{A_{11}/A} \tag{5.1}$$

$$t_{B/C} = A_{11} \times \delta_{A_{11}/B} \tag{5.2}$$

$$\Delta_A = t_{A/C} - t_{B/C} \tag{5.3}$$

$$\Delta_C = t_{B/C} \tag{5.4}$$

Also above defined terms are shown in Figure 5.1

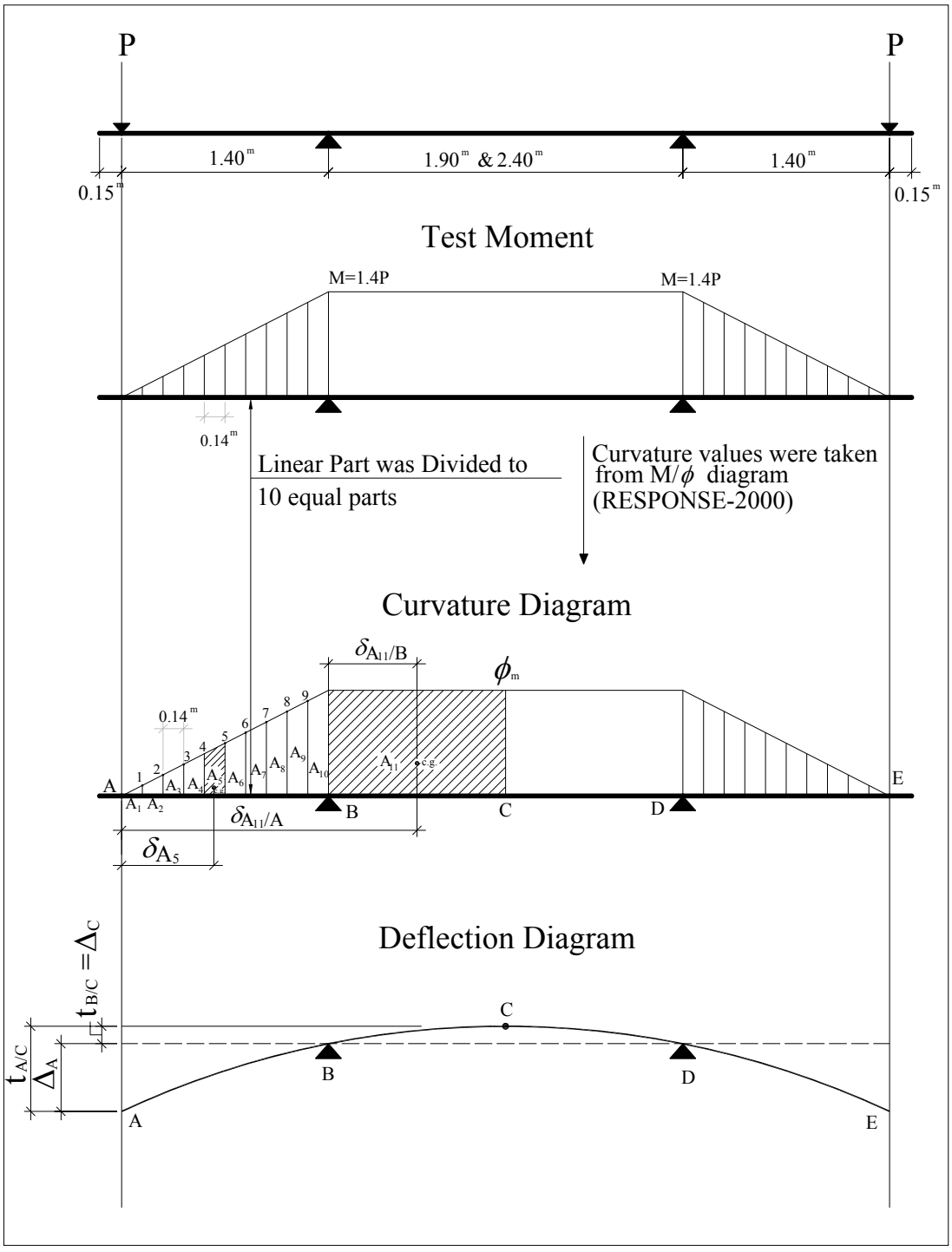

Figure 5.1 Procedure for calculating Load – Deflection Curves.

Calculated load-deflection curves are shown on the same chart of measured values and named as "Analytical". On the mid deflection charts, the average of two load cells values were used in the y-axis. In the tip deflection charts, the measured displacement values were drawn against the corresponding load cell readings i.e. left tip deflection vs. left load cell and right tip deflection vs. right load cell. Test results for deflection values were corrected with the support settlement data. The measured left and right support settlement values were close to each other and the average of them were added to mid deflection values and subtracted from the tip deflection values. The experimental and analytical tip and mid deflection curves are given in Figure 5.2 – 5.7.

In the analytical calculation of load–deflection curves, material and geometric properties of the specimens given in Chapter 3 were used. Material properties include yield and ultimate strength for longitudinal, transverse and compression reinforcement, and compressive strength for concrete. Geometric properties include the section dimensions and clear cover dimension which had been determined after the tests.

The main idea behind this analytical study is to obtain the experimental deflection curves analytically. The comparison of the experimental and analytical curves is made for the initial elastic region, for the slope of the post cracking region and for the ultimate strength.

The ultimate strength of all tests is predicted with a reasonable accuracy. The difference between the experimental and analytical ultimate is generally within 5%. The only exception is the experiment TS26 in which bond failure occurred. The ultimate point in this experiment was reached prior of yielding of beam by an early lap splice failure. In all other experiments, beams failed in a ductile manner with yielding of longitudinal reinforcement, Figure 5.2.

Since the elastic region occurs only in the very early stages, it is hard to differentiate the curves. Therefore, this portion of the curves are zoomed in and given on the same

chart. Investigation of these curves showed that the elastic portion of all experimental curves is predicted very accurately.

The slope of the measured deflection curves are also predicted acceptably by the analytical ones for all specimens. The slip of the bars not included in the analytical calculations. Since all bars were deformed and a minimum amount of cover concrete was around the bars, slip was not a primary concern in the calculations. The comparison charts support this issue by matching well on the top of each other.

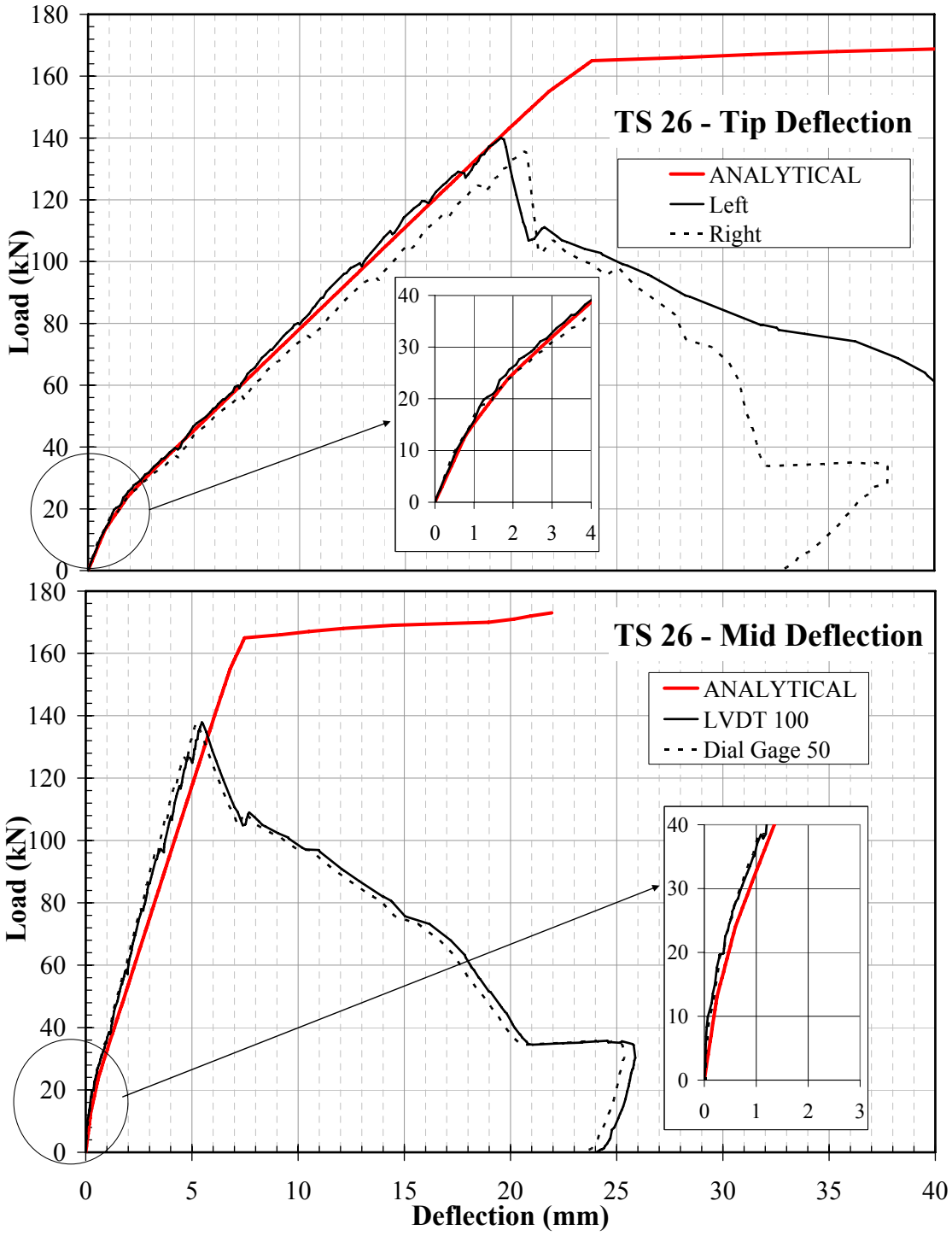

Figure 5.2 Load Deflection curves of TS26.

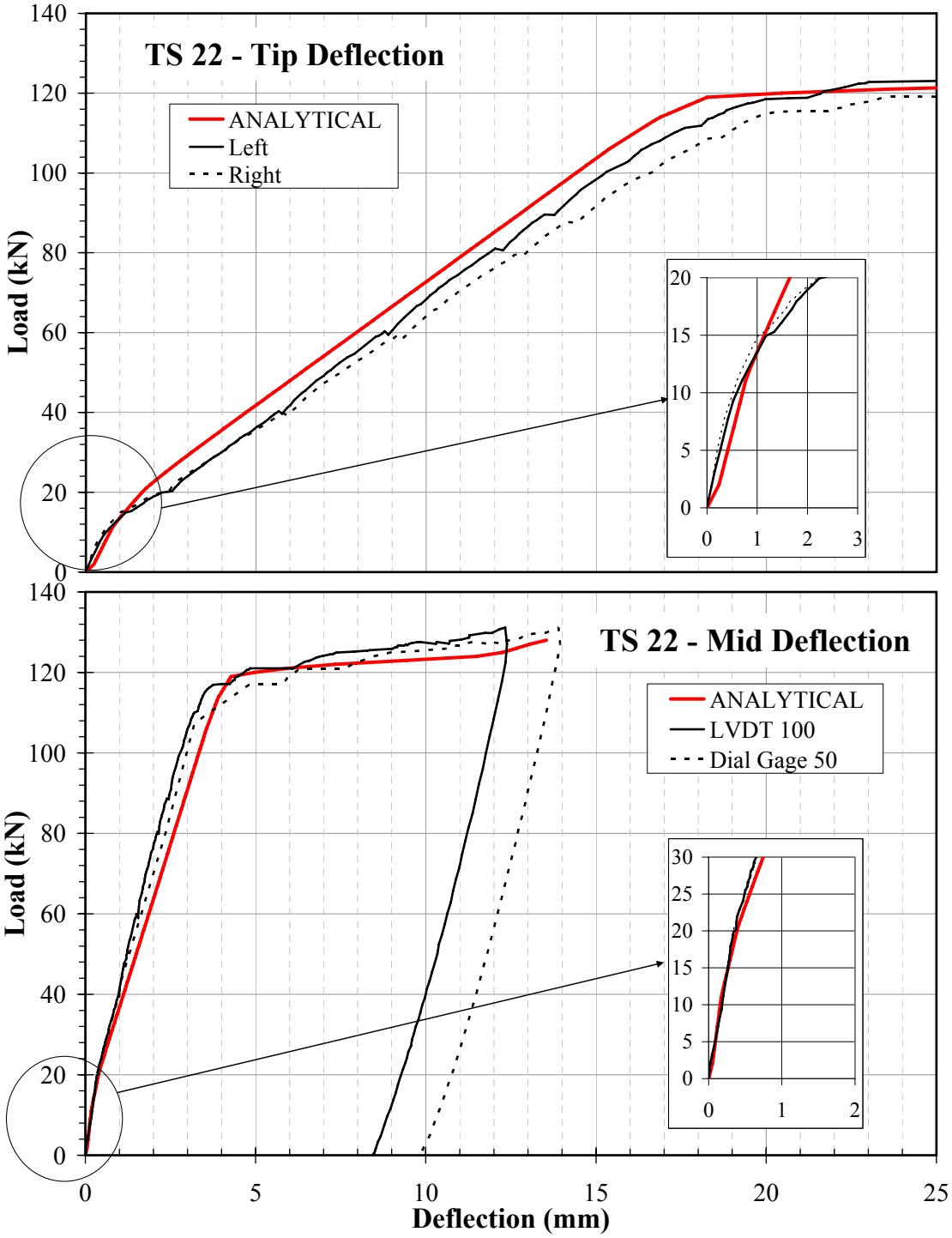

Figure 5.3 Load Deflection curves of TS22.

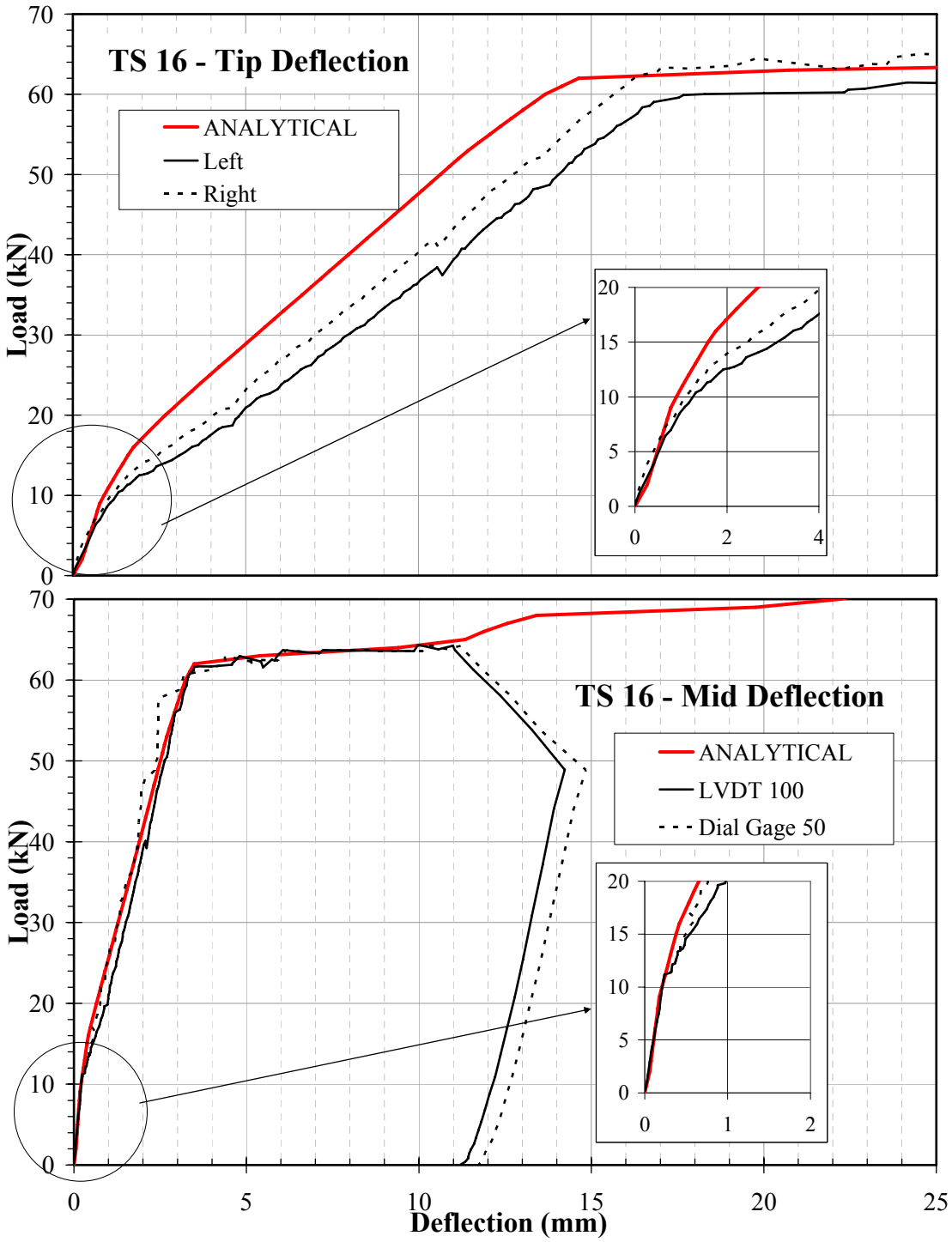

Figure 5.4 Load Deflection curves of TS16.

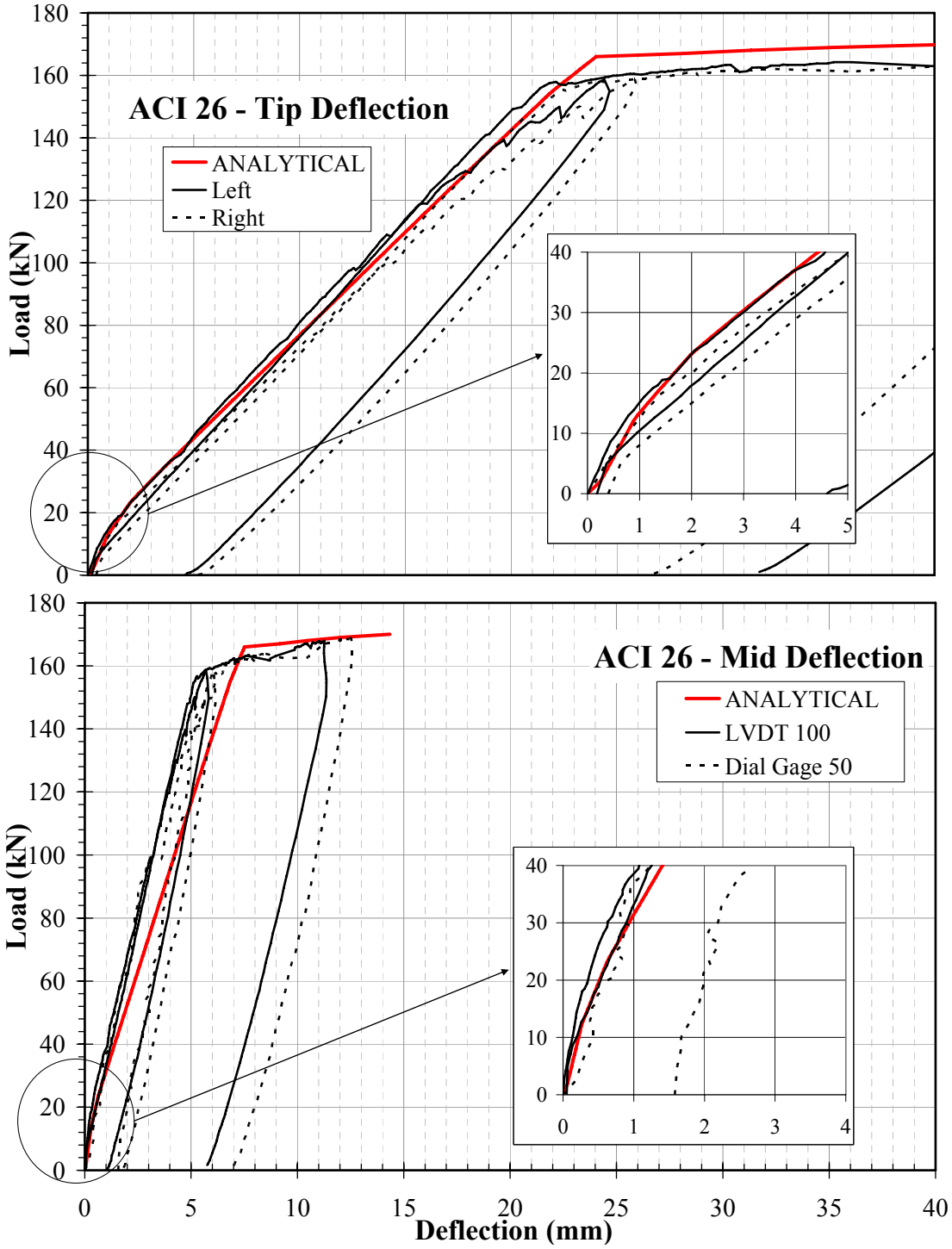

Figure 5.5 Load Deflection curves of ACI26

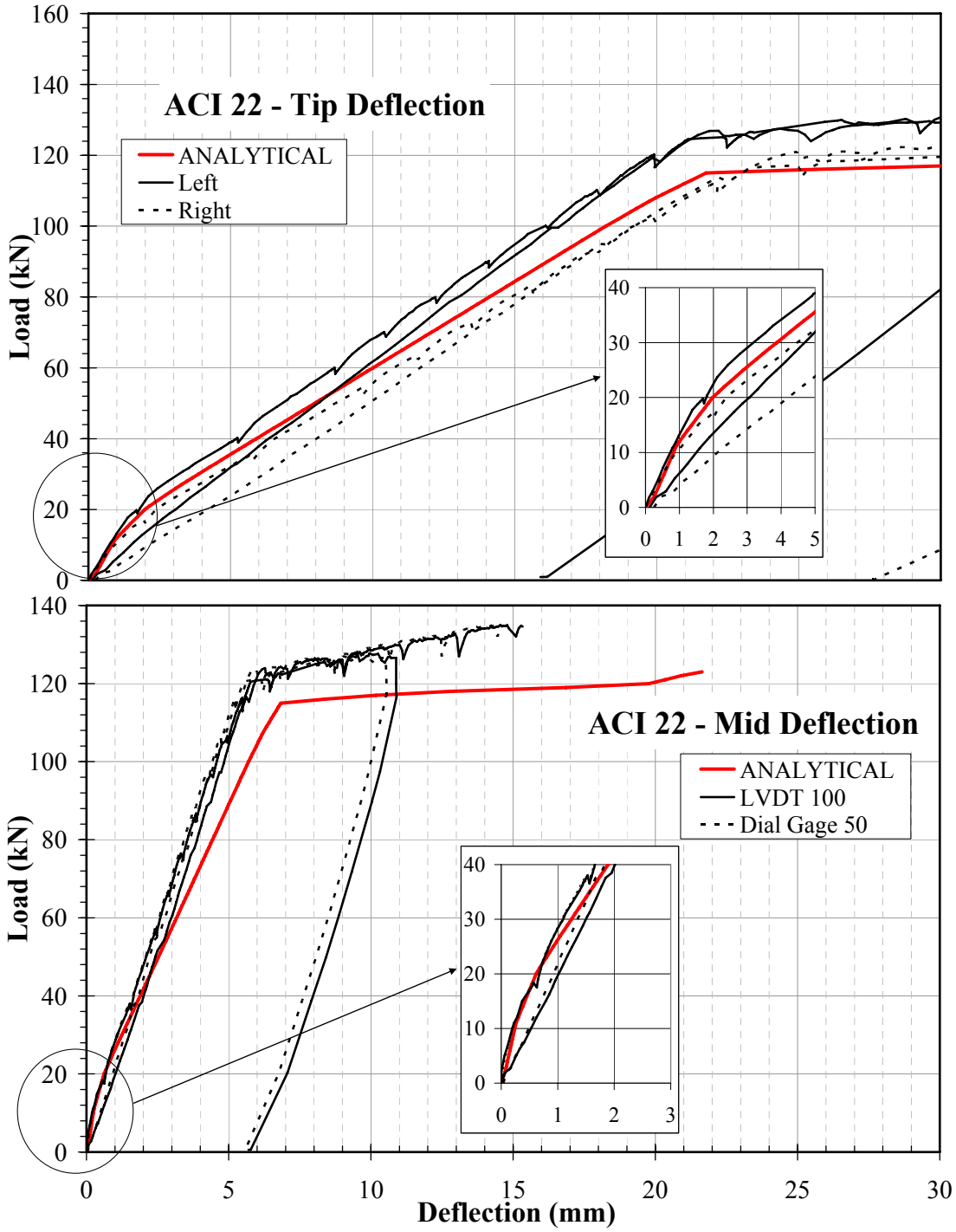

Figure 5.6 Load Deflection curves of ACI22

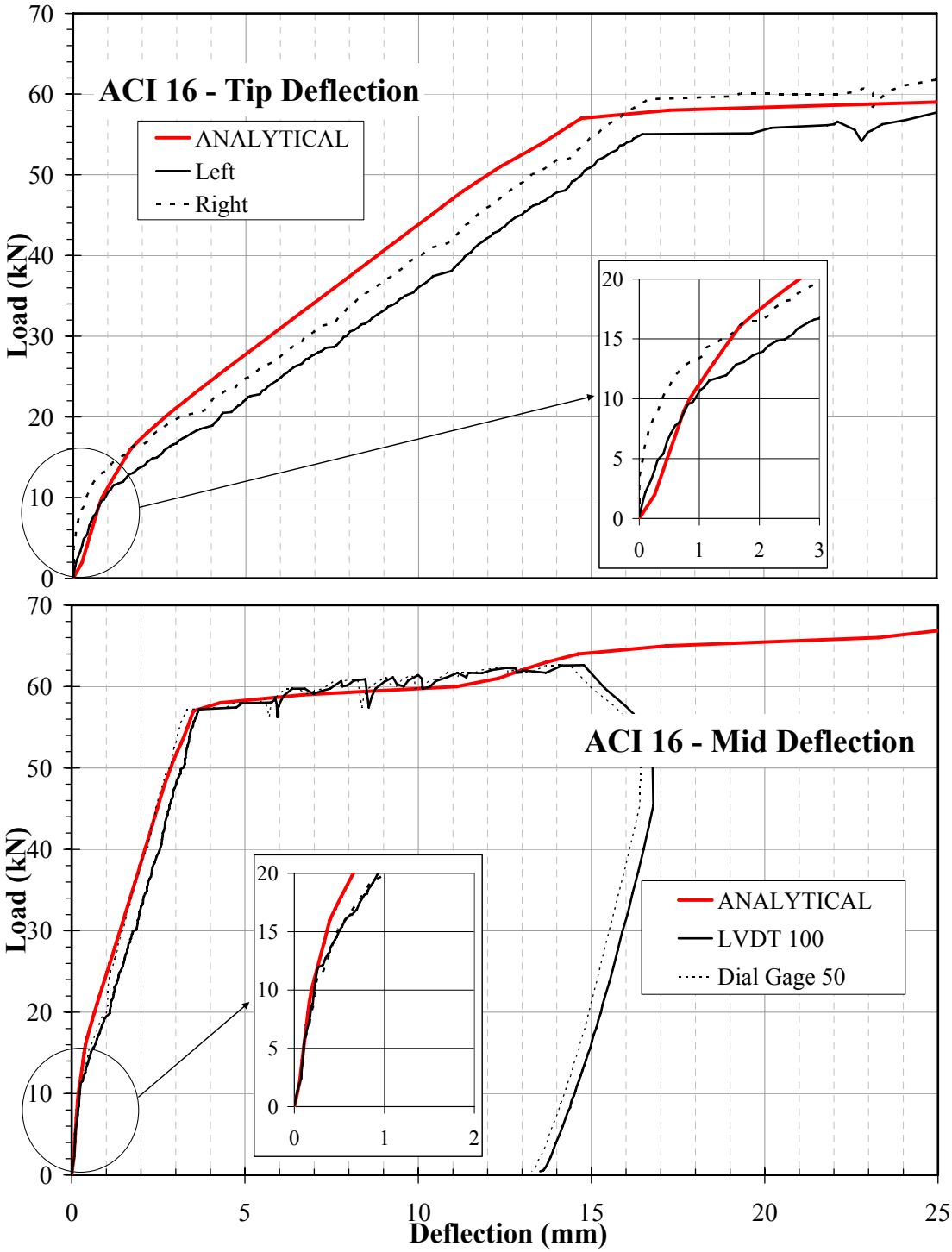

Figure 5.7 Load Deflection curves of ACI16

5.3. Reinforcement Strain Profiles

During the test, strains were measured both on longitudinal and transverse reinforcement. As expected strain at the free end of bar is very close to zero and it increases through the lap splice until the maximum steel strain reached at the continuous end of the lap splice. For each specimen strain, at yielding load, are presented both with tables and charts.

The data acquisition system was capable of acquiring data from strain gage based transducers. In other words, the data acquisition system reads from a full Wheatstone bridge of strain gages. All the load cells and displacement based transducers in the laboratory are this kind. The strain gages on the bars, however, are Quarter Bridge. Therefore, strain gages were completed to full Wheatstone bridge. The reliability of the strain gage readings was low for this reason. The evaluation of the strain gauge readings should be considered regarding this limitation.

5.3.1. TS26

As previously defined in Chapter 4, Figure 4.3 strain gauges with numbers 1, 2, 3 were located on the longitudinal edge bar and 4, 5, 6 were located on the longitudinal mid bar. According to strain values at the ultimate load which is approximately 138 kN, both the middle and edge bars were not yielded. These values are as expected because the failure of TS26 was side and bottom face splitting of the concrete cover and after that point failure was sudden and brittle. After failure point no more strain increase in longitudinal bars were measured. Table 5.1 and Figure 5.8 summarize the strain values for TS26 in microstrain ($\mu\varepsilon$).

Table 5.1 Longitudinal reinforcement strains of TS26.

Strain gauge locations	Strain Gauge Number	Strain at Yielding Load (με)
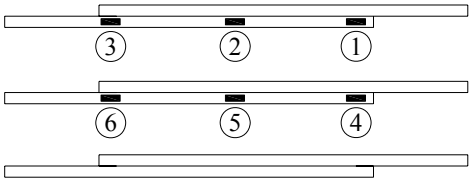	1	45
	2	1032
	3	1736
	4	108
	5	544
	6	1377

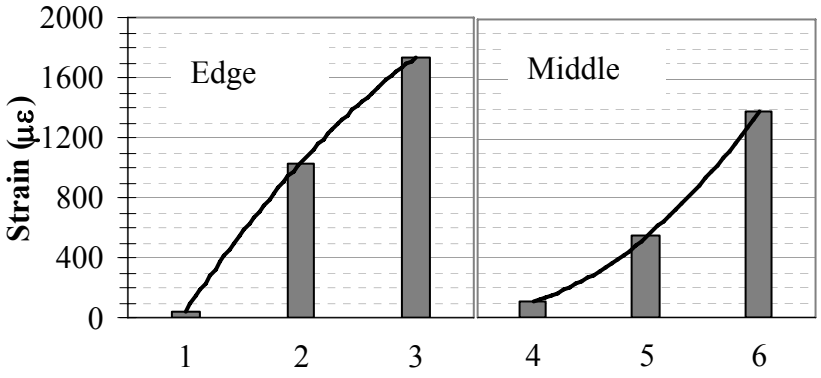

Figure 5.8 Strain values at ultimate for longitudinal reinforcements of TS26.

Strain gauges from 7 to 12 were located on transverse reinforcement. Their locations were described in Chapter 4 and shown in Figure 4.3. Any data could not be recorded from strain gauge 7, because it was broken down during casting of concrete. All strain gauges almost have the same strain values and prior to ultimate load strains on transverse reinforcement were small. Strains in transverse reinforcement were shown in Table 5.2 and Figure 5.9 Strain gauges 7, 9 and 11 are along the mid part of the beam and strain gauges 8, 10 and 12 are along the edge of the beam.

Table 5.2 Transverse reinforcement strains of TS26.

Strain gauge locations	Strain Gauge Number	Strain at Yielding Load (με)
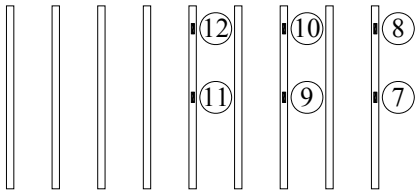	7	NA
	9	420
	11	72
	8	365
	10	290
	12	246

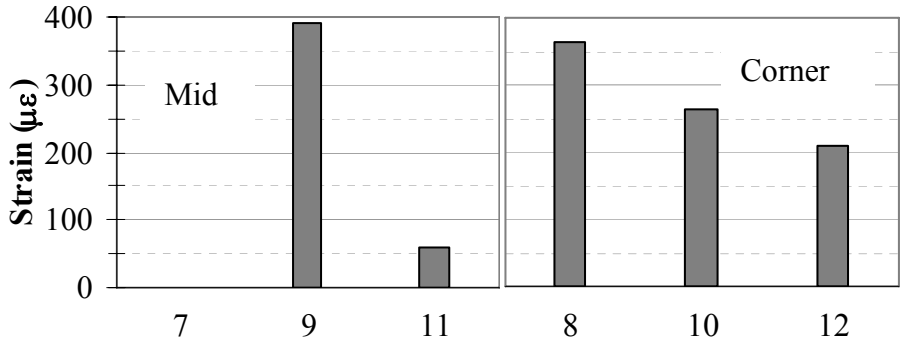

Figure 5.9 Strain values at ultimate for transverse reinforcements of TS26.

5.3.2. TS22

According to acquired data strain gauge 3 gave meaningless results. It was located at the continuous edge of the lap splice region and where maximum strain is expected. On the other hand middle bar strain gage 6 gave the maximum stress as expected. According to strain values at the yield load which was approximately taken as 120 kN, both the middle and edge bars were exceeded their yielding strain. TS22 failed as a result of yielding of longitudinal reinforcement followed by crushing of concrete. Table 5.3 and Figure 5.10 summarize the strain values for TS22 in microstrain (με).

Table 5.3 Longitudinal reinforcement strains of TS22.

Strain Gauge Locations	Strain Gauge Number	Strain at Yielding Load (με)
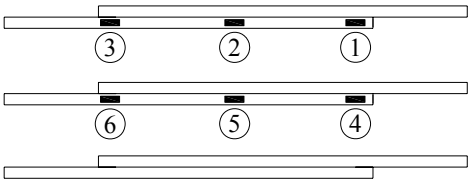	1	2
	2	1347
	3	NA
	4	10
	5	1414
	6	2732

Figure 5.10 Strain values at yielding for longitudinal reinforcements of TS22.

Locations of strain gauges were similar to TS26. Strains in transverse reinforcement were shown in Table 5.4 and Figure 5.11 in microstrain (με).

Table 5.4 Transverse reinforcement strains and stresses of TS22.

Strain Gauge Locations	Strain Gauge Number	Strain at Yielding Load (με)
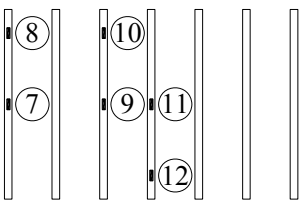	7	947
	9	45
	11	362
	8	1587
	10	108
	12	212

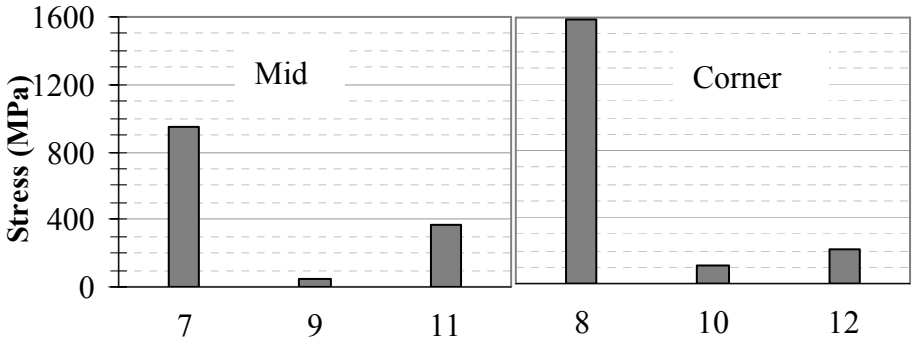

Figure 5.11 Strain values at yielding for transverse reinforcements of TS22.

5.3.3. TS16

According to strain values at the yield load, which was approximately 62 kN, both the middle and edge bars were yielded. Middle and edge bars exceeded their yield strain value. Since the failure of TS16 was flexural, yielding of longitudinal reinforcement should be expected. The stress distribution along the lap splice is increasing almost linearly. Table 5.5 and Figure 5.12 summarize the strain and stress values for TS16 in microstrain (με).

Table 5.5 Longitudinal reinforcement strains and stresses of TS16.

Strain Gauge Locations	Strain Gauge Number	Strain at Yielding Load (με)
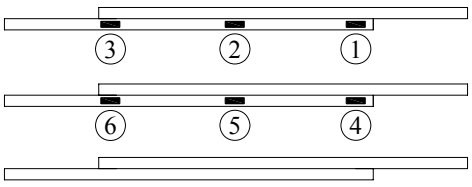	1	74
	2	1287
	3	4761
	4	62
	5	1213
	6	4985

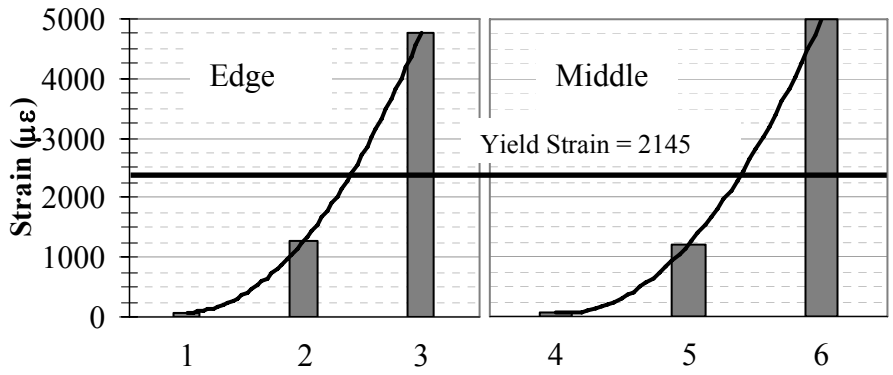

Figure 5.12 Strain values at yielding for longitudinal reinforcements of TS16.

No data could be recorded from strain gauge 9, because it was broken during casting of concrete. Strains in transverse reinforcement were shown in Table 5.6 and Figure 5.13 in microstrain (με).

Table 5.6 Transverse reinforcement strains and stresses of TS16.

Strain Gauge Locations	Strain Gauge Number	Strain at Yielding Load (με)
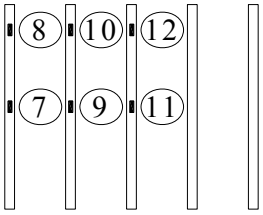	7	148
	9	NA
	11	5
	8	378
	10	222
	12	153

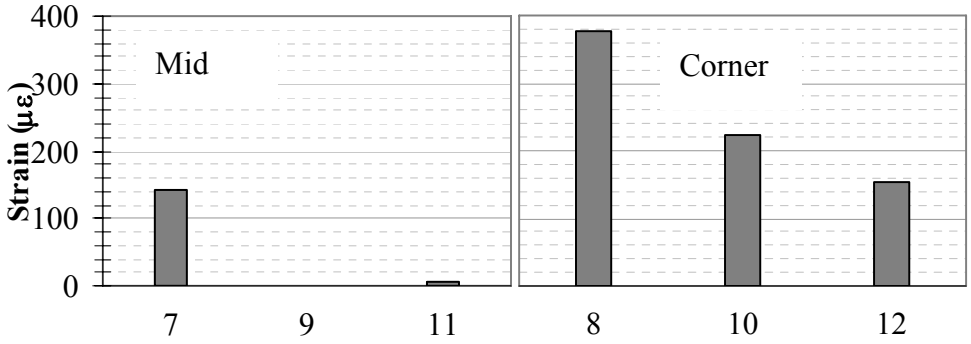

Figure 5.13 Strain values at yielding for transverse reinforcements of TS16.

5.3.4. ACI26

As previously defined in Chapter 4, Figure 4.21, strain gauges with numbers 1, 2, 3 were located on the edge bar and 4, 5, 6 were located on mid bar. Strain gage 6 did not give reasonable results. According to strain values at the ultimate load, which was approximately 159 kN, both the middle and edge bars yielded. Table 5.7 and Figure 5.14 summarize the strain values for ACI26 in microstrain (με).

Table 5.7 Longitudinal reinforcement strains and stresses of ACI26.

Strain Gauge Locations	Strain Gauge Number	Strain at Yielding Load (με)
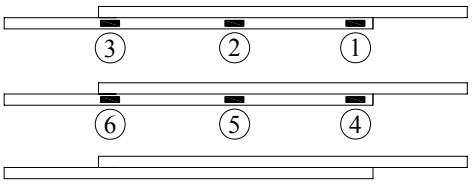	1	14
	2	787
	3	2800
	4	151
	5	1443
	6	NA

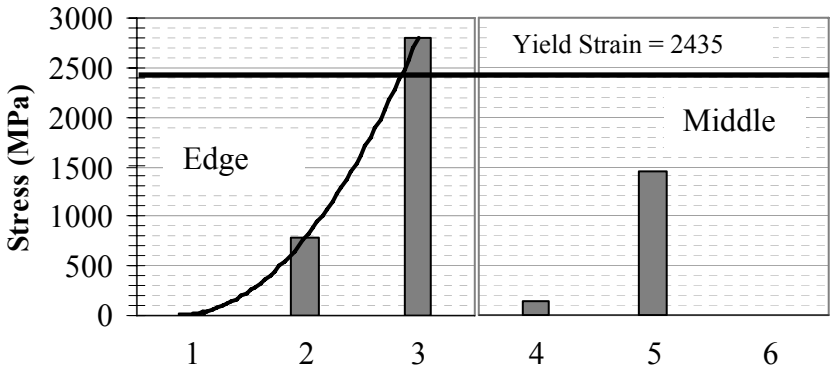

Figure 5.14 Strain values at yielding for longitudinal reinforcements of ACI26.

Stresses in transverse reinforcement were shown in Table 5.6 and Figure 5.15 in microstrain (με). Strain gauges 7, 9 and 11 are along the mid part of the beam and strain gauges 8, 10 and 12 are along the corner of the beam.

Table 5.8: Transverse reinforcement strains of ACI26.

Strain Gauge Locations	Strain Gauge Number	Strain at Yielding Load (με)
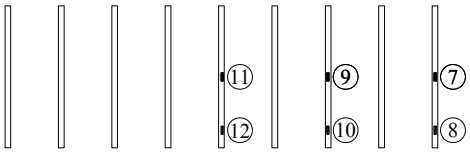	7	143
	9	NA
	11	32
	8	-357
	10	-228
	12	138

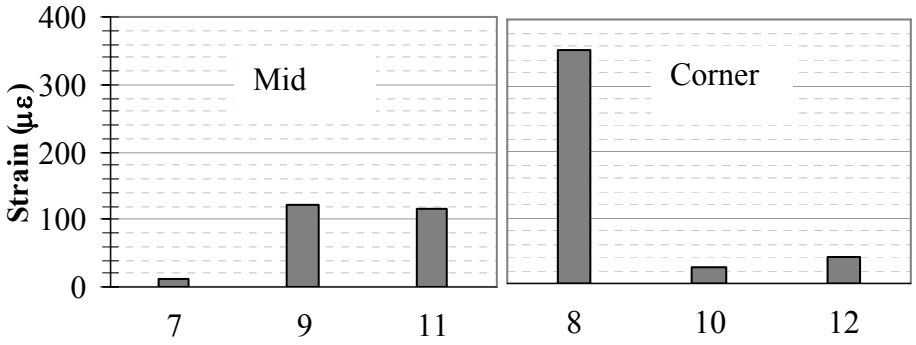

Figure 5.15 Strain values at yielding for transverse reinforcements of ACI26.

5.3.5. ACI16

Strain gauges with numbers 1, 2, 3 were located on the edge bar and 4, 5, 6 were located on mid bar. According to strain values at the ultimate load, which was approximately 55 kN, only the edge bar were yielded. Table 5.7 and Figure 5.16 summarize the strain values for ACI16 in microstrain (με).

Table 5.9 Longitudinal reinforcement strains and stresses of ACI16.

Strain Gauge Locations	Strain Gauge Number	Strain at Yileding Load (με)
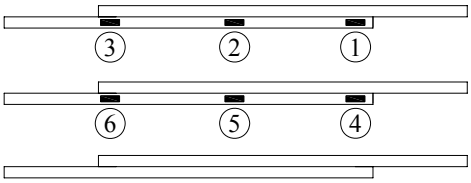	1	2
	2	493
	3	1890
	4	33
	5	1467
	6	1187

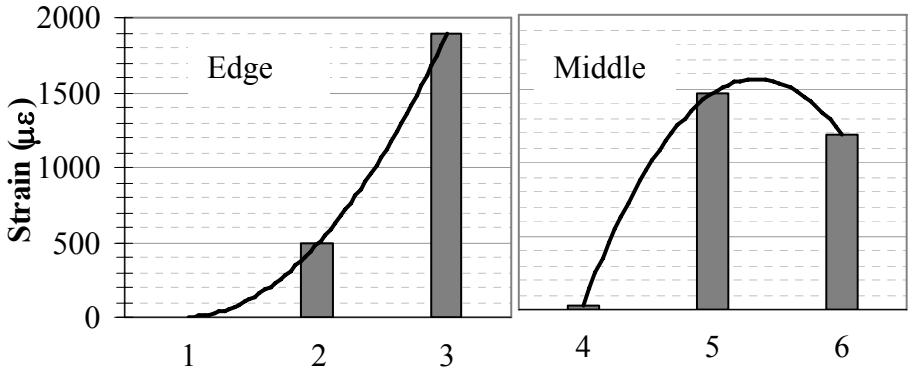

Figure 5.16 Strain values at yielding for longitudinal reinforcements of ACI16.

Locations of strain gauges were similar to other specimens. Strains in transverse reinforcement are shown in Table 5.8 and Figure 5.17 microstrain (με). Strain gauges 7, 9 and 11 are along the mid part of the beam and strain gauges 8, 10 and 12 are along the edge of the beam.

Table 5.10 Transverse reinforcement strains and stresses of ACI16.

Strain Gauge Locations	Strain Gauge Number	Strain at Yielding Load (με)
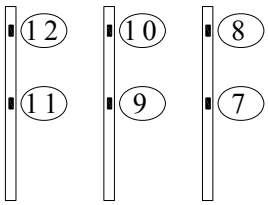	7	349
	9	37
	11	304
	8	156
	10	56
	12	257

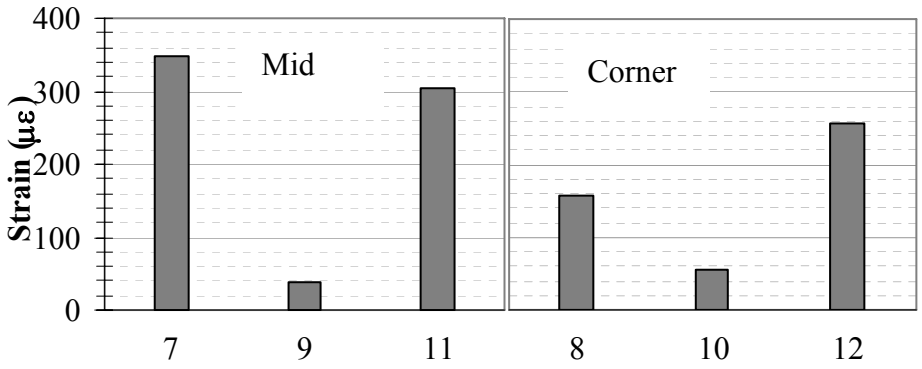

Figure 5.17 Strain values at yielding for transverse reinforcements of ACI16.

As seen form bar charts and tables, near the free end, strains on the longitudinal bars are close to zero and increasing along the bar. This is the expected strain distribution along a lap splice. The maximum strains in all specimens except TS26 exceed their yield values. Only for ACI16's strain values were smaller than the yield strain value. This may be occurred due to data acquisition system.

Examination of the strains on the transverse reinforcement showed that strain distribution on the stirrups is not uniform over the lap splice. Stirrups at the ends of the lap splice showed higher strain and they decreased towards the middle of splice. At the yielding of the beams, the stirrup strains at the end of the splices were approximately 350 με. The strain values of the stirrups decrease to approximately 200 με at the center of the lap splice.

CHAPTER 6

CASE STUDY

6.1. General

A case study was conducted to compare the lap splice lengths calculated according to both TS500 and ACI318-05 specifications. In this chapter information about case study is given and the results are evaluated in detail.

6.2. Explanation of Case Study

In order to calculate lap splice lengths for tension reinforcement in flexural members, basically compressive strength of concrete and yield strength of steel have to be defined. These two variables are adequate for TS500 approach. In addition to these variables, ACI318-05 specification requires clear cover and spacing between bars and transverse reinforcement ratio. Minimum requirements in TS500 were used to determine these variables. TS500 requirements were previously defined in Chapter 3. According to TS500 standard, spacing between the lap spliced bars need to be minimum one and half bar diameter. Otherwise, calculated development length has to be multiplied with 1.2. On the other hand, TS500 requires only one bar diameter clear cover and 20 mm as minimum for the structural members that are not exposed to weather. In ACI318-05, clear cover limit is 38 mm (1.5 in) for the structural members that are not exposed to weather. This large cover highly improves the performance of lap splices.

In this case study the new design expressions [9] proposed by ACI Committee 408 was also considered.

6.2.1. Section Properties

As previously mentioned, reinforcement configuration, clear cover dimensions and transverse reinforcement were calculated according to TS500 requirements. In order to calculate transverse reinforcement, 400 mm section depth is taken into consideration to be consistent with the specimens used in experimental study. Similarly, three bars were considered in the longitudinal direction. Details of sections, which were used in lap splice calculations, are summarized in Table 6.1 and the details of the variables used in the table are given in Figure 6.1.

Table 6.1 Values of variables used in Case Study

Section ID	d_b (mm)	d_m (mm)	ϕ_t (mm)	$2c_{si}$ (mm)	c_{bb} (mm)	c_{so} (mm)	b_w (mm)	h (mm)	Stirrup
S12	12	24	8	25	20	20	214	400	ϕ8/100
S14	14	24	8	25	20	20	224	400	ϕ8/100
S16	16	24	8	25	20	20	234	400	ϕ8/100
S18	18	24	8	27	20	20	248	400	ϕ8/100
S20	20	24	8	30	20	20	264	400	ϕ8/100
S22	22	24	8	33	22	22	284	400	ϕ8/100
S24	24	24	8	36	24	24	304	400	ϕ8/100
S25	25	24	8	37.5	25	25	314	400	ϕ8/100
S26	26	24	8	39	26	26	324	400	ϕ8/100
S30	30	24	8	45	30	30	380	400	ϕ8/100
S32	32	24	8	48	32	32	400	400	ϕ8/100

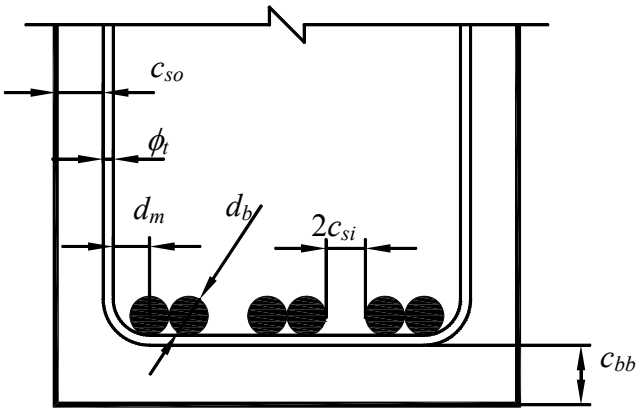

Figure 6.1 Details for variables defined in equations and case study.

6.2.2. Case Study Results

This case study was conducted using 9 different concrete strengths. These are 16, 18, 20, 25, 30, 35, 40, 45 and 50 MPa. It is obvious that lap splice length is decreasing with increasing concrete strength. Although ℓ_d / d_b ratio is changing for different concrete strengths, the trend is similar for all concrete strengths. Thus, results are interpreted here, only for concrete strengths 20, 35, 50 MPa.

Since this case study evaluates design provisions, all the required multipliers are included in the calculation. Similar to the conducted tests, all bars were considered to be lap spliced at the same location. Therefore the calculated development lengths were multiplied by 1.3 in the ACI 318 approach and by 1.5 in the TS 500 approach in order to calculate the required lap splice length. There is no such increase in the new ACI 408 proposal.

As can be seen in the last column of Table 6.1, the required minimum transverse reinforcement over the splice length is excessively high. The spacing of the transverse reinforcement should be equal or less than the ¼ of the beam height or 200 mm. according to TS 500 at every 100 mm a 8 mm diameter stirrup is required

along the lap splice according to TS 500. ACI 318 does not ask any special stirrup configuration along the lap splice.

Figure 6.2 shows three charts prepared for 20, 35 and 50 MPa concrete strength. As can be seen from the figures, the required splice length decreases as the concrete strength increases.

The upper bounds of the charts are drawn by either ACI408 Basic or ACI318-05 Basic equation. They give over conservative results as compared to other expressions. The main reason is that both Basic equations do not consider the effect of transverse reinforcement even a minimum amount. It should be noted that, the application of these basic equations are not very simple. Designer needs to check many conditions in order to use simple equations.

After the Basic expressions, TS 500 approach gives the highest results. The main reason for this high splice length requirement is the α_o=1.5 multiplier. Specimens in this study were prepared without using this multiplier and behaved well except TS26 in which the main problem was inadequate cover but not splice length.

ACI 318-05 Advanced and ACI 408 Advanced expressions give the lowest lap splice lengths. The main reason of this low values is the high amount of transverse reinforcement used in the case study according to TS 500. The advanced equations are very sensible to transverse reinforcement. To ensure safety while decreasing the splice length using the transverse reinforcement effect, there is an upper limit for the amount of K_{tr} and K'_{tr} value. TS 500 curve lies in between the basic and advanced curves of ACI 318-05 and ACI 408. It should be noted that, TS 500 approach is much simpler as compared to other approaches.

ACI 408 advanced approach does not consider any multiplier for lap splice length calculations. ACI 408 Advanced approach requires larger lengths for development length of bars (not splice length) as compared to ACI 318-05 approach for

development length. Briefly, the safety margin is increased for development length in this approach and the multiplier is decreased to 1.0 for many cases for splice length calculations. The development length expression in ACI 408 gives close values to that of splice length expression (1.3 × development length) of ACI 318-05.

It should be noticed that beams for case study were designed according to TS 500 limitations. In all three cases given in Figure 6.2, ACI 318-05 Advanced and ACI 408 Advanced expressions give the shortest splice lengths. TS26 beam which was failed prematurely due to bond problem had a ℓ_d / d_b ratio of 34. The multiplier 1.5 for the spliced length was not applied in the test. Including the multiplier, however, in the case study, ACI 318-05 approach and ACI 408 Advanced Approach required ℓ_d / d_b ratio of 36 and 38, respectively. These short splice lengths arise premature bond failure concerns. Here the problem is the cover dimensions or cover dimensions to bar diameter ratio (c_b/d_b, c_{so}/d_b). For large diameter bars, since their flexural stiffness is higher even a ratio of 1.0 becomes insufficient. For such cases increasing the lap splice length is not an effective solution. Instead, the cover dimension needs to be increased.

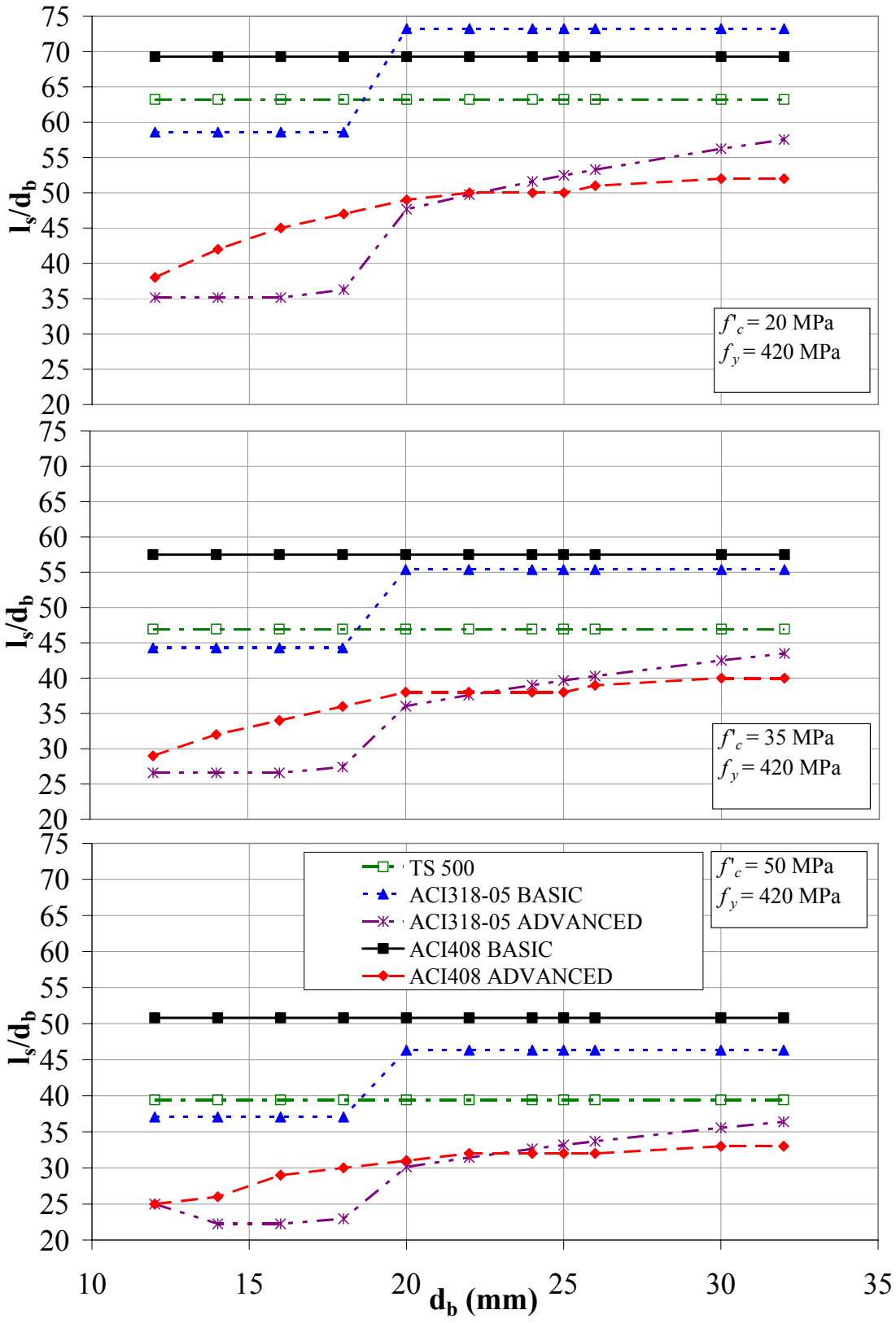

Figure 6.2 ℓ_d / d_b vs d_b curves for 5 different calculation methods

CHAPTER 7

CONCLUSIONS

After realizing that there are no specific tests in the literature for the minimum limitations of Codes, an experimental research was initiated at the Structural Mechanics Laboratory of the Middle East Technical University. In this scope, totally 6 beams were prepared according to TS 500 and ACI 318-05. Clear cover, spacing between bars, amount of transverse reinforcement, and splice length was calculated according to the minimum requirements given in the Codes. The results of the tests and analytical studies were presented in the previous chapters. A case study was also conducted on this topic and discussed. Based on the tests conducted and analytical studies, the following conclusions can be drawn:

- If the minimum cover, spacing, and transverse reinforcement requirements are met, specimens produced according to ACI 318-05 behave satisfactorily with a flexural failure at the ultimate stage. It should be noted that, the multiplier 1.3 for splice length calculation was not considered in the design of beams.

- While TS22 and TS16 specimens showed acceptable behavior with flexural failure at the ultimate stage, TS26 beam failed in a sudden and brittle manner prior to the yielding of the beam with a side and face splitting bond failure. It should be noted that the multiplier 1.5 for the lap splice length was not applied in the calculations of TS 500 specimens.

- The Turkish Standard for Building Code requires much less cover concrete as compared to ACI 318-05. This small cover does not cause any problem for

small diameter bars. For large diameter bars, however, the beam can not show the expected performance. The reason for the bond failure of TS26 may not be the inadequate lap length but inadequate concrete cover over the spliced bars.

- ACI 408 proposal does not include the multiplier 1.3 for splice length calculation in many cases. The safety margins, however, increased in this approach. ACI 408 Advanced expression requires almost the same splice lengths as compared to ACI 318-05 Advanced expression including a 1.3 multiplier.

- ACI 318-05 Advanced and ACI 408 Advanced expressions calculate splice lengths similar to the splice length realized in TS26 specimen. The splice length of this beam was calculated according to TS 500 without multiplier 1.5. This beam failed due to splitting of cover concrete. It can be said that ACI 318-05 Advanced and ACI 408 Advanced expressions would predict the splice length unsafely for this specimen.

- TS 500 limitations for minimum cover dimensions of large bars need to be revised. Although one bar diameter net cover is adequate for bars up to 22 mm, it is found inadequate for 26 mm diameter bars.

REFERENCES

[1] Abrams, D.A., "Tests of Bond Between Concrete and Steel", University of Illinois Bulletin, No.71, 1913

[2] Azizinamini, A., Chisala, M., Ghosh, S. K., "Tension Development Length of Reinforcing Bars Embedded in High-Strength Concrete", Engineering Structures, Vol.17, No.7, pp.512-522, 1995

[3] Azizinamini, A., Stark, M., Roller, J. J., Ghosh, S. K., "Bond Performance of Reinforcing Bars Embedded in High-Strength Concrete," ACI Structural Journal, V. 90, No. 5, pp. 554-561, Sep.-Oct. 1993

[4] Chamberlin, S.J., "Spacing of Spliced Bars in Beams", Journal of the American Concrete Institute, V. 29, No. 8, Proceedings V. 54, pp. 689-697, Feb. 1958

[5] Canbay, E., Frosch, R.J., "Bond Strength of Lap-Spliced Bars", ACI Structural Journal, V. 102, pp. 605-614, July 2005

[6] Canbay, E., Frosch, R.J., "Design of Lap-Spliced Bars: Is Simplification Possible?", ACI Structural Journal, V. 103, pp. 443-451, May 2006

[7] Chinn, J., Ferguson, P.M., Thompson, J.N., “Lapped Splices in Reinforced Concrete Beams”, Journal of the American Concrete Institute, V. 27, No. 2, Proceedings V. 52, pp. 201-213, Oct. 1955

[8] Darwin, D., Zuo, J., Tholen, M.L., Idun, E.K., “Development Length Criteria for Conventional and High Relative Rib Area Reinforcing Bars”, ACI Structural Journal, V.93, No.3, pp.347-359,May-June 1996

[9] Darwin, D., Lutz L. A., Zuo, J., “Recommended Provisions and Commentary on Development and Lap Splice Lengths for Deformed Reinforcing Bars in Tension”, ACI Structural Journal, V.102, No.3, pp.347-359,May-June 1996

[10] Ferguson, P.M., Breen, J.E., “Lapped Splices for High Strength Reinforcing Bars, Part I & II”, Journal of the American Concrete Institute, No. 9, Proceedings V. 62, pp. 1063-1077, Sept. 1965

[11] Ferguson, P.M., Briceno, E.A., “Tensile Lap Splices-Part I: Retaining Wall Type, Varying Moment Zone”, *Research Report* No. 113-2, Center for Highway Research, The University of Texas at Austin, July 1969

[12] Ferguson, P. M., Krishnaswamy, C. N., “Tensile Lap Splices-Part 2: Design Recommendation for Retaining Wall Splices and Large Bar Splices,” Research Report No. 113-2, Center for Highway Research, The University of Texas at Austin, 60 pp, Apr. 1971

[13] Goto, Y., “Cracks Formed in Concrete Around Deformed Tension Bars”, ACI Journal, Title No.68-26, pp. 244-251, April, 1971

[14] Hamad, B. S., Najjar, S. S. and Jumma G. K. “Correlation between Roles of Transverse Reinforcement and Steel Fibers in Confining Tension Lap Splices in High-Strength Concrete”, ACI Structural Journal, V. 100, pp. 19-24, January 2003

[15] Orangun, C.O., Jirsa, J.O., Breen, J.E., “A Reevaluation of Test Data on Development Length and Splices”, ACI Journal, Title No.74-11, pp.114-122, March 1977

[16] Rezansoff, T., Konkankar, U. S., Fu, Y. C., “Confinement Limits for Tension Lap Splices under Static Loading”, Canadian Journal of Civil Engineering, Vol. 19, pp. 447-453, 1992 -

[17] Sakurada, T., Morohashi, N., Tanaka, R., “Effect of Transverse Reinforcement on Bond Splitting Strength of Lap Splices”, Transactions of the Japan Concrete Institute, Vol.15, pp.573-580, 1993

[18] Sozen, M.A., Moehle, J.P., “Development and Lap-Splice Lengths for Deformed Reinforcing Bars in Concrete”, The Portland Cement Association & The Concrete Reinforcing Steel Institute, 109 p., Aug. 1990

[19] Thompson, M. A., Jirsa, J. O., Breen, J. E., Meinheit, D. F., “The Behavior of Multiple Lap Splices in Wide Sections,” Research Report No. 154-1, Center for Highway Research, The University of Texas at Austin, 75 pp, Feb. 1975

[20] Zekany, A. J., Neumann, S., Jirsa, J. O., Breen, J. E., “The Influence of Shear on Lapped Splices in Reinforced Concrete,” Research Report 242-2, Center for Transportation Research, Bureau of Engineering Research, University of Texas at Austin, 88 pp, July 1981

[21] Zuo, J., Darwin, D., "Splice Strength of Conventional and High Relative Rib Area Bars in Normal and High Strength Concrete," ACI Structural Journal, V. 97, No.4, pp. 630-641, July-Aug. 2000

[22] "TS-500 February 2000, Requirements for Design and Construction of Reinforced Concrete Structures," Middle East Technical University, Ankara, 2003. [Translated and Printed with Permission from Turkish Standards Institute]

[23] ACI Committee 318, "Building Code Requirements for Structural Concrete (ACI318-77) and Commentary (318R-77)," American Concrete Institute, Farmington Hills, Detroit, 2002.

[24] ACI Committee 318, "Building Code Requirements for Structural Concrete (ACI318-05) and Commentary (318R-05)," American Concrete Institute, Farmington Hills, Michigan, 2002, 443 pp.

[25] ACI Committee 408, 2003, "Bond and Development of Straight Reinforcing Bars in Tension (ACI 408R-03)," American Concrete Institute, Farmington Hills, Mich., 49 pp.

[26] Bentz C. E., Response-2000, Reinforced Concrete Sectional Analysis using the Modified Compression Field Theory, Version 1.0.5, 2000.

APPENDIX A

LAP SPLICE CALCULATIONS FOR SPECIMENS

In this appendix detailed calculation for lap splice lengths of beam specimens determined. For all six specimens material properties defined below are used.

f'_c = 30 MPa = 4350 psi f_{cd} = 20 MPa f_{ctd} = 1.278 MPa

f_y = 420 MPa = 60900 psi f_{yd} = 365 MPa

- ACI26

b_w = 306.2 mm = 12.055 in.

d = 340.9 mm = 13.42 in.

d_b = 26 mm = 1.024 in. d_{tr} = 8 mm = 0.3150 in.

c_c = 38.1 mm = 1.50 in.

c_s = 25.4 mm = 1.00 in.

$$c = \text{Min}\left(\frac{25.4+26}{2}, 38.1\right)\text{mm} = 26\text{ mm} = 1.024\text{ in.}$$

$$A_{tr} = \frac{\pi \cdot 0.315^2}{4} 2 = 0.1558\text{ in}^2$$

$s \le d/2$ & 24 in → s = Min(170.45, 610) mm = 6.711 in.

$$A_v = 0.75\sqrt{f'_c}\frac{b_w s}{f_y} \quad \rightarrow s = \frac{A_v f_y}{0.75 b_w \sqrt{f'_c}} = \frac{0.1558 \times 60900}{0.75 \times 12.055 \times \sqrt{4350}} = 15.91\text{ in.}$$

$$K_{tr} = \frac{A_{tr} f_{yt}}{1500 sn} = \frac{0.1558 \times 60900}{1500 \times 6.711 \times 3} = 0.314$$

$$\frac{c_b + K_{tr}}{d_b} = \frac{1.024 + 0.314}{1.024} = 1.307$$

$$\ell_d = \frac{3}{40}\frac{f_y}{\sqrt{f_c'}}\frac{\psi_t\psi_e\psi_s\lambda}{\left(\frac{c_b + K_{tr}}{d_b}\right)}d_b = \frac{3}{40}\frac{60900}{\sqrt{4250}}\frac{1}{1.307}1.024 = 54.257\,\text{in} = 13800\ \text{mm}$$

ACI22

b_w = 285 mm = 11.22 in.

d = 342.9 mm = 13.50 in.

d_b = 22 mm = 0.866 in. d_{tr} = 8 mm = 0.3150 in.

c_c = 38.1 mm = 1.50 in.

c_s = 25.4 mm = 1.00 in.

$$c = \text{Min}\left(\frac{25.4 + 22}{2}, 38.1\right)\text{mm} = 23.7\ \text{mm} = 0.933\ \text{in.}$$

$$A_{tr} = \frac{\pi \cdot 0.315^2}{4}2 = 0.1558\ \text{in}^2$$

$s \le d/2$ & 24 in → s = Min(171.45, 610) mm = 6.75 in.

$$A_v = 0.75\sqrt{f_c'}\frac{b_w s}{f_y} \quad \rightarrow s = \frac{A_v f_y}{0.75 b_w \sqrt{f_c'}} = \frac{0.1558 \times 60900}{0.75 \times 11.22 \times \sqrt{4350}} = 17.1\ \text{in.}$$

$$K_{tr} = \frac{A_{tr} f_{yt}}{1500sn} = \frac{0.1558 \times 60900}{1500 \times 6.81 \times 3} = 0.313$$

$$\frac{c_b + K_{tr}}{d_b} = \frac{0.933 + 0.313}{0.866} = 1.439$$

$$\ell_d = \frac{3}{40}\frac{f_y}{\sqrt{f_c'}}\frac{\psi_t\psi_e\psi_s\lambda}{\left(\frac{c_b + K_{tr}}{d_b}\right)}d_b = \frac{3}{40}\frac{60900}{\sqrt{4250}}\frac{1}{1.439}0.866 = 41.68\,\text{in} = 1060\ \text{mm}$$

- ACI16

b_w = 225 mm = 10.4 in.

c = Min $\left(\frac{25.4+16}{2}, 38.1\right)$ mm = 20.7 mm = 0.815 in.

d_b = 16 mm = 0.6299 in. d_{tr} = 8 mm = 0.3150 in.

c_c = 38.1 mm = 1.50 in.

c_s = 25.4 mm = 1.00 in.

$A_{tr} = \frac{\pi \cdot 0.315^2}{4} 2 = 0.1558$ in²

$s \leq$ d/2 & 24 in → s = Min(173, 610) mm = 6.81 in.

$A_v = 0.75\sqrt{f_c'}\frac{b_w s}{f_y}$ → $s = \frac{A_v f_y}{0.75 b_w \sqrt{f_c'}} = \frac{0.1558 \times 60900}{0.75 \times 10.04 \times \sqrt{4350}} = 19.1$ in.

$$K_{tr} = \frac{A_{tr} f_{yt}}{1500 sn} = \frac{0.1558 \times 60900}{1500 \times 6.81 \times 3} = 0.310$$

$$\frac{c_b + K_{tr}}{d_b} = \frac{0.815 + 0.310}{0.6299} = 1.786$$

$$\ell_d = \frac{3}{40}\frac{f_y}{\sqrt{f_c'}}\frac{\psi_t \psi_e \psi_s \lambda}{\left(\frac{c_b + K_{tr}}{d_b}\right)} d_b = \frac{3}{40}\frac{60900}{\sqrt{4250}}\frac{0.8}{1.786} 0.6299 = 19.54\,\text{in} = 496.3\text{mm} \approx 500\text{ mm}$$

- TS26

b_w = 306 mm

d = 341 mm

d_b = 26 mm

c_c = 26 mm

c_s = 39 mm

$$\ell_b = \left(0.12 \frac{f_{yd}}{f_{ctd}} \phi\right) \geq 20\phi$$

$$\ell_b = \left(0.12\frac{365}{1.278}26\right) = 34.6\phi = 890 \text{ mm}$$

- TS22

b_w = 284 mm

d = 359 mm

d_b = 22 mm

c_c = 20 mm

c_s = 25 mm

$$\ell_b = \left(0.12\frac{f_{yd}}{f_{ctd}}\phi\right) \geq 20\phi$$

$$\ell_b = \left(0.12\frac{365}{1.278}22\right) = 34.6\phi = 750\,\text{mm}$$

- TS16

b_w = 234 mm

d = 364 mm

d_b = 16 mm

c_c = 20 mm

c_s = 25 mm

$$\ell_b = \left(0.12\frac{f_{yd}}{f_{ctd}}\phi\right) \geq 20\phi$$

$$\ell_b = \left(0.12\frac{365}{1.278}16\right) = 34.6\phi = 550\,\text{mm}$$

APPENDIX B

THEORETICAL MOMENT CURVATURE DIAGRAMS OF SPECIMENS

In this appendix theoretical moment curvature diagrams, acquired from RESPONSE-2000, are shown.

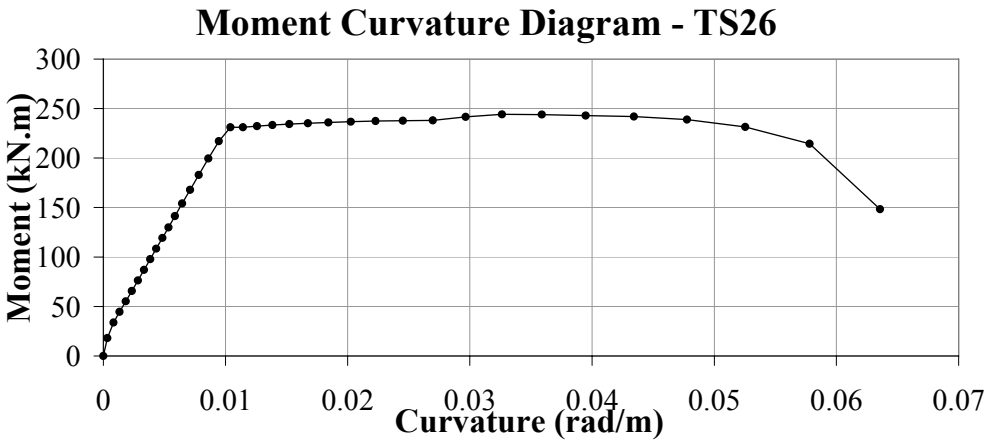

Figure B.1. Moment Curvature Diagram – TS26.

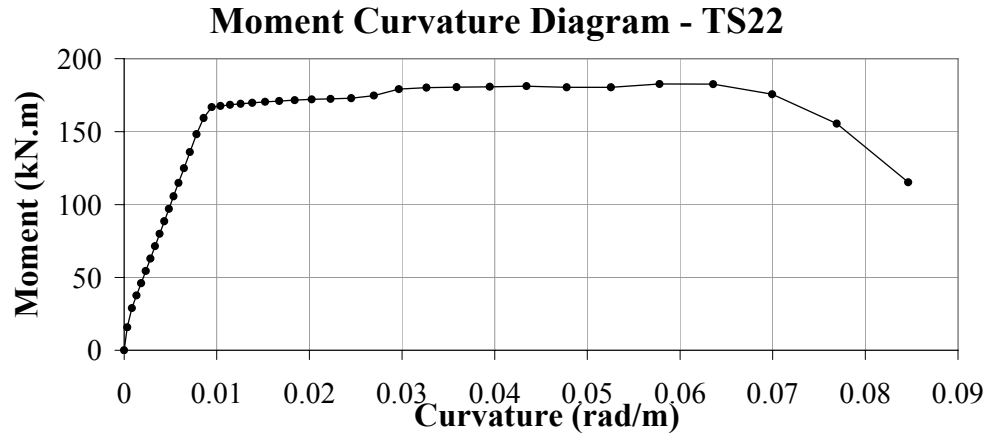

Figure B.2. Moment Curvature Diagram – TS22

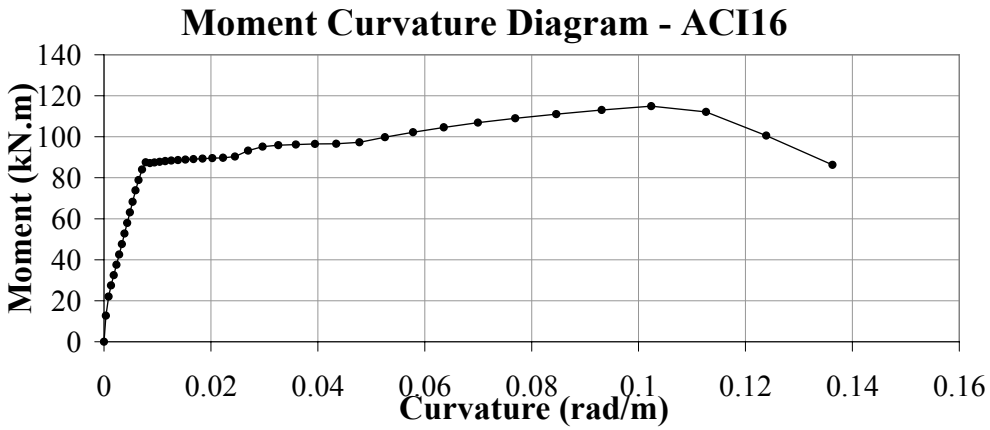

Figure B.3. Moment Curvature Diagram – TS16.

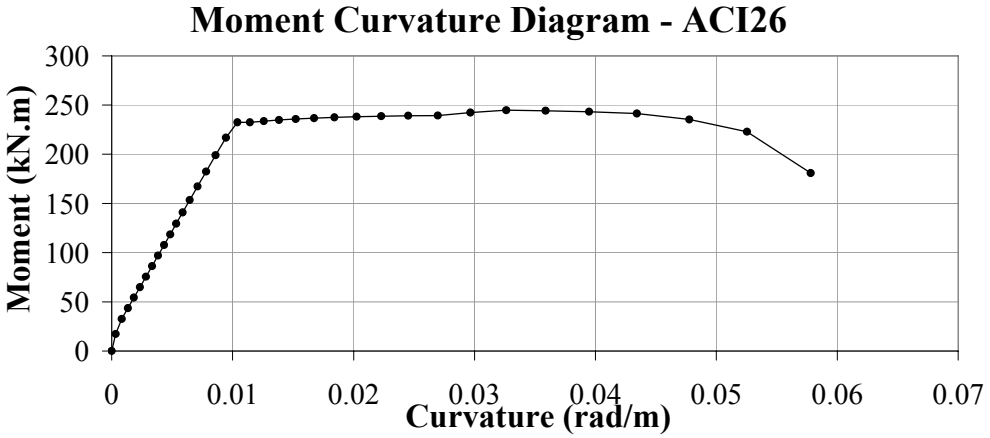

Figure B.4. Moment Curvature Diagram – ACI26.

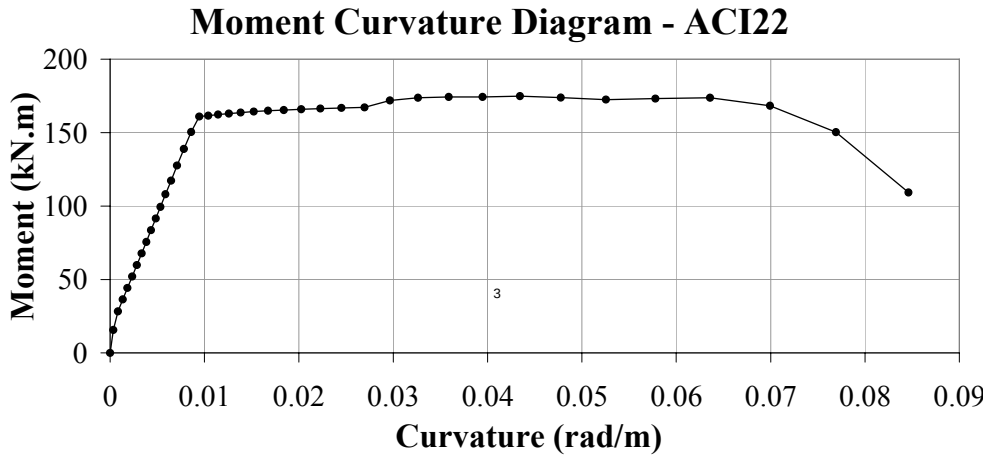

Figure B.5. Moment Curvature Diagram – ACI22.

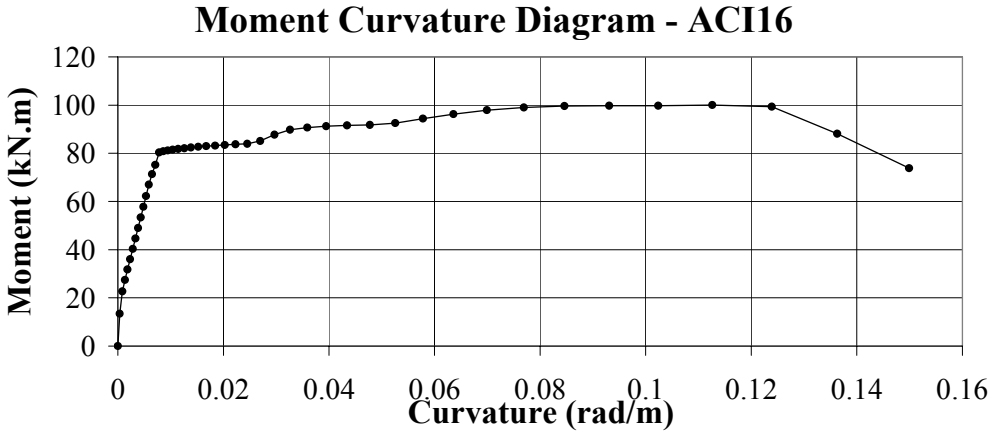

Figure B.5. Moment Curvature Diagram – ACI16.